



Impact of Forest Drought Response on Land-Atmosphere Interactions



Hao-wei Wey

Hamburg 2020

Hinweis

Die Berichte zur Erdsystemforschung werden vom Max-Planck-Institut für Meteorologie in Hamburg in unregelmäßiger Abfolge herausgegeben.

Sie enthalten wissenschaftliche und technische Beiträge, inklusive Dissertationen.

Die Beiträge geben nicht notwendigerweise die Auffassung des Instituts wieder.

Die "Berichte zur Erdsystemforschung" führen die vorherigen Reihen "Reports" und "Examensarbeiten" weiter.

Anschrift / Address

Max-Planck-Institut für Meteorologie
Bundesstrasse 53
20146 Hamburg
Deutschland

Tel./Phone: +49 (0)40 4 11 73 - 0

Fax: +49 (0)40 4 11 73 - 298

name.surname@mpimet.mpg.de

www.mpimet.mpg.de

Notice

The Reports on Earth System Science are published by the Max Planck Institute for Meteorology in Hamburg. They appear in irregular intervals.

They contain scientific and technical contributions, including Ph. D. theses.

The Reports do not necessarily reflect the opinion of the Institute.

The "Reports on Earth System Science" continue the former "Reports" and "Examensarbeiten" of the Max Planck Institute.

Layout

Bettina Diallo and Norbert P. Noreiks
Communication

Copyright

Photos below: ©MPI-M

Photos on the back from left to right:
Christian Klepp, Jochem Marotzke,
Christian Klepp, Clotilde Dubois,
Christian Klepp, Katsumasa Tanaka



Impact of Forest Drought Response on Land-Atmosphere Interactions



Hao-wei Wey

Hamburg 2020

Hao-wei Wey

aus Neu-Taipeh, Taiwan

Max-Planck-Institut für Meteorologie
The International Max Planck Research School on Earth System Modelling
(IMPRS-ESM)
Bundesstrasse 53
20146 Hamburg

Tag der Disputation: 12. Februar 2021

Folgende Gutachter empfehlen die Annahme der Dissertation:

Prof. Dr. Martin Claussen

Prof. Dr. Julia Pongratz

Vorsitzender des Promotionsausschusses:

Prof. Dr. Dirk Gajewski

Dekan der MIN-Fakultät:

Prof. Dr. Heinrich Graener

Title Cover:

Aerial image of forest in San Juan Bautista, Peru, located in the Western Amazon.

Photo by David Geere.

Hao-wei Wey

Impact of Forest Drought Response on Land-Atmosphere Interactions

ABSTRACT

The Amazon forests are one of the largest ecosystem carbon pools on Earth. Although more frequent and prolonged droughts have been predicted under future climate change there, the vulnerability of Amazon forests to drought has yet remained largely uncertain, as most land surface models failed to capture the vegetation responses to drought. In this study, the ability of the state-of-the-art land surface model JSBACH to simulate the drought responses of Leaf Area Index (LAI) and litter production in the Amazon forests is evaluated and several weaknesses are found. Based on the evaluation, an improved version of JSBACH is presented, which is modified based on intensive field measurement from the artificial drought experiments. In the modified JSBACH, a dependency of leaf growth on carbon allocation to leaves is added, and leaf shedding rate is separated into two parts representing aging and water stress. The modified JSBACH is shown to capture the drought responses at different sites in the Amazon.

We then couple the modified JSBACH with the atmospheric model ECHAM to simulate the impacts of drought under RCP8.5 scenario. As the vegetation drought response was poorly simulated, we separate the complex drought effects of the Amazon forests to give more insights, which has not been done before. The drought effects are separated into (1) the direct effect resulting from declining soil moisture and stomatal responses, and (2) the LAI effect due to leaf shedding from drier soil. It is shown that the LAI effect accounts for 35% of reduced natural carbon uptake and 12% of surface warming by the end of the 21st century. A comparison with results simulated by the standard JSBACH shows that the model uncertainty associated with LAI and litter production is large for biogeochemical effects, and smaller for biogeophysical effects.

In addition, the drought-induced tree mortality is implemented to the model to estimate the impacts. Compared with model version without a drought mortality, the carbon storage is reduced for more than 60%. The results highlight the importance for land surface models to incorporate drought deciduousness and drought mortality for tropical rainforests, in order to have better future climate projections.

ZUSAMMENFASSUNG

Die Amazonas-Regenwälder sind einer der größten Ökosystemkohlenstoffspeicher auf der Erde. Obwohl aufgrund des zukünftigen Klimawandels häufigere und längere Dürreperioden für die Region vorhergesagt wurden, ist die Vulnerabilität der Amazonaswälder für Dürren bisher weitgehend ungewiss, da die meisten Landoberflächenmodelle die Reaktion der Vegetation auf Dürren nicht erfassen konnten. In dieser Studie wird die Fähigkeit des hochmodernen Landoberflächenmodells JSBACH bewertet, die Reaktionen des Blattoberflächenindex (LAI) und der Streuproduktion in den Amazonaswäldern auf Dürre zu simulieren, und mehrere Schwachstellen werden festgestellt. Basierend auf der Evaluation wird eine verbesserte Version von JSBACH vorgestellt. Diese wurde auf der Grundlage von intensiven Feldmessungen künstlicher Dürreexperimente modifiziert. Im modifizierten JSBACH ist eine Abhängigkeit des Blattwachstums von der Kohlenstoffzuteilung auf die Blätter integriert und die Blattabwurfrate wird in zwei Teile aufgeteilt, die Alterung und Wasserstress repräsentieren. Es wird gezeigt, dass das modifizierte JSBACH die Reaktion auf Dürre an verschiedenen Standorten im Amazonasgebiet erfasst.

Das modifizierte JSBACH wird darüber hinaus mit dem atmosphärischen Modell ECHAM gekoppelt, um die Auswirkungen von Dürre unter dem RCP8.5-Szenario zu simulieren. Da die Reaktion der Vegetation auf Dürre schlecht simuliert wurde, separieren wir die komplexen Dürreauswirkungen der Amazonaswälder, um bessere Einblicke zu erhalten, was bisher noch nicht gemacht wurde. Die Dürreeffekte werden unterteilt in (1) den direkten Effekt, der sich aus der abnehmenden Bodenfeuchtigkeit und den stomatären Reaktionen ergibt, und (2) den LAI-Effekt aufgrund des Blattabwurfs durch trockenere Böden. Es wird gezeigt, dass der LAI-Effekt zum Ende des 21. Jahrhunderts für 35% der verringerten natürlichen Kohlenstoffaufnahme und 12% der Oberflächenerwärmung verantwortlich ist. Ein Vergleich mit Ergebnissen, die mit der JSBACH-Standardversion simuliert wurden, zeigt, dass die Modellunsicherheit im Zusammenhang mit dem LAI und der Streuproduktion für biogeochemische Effekte groß und für biogeophysikalische Effekte kleiner ist.

Darüber hinaus wird die dürreinduzierte Baumsterblichkeit in das Modell implementiert, um die Auswirkungen abzuschätzen. Verglichen mit der Modellversion ohne Trockenheitsmortalität ist die Kohlenstoffspeicherung um mehr als 60% reduziert. Die Ergebnisse zeigen, wie wichtig es für Landoberflächenmodelle ist, Blattabwurf und Mor-

talität durch Dürre bei tropischen Regenwäldern einzubeziehen, um bessere Zukunftsklimaprojektionen zu erhalten.

ACKNOWLEDGMENTS

Eat fruits; thank trees. Eat rice; thank fields.

— Taiwanese proverb

First of all, I would like to express my deepest gratitude to my supervisor and co-supervisor, Julia Pongratz and Kim Naudts, for their insightful guidance and tremendous support throughout the whole period of my study. A beautiful taste for science that they have shown to me is what I will continue to pursue no matter where I go. I thank my panel chair, Martin Claußen, for his academic supervision on this work from a macroscopic point of view. I thank Eva-Maria Pfeiffer and Udo Schickhoff for being part of my doctoral examination commission and providing invaluable suggestions.

I thank Julia Nabel for her many critical comments and for helping me understand the model JSBACH as well as the gap between the modeled world and the reality. I thank Lena Boysen, Thomas Raddatz, Christian Reick and Jürgen Bader for the inspiring discussions. I thank Tobias Stacke and Philipp de Vrese for the discussion and help related to soil physics in the model. Many colleagues and friends have helped make my life and working environment during the past few years enjoyable. They are Guilherme, Cathy, Sirisha, Pin-hsin, Zoé, Meike, Nora, Josephine, Mateo, Suman, Diego, István, Sally, Alex, Johannes, Dorothea, Sebastian, and many others. I thank Guilherme, Mateo and Nora for proofreading the thesis, and Meike for translating the abstract.

I thank the IMPRS-ESM for generously providing the resources we need. My sincere gratitude goes to Antje Weitz, Cornelia Kampmann and Michaela Born, for their assistance with various administrative tasks and answering every single question I sent to them. Especially, Antje Weitz has my heartfelt respect, for being always so caring and able to remember surprisingly many details of my personal life each time we met.

I am more than grateful to my family: my parents, sisters, *a-má*, *a-koo*, for their unconditional mental and material support from beyond the oceans. Finally, I want to thank my partner, for the patience and understanding she gave me during my difficult time, for the countless hours she spent on the regional trains just to be in Hamburg with me, and for everything she has done for me. The time we spent together finishing our theses will always be cherished in my life.

Bān-tshian giân-gí, lóng-sī tsi't-kù – Kám-siā lí.

CONTENTS

1	INTRODUCTION	1
1.1	The drought-threatened Amazon forests under the changing climate	1
1.2	Drought effects in the Amazon forests: What have we learned from the observations?	2
1.3	The gaps between observations and simulations	3
1.4	Drought effects under future climate	4
1.5	Thesis overview	5
2	EVALUATING AND IMPROVING THE SIMULATED VEGETATION DROUGHT RESPONSES AT THE AMAZON FORESTS	7
2.1	Introduction	7
2.2	Methods	11
2.2.1	The starting point: JSBACH v3.2 (FOM branch)	11
2.2.2	Site description	15
2.2.3	Model modifications and parameter tuning	16
2.2.4	Simulation protocol	17
2.3	Results	18
2.4	Discussion	26
2.4.1	LAI	26
2.4.2	Leaf litter production	27
2.4.3	Implications for future model development	28
2.5	Conclusions	29
3	SEPARATING THE DIRECT AND LAI EFFECTS OF DROUGHT UNDER FUTURE CLIMATE	31
3.1	Introduction	31
3.2	Methods	33
3.2.1	Model configuration	33
3.2.2	Simulations	35
3.3	Results	37
3.3.1	Future decline of precipitation simulated by MPI-ESM	37
3.3.2	Biogeochemical effects: The carbon budgets	38
3.3.3	Biogeophysical effects	43
3.3.4	Comparing the standard and modified JSBACH	48
3.4	Discussion	52
3.4.1	Improvement of JSBACH under coupled mode	52
3.4.2	Biogeochemical and biogeophysical effects due to LAI	52
3.5	Conclusions	54
4	MODELING DROUGHT-INDUCED TREE MORTALITY AND ITS IMPACTS UNDER FUTURE CLIMATE	57

4.1	Introduction	57
4.2	Methods	59
4.2.1	Implementation of drought mortality	59
4.2.2	Evaluation at TFE site at TAP	60
4.2.3	Simulation protocol	60
4.3	Results	61
4.4	Discussions and Conclusions	66
5	CONCLUSIONS AND OUTLOOKS	69
5.1	Conclusions	69
5.2	Outlooks	72
A	APPENDIX TO CHAPTER 3	75
A.1	The drought effects outside the Amazon	75
B	APPENDIX TO CHAPTER 4	77
B.1	Alternatives for implementing drought mortality	77
B.2	Methods	78
C	FORMAL REMARK ABOUT THE USE OF "WE" IN THIS THE- SIS	79
	BIBLIOGRAPHY	81

LIST OF FIGURES

- Figure 2.1 Location of the two throughfall exclusion experiments used in this study. Left: Tapajós National Forest (TAP); Right: Caxiuanã National Forest (CAX). 15
- Figure 2.2 Taylor Diagrams of observational and simulated LAI at EXP plot for the first 2 years. The standard JSBACH is also shown on the diagram with the label "default". 18
- Figure 2.3 Time evolution of soil moisture (upper half) and LAI (lower half) of both observation and simulations at TAP. (Top) standard (Bot) modified JSBACH. Dots: observation; Lines: simulations. 20
- Figure 2.4 LAI versus relative soil moisture at the EXP plot at TAP. (Top) observation (slope = 5.53, $r = 0.519$) (Mid) standard JSBACH (slope = 16.7, $r = 0.831$) (Bot) modified JSBACH (slope = 3.45, $r = 0.702$). Relative soil moisture is calculated as volumetric soil moisture divided by field capacity. Red lines are regression lines. The regression line in the middle is calculated only when relative soil moisture < 0.65. 21
- Figure 2.5 Time evolution of soil moisture (upper half) and leaf litter production (lower half) of both observation and simulations at TAP. (Top) standard (Bot) modified JSBACH. Dots: observation; Lines: simulations. 22
- Figure 2.6 Time evolution of soil moisture (upper half) and LAI (lower half) of both observation and simulations at CAX. (Top) The standard and (Bot) modified JSBACH. Dots: observation; Lines: simulations. 24
- Figure 2.7 Time evolution of soil moisture (upper half) and leaf litter production (lower half) of both observation and simulations at CAX. (Top) The standard and (Bot) modified JSBACH. Dots: observation; Lines: simulations. 25
- Figure 3.1 Cover fraction of the 11 Plant Functional Types in TRENDYv7. 34

- Figure 3.2 (Top and lower left) Precipitation between the end of the 21st century (2071–2085) and the 20th century (1971–2000). (Lower right) 1971–2000 averaged precipitation. Dots: All ensemble members agree on the sign of change. 38
- Figure 3.3 (a) Difference of soil moisture between 2071–2085 and 1971–2000 (m^3/m^3). (b) Difference of LAI because of difference in soil moisture in (a) during 2071–2085. (c) The seasonality of soil moisture of the historical and future (21sm-21L) experiments. The difference represents the direct effect. (d) The seasonality of LAI of 21sm-20L and 21sm-21L. The difference represents the LAI effect. Note the different scales of differences (the right y-axis) in (c) and (d). Dots: All ensemble members agree on the sign of change. The boxes in (a) and (b) indicate the Northern and Southern Amazon as defined in a study analyzing the precipitation of CMIP5 models over tropical South America (Yin et al., 2013). 39
- Figure 3.4 Evolution of (a) soil moisture and LAI (b) gross primary production (GPP) (c) autotrophic respiration (R_a)(d) NPP (e) soil respiration (R_s) (f) net ecosystem production (NEP) in the Amazon forests during the 21st century. Blue lines indicate 21sm-21L, which is the all-interactive simulation. Brown lines and green lines represent direct and LAI effects respectively. Dashed lines are linear regression lines and are shown only when $p < 0.05$. The region over which the area mean is taken is the boxes in Fig. 3.3. 40
- Figure 3.5 The direct and LAI effects on carbon budget components in the Amazon forests during 2071–2085. Bars represent ensemble means and whiskers represent range of ensemble members. R_a : Autotrophic respiration. R_s : Soil respiration. 42
- Figure 3.6 Comparison of NPP, soil respiration (R_s) and NEP due to the direct (brown) and LAI effects (green) during 2015–2030 and 2070–2085. Whiskers represent range of ensemble members. 42
- Figure 3.7 (a) The spatial pattern of the direct effect on NEP. (b) The spatial pattern of the LAI effect on NEP. Dots: All ensemble members agree on the sign of change. 43

- Figure 3.8 Evolution of (a) soil evaporation (b) transpiration (c) latent heat flux (d) low cloud cover (e) net surface solar radiation (f) surface temperature in the Amazon forests during the 21st century. Blue lines indicate 21sm-21L, which is the all-interactive reference simulation. Brown lines and green lines represent direct and LAI effects respectively. Dash lines are linear regression lines and are shown only when $p < 0.05$. The region over which the area mean is taken is the boxes in Fig. 3.3. Note the different scales of 21sm-21L (the right y-axis) and the drought effects (the left y-axis). 44
- Figure 3.9 The direct and LAI effects on energy budget in the Amazon forests during 2071–2085. Bars represent ensemble means and whiskers are ensemble ranges. Soil evap: Soil evaporation. Rsn: Net surface shortwave radiation. Precip: Precipitation. PET: potential evapotranspiration. Aridity: Aridity Index, calculated as the ratio between precipitation and PET. NA: Northern Amazon. SA: Southern Amazon. 46
- Figure 3.10 (a) Change in annual precipitation due to the direct effect during 2071–2085 (mm/day). (b) North-south cross section of wind and moisture field. Vector: (meridional wind, pressure velocity ($-10 \times \omega$)); contour: change in specific humidity; shading: specific humidity in the wet (21sm-20L) experiment. 47
- Figure 3.11 The comparison of the standard and modified JSBACH of the direct and LAI effects on carbon budget components in the Amazon forests during 2071–2085. Bars represent ensemble means and whiskers represent range of ensemble members. Ra: Autotrophic respiration. Rs: Soil respiration. The lower panel is the same as Fig. 3.5. 49

- Figure 3.12 The comparison of the standard and modified JSBACH of the direct and LAI effects on energy budget in the Amazon forests during 2071–2085. Bars represent ensemble means and whiskers are ensemble ranges. Soil evap: Soil evaporation. Rsn: Net surface shortwave radiation. Precip: Precipitation. PET: potential evapotranspiration. Aridity: Aridity Index, calculated as the ratio between precipitation and PET. NA: Northern Amazon. SA: Southern Amazon. The lower panel is the same as Fig. 3.9. 51
- Figure 4.1 Precipitation over the Amazon from 1852 to 2014 (top) and from 2015 to 2085 under RCP8.5 (bottom). Note that a positive trend exists for the historical period (1852–2014), but not for the future scenario. 62
- Figure 4.2 Comparisons of total vegetation carbon between the simulations of the (Top) spin-up and (Mid) historical period; (Bot) Comparisons of LAI between the simulations of the historical period. 63
- Figure 4.3 Comparisons between observation from Brienen et al., 2015 and the simulations. 64
- Figure 4.4 Comparisons of biomass map pattern from (a) observation (Saatchi et al., 2007), (b) STND, (c) LFSO, and (d) MORT. Note that the colorbars are different among figures. The black boxes indicate the Northern and Southern Amazon, and the red box is northwestern Amazon, as defined in Yin et al., 2013. 65
- Figure 4.5 Comparisons between models of (Upper) vegetation carbon and (Lower) net primary production (NPP). Note that MORT has a shifted y-axis as shown at the right hand side (red). 66
- Figure 4.6 Comparison of the difference in vegetation carbon between 2015 and 2085. (Left) STND (Mid) LFSO (Right) MORT. 66
- Figure A.1 Precipitation from the direct effect in (Upper) globally prescribed and (Lower) only South America prescribed experiments. 76
- Figure B.1 Climatic water deficit (CWD) accumulated with 12 months. The mortality data is from Brienen et al., 2015. X-axis: CWD; Y-axis: biomass mortality. 77

Figure B.2 (Upper) Soil moisture and (Lower) growth efficiency at both control (CTR) and drought (EXP) plots as simulated by the modified JSBACH. 78

LIST OF TABLES

Table 2.1	Summary of the Plant Functional Types (PFTs) in JSBACH and the respective phenological categories. 12
Table 2.2	Summary of symbols used in the standard JSBACH. See text for details. 14
Table 2.3	Summary of difference between standard and modified JSBACH. See text for details. 19
Table 2.4	Comparison between the standard and modified version of JSBACH at TAP, including simulated bias, differences of standard deviation (dSDev) between simulation and observation, centered root-mean-square deviation (CRMSD), and correlation coefficient with observation (CCoef). At the CTR plot, data from all years are used for calculation, while at the EXP plot, only data from the first 2 years are used. Values in bold indicates the respective model version performs better than its counterpart. Values in italic indicates the correlation is insignificant ($p > 0.1$). 23
Table 2.5	Comparison between the standard and modified version of JSBACH at CAX, including simulated bias, differences of standard deviation between simulation and observation (dSDev), CRMSD, and correlation coefficient with observation (CCoef). At the CTR plot, data from all years are used for calculation, while at the EXP plot, only data from the first 2 years are used. Values in bold indicates the respective model version performs better than its counterpart. Values in italic indicates the correlation is insignificant ($p > 0.1$). 26

Table 3.1	<p>Design of the coupled experiments. 21sm-21L (sm: soil moisture; L: LAI) is the reference experiment where both the soil moisture and LAI are interactive. In 20sm-20L the soil moisture is prescribed with the 1971–2000 climatology and the LAI is interactive. In 21sm-20L the soil moisture is prescribed from 21sm-21L and the LAI is prescribed from 20sm-20L. The difference between 21sm-20L and 20sm-20L reveals the direct effect of drought from soil moisture and stomatal closure alone. The difference between 21sm-21L and 21sm-20L reveals the LAI effect of drought from the LAI reduction due to drier soil. The experiments are run with both the standard and modified JSBACH. For each experiment five ensemble members are conducted with different initial date. 36</p>
Table 4.1	<p>Comparison between LFSD (leaf shedding version) and MORT (both leaf shedding and mortality) of JSBACH at TAP, including simulated bias, differences of standard deviation (dSDev) between simulation and observation, centered root-mean-square deviation (CRMSD), and correlation coefficient with observation (CCoef). At both CTR and EXP plot, data from all years are used for calculation. Values in bold indicates the respective model version performs better than its counterpart. Values in italic indicates the correlation is insignificant ($p > 0.1$). 61</p>

ACRONYMS

AGB	aboveground biomass
AMIP	Atmospheric Model Intercomparison Project
CAX	Caxiuanã National Forest
CWD	Climatic Water Deficit
CMIP	Coupled Model Intercomparison Project
CRMSD	centered root-mean-square deviation
DGVM	Dynamic Global Vegetation Model

ENSO	El Niño-Southern Oscillation
ESM	Earth System Model
ET	evapotranspiration
GHG	greenhouse gas
GLACE	Global Land-Atmosphere Coupling Experiment
GLACE-CMIP5	Global Land-Atmosphere Coupling Experiment–Coupled Model Intercomparison Project Phase 5
ILAMB	International Land Model Benchmarking
INDC	Intended Nationally Determined Contribution
MODIS	Moderate Resolution Imaging Spectroradiometer
MPI-ESM	Max Planck Institute Earth System Model
NPP	Net Primary Production
NSC	nonstructural carbohydrate
PET	Potential Evapotranspiration
PFT	Plant Functional Type
R_a	autotrophic respiration
R_s	soil respiration
REW	relative extractable water
SDTF	Seasonally Dry Tropical Forests
SIC	sea ice concentration
SLA	Specific Leaf Area
SST	sea surface temperature
TAP	Tapajós National Forest
TFE	Throughfall Exclusion Experiment
VPD	vapor pressure deficit

INTRODUCTION

1.1 THE DROUGHT-THREATENED AMAZON FORESTS UNDER THE CHANGING CLIMATE

The Amazon forests are the largest intact tropical forests in the world and account for 25% of the natural carbon sink in global forests (Pan et al., 2011; Friedlingstein et al., 2019). As nearly one third of emitted CO₂ is stored in land, the Amazon forests alone are able to play an important role in the carbon cycle. In fact, the intact forests in the Amazon are estimated to have mitigated the carbon emissions of the Amazonian countries (Phillips et al., 2017). Moreover, the Amazon is one of the most biodiverse ecosystems on Earth. Depending on different estimation methods, the Amazon has about 14,000 to 50,000 plant species, which are 4% – 13% of the world (Hubbell et al., 2008; Cardoso et al., 2017; Christenhusz and Byng, 2016). The importance of the Amazon forests is also manifested in, for instance, the Intended Nationally Determined Contribution (INDC) of Brazil¹, which aims to achieve zero illegal deforestation in Brazilian Amazonia² by 2030. In addition, tropical forests have been pointed out to have large potential for climate mitigation via reforestation (Busch et al., 2019). It is therefore crucial to enhance our understanding on the interaction between the Amazon forests and climate.

Importance of the Amazon forests

However, the Amazon forests, located in a warm and moist climate, will likely be subject to a drier climate and more meteorological droughts in the future. Meteorological drought is defined as a prolonged time with precipitation below average and is able to impact plants by limiting the soil moisture. It has been predicted that meteorological drought will become more frequent and prolonged in many places of the world, including the Amazon basin (e.g., Malhi et al., 2008; Joetzjer et al., 2013; Chadwick et al., 2015; Duffy et al., 2015; Cook et al., 2020). As the precipitation pattern in the Amazon basin is affected by the sea surface temperature (SST) of tropical Atlantic and El Niño-Southern Oscillation (ENSO), both of which will change under a warming climate, it is predicted that the annual mean precipitation will decrease, and the dry season will become longer (Ruiz-Vásquez et al., 2020). In addition, more extreme dry years are likely to hap-

More droughts in the Amazon under climate change

¹ The intended reductions in greenhouse gas emissions submitted by each country to the United Nations Framework Convention on Climate Change (UNFCCC).

² Brazilian Amazonia accounts for about 60% of the area of the Amazon rainforest.

pen. Due to the importance of the Amazon forests, it is desirable to understand how future drought will affect the Amazon forests.

*Responses of trees to
water shortage*

Generally, the responses of trees to water shortage contains several stages. On the short term, plants under drought conditions can save water by reducing transpiration through stomatal closure. Later, if low soil moisture persists, leaf shedding can also happen. If the water shortage continues without relief, tree death will eventually take place. However, tropical rainforests have been seen as more resilient to drought, such that the applicability of the theoretical framework to the Amazon forests remains unclear for several reasons. First, the rooting depth of trees in tropical rainforests is deeper, such that the trees are able to access water at deeper soil or reaching the water table. In addition, the number of tree species at stand-level can be much higher compared to other forest biomes. Vast differences in traits are found among tree species. For example, it has been shown that the hydraulic strategies of isohydric (stomata close rapidly during drought to maintain a minimum leaf water potential) and anisohydric (stomata remain open during drought, allowing leaf water potential to decrease) strategies exist as a continuum among species (Klein, 2014), which complicates the prediction of stomatal closure effect of the forests as a whole. Due to the complexity of tropical rainforests, observations and experiments directly obtained from the drought in the Amazon forests are required.

1.2 DROUGHT EFFECTS IN THE AMAZON FORESTS: WHAT HAVE WE LEARNED FROM THE OBSERVATIONS?

*Past droughts in
2005 and 2010*

Several drought events have taken place in the Amazonia since the beginning of the 21st century, including the years of 2005 and 2010. In both years, the drought can be attributed to the combination of El Niño and an anomalously warm tropical North Atlantic Ocean during the dry season (Marengo et al., 2008; Zeng et al., 2008; Lewis et al., 2011). The drought in 2005 was a 1-in-100-year event, with about 1.9 million km² of area having dry-season precipitation reduced for more than 1 standard deviation. The drought in 2010 was even more spatially extensive with multiple epicenters in north-central Bolivia, the Brazilian state of Mato Grosso, and also the southwestern Amazon as in 2005 (Lewis et al., 2011).

*Impacts from past
droughts*

From the two drought events in the Amazon forests, studies of both remote sensing-based and in-situ observations have found prominent effects. Satellite microwave observations showed that during the 2005 drought, the canopy structure and water content declined, and the decrease in canopy backscatter persisted for years (Saatchi et al., 2013). The forest structure measured by LiDAR waveforms before and after 2005 also showed a change in forest structure and a significant loss

of carbon (Yang et al., 2018). The 2010 drought has also been shown to have large impacts on carbon budgets. Atmospheric measurements have suggested that the Amazon was a carbon source of 0.5 PgC/yr, instead of the usual close-to-neutral during the 2010 drought (Gatti et al., 2014), with the emission from biomass burning being more than doubled during the drought (Laan-Luijckx et al., 2015). Ground-based observation on mortality and growth from an extensive forest plot network also showed that during the 2010 drought, the Amazon forest did not gain biomass. The net biomass impact was driven by both an increase in biomass mortality and a decline in biomass productivity (Feldpausch et al., 2016).

In addition to the observations and measurements on the past drought events, field-campaigns to simulate drought in the forests have also been conducted. These artificial rainfall reduction experiments can help us understand how trees react to drought at stand-level. At the same time, detailed information on soil and tree physiology are provided through intensive measurements to facilitate the investigation of mechanisms. It is shown that the LAI³ is decreased and leaf litter is increased at drought plots, where the precipitation levels are artificially reduced (Nepstad et al., 2002; Fisher et al., 2007). In the experiments, the tree mortality started to increase after two years, indicating a threshold of drought intensity for the tree mortality to increase.

Artificial drought experiments

1.3 THE GAPS BETWEEN OBSERVATIONS AND SIMULATIONS

Despite the abundant data from the observations, the simulation of forest drought response by current vegetation models has so far gained only limited success. The CMIP5 models have been shown to overestimate the responses of GPP and LAI to hydrological anomalies (Huang et al., 2016). When compared with observations from the artificial droughts experiments, only few models manage to capture the timing and magnitude of the responses including leaf shedding, changes in autotrophic respiration (R_a), and enhanced mortality (Powell et al., 2013; Joetzjer et al., 2014). Results from modeling studies also lack consistency. When the Amazonian response of productivity to climate change was evaluated with five vegetation models, although similar responses to warming have been found, the underlying mechanisms were different across the models (Rowland et al., 2015a). It has also been shown that soil moisture stress is a major source of carbon cycle uncertainty in the simulations of Earth System Models (ESMs), due to the overly-simplified representation of the vegetation drought response in the land surface models within ESMs (Trugman et al., 2018).

Limitations of models

³ Defined as one-sided leaf area per unit ground area.

The Global Land-Atmosphere Coupling Experiment–Coupled Model Intercomparison Project Phase 5 (GLACE-CMIP5) aims to quantify the influence of soil moisture on the climate and land-atmosphere interaction. It is a model intercomparison project of an ensemble of ESMs. By comparing results of the reference simulation and simulation with prescribed soil moisture at the historical level of climatology mean (1971–2000), the effect of soil moisture is quantified. The GLACE-CMIP5 experiments have been applied to investigate the future influences of soil moisture in terms of biogeophysical effects (e.g., Berg et al., 2016; May et al., 2017; Lorenz et al., 2016; Zhou et al., 2019) and biogeochemical effects of terrestrial carbon budget (Green et al., 2019). It has been shown that net biome productivity is reduced in the Amazon forests (Green et al., 2019). However, as the vegetation drought responses are not well simulated by the models, biases and uncertainties might exist in the results.

1.4 DROUGHT EFFECTS UNDER FUTURE CLIMATE

Under future climate, the task of predicting the drought responses of the Amazon forests and the impacts on land-atmosphere interactions is more complicated. From the atmospheric point of view, the future strength and patterns of circulation may be perturbed. For example, the Walker circulation has been shown to strengthen due to the warming climate (L’Heureux et al., 2013; McGregor et al., 2014; Barichivich et al., 2018), which affects the precipitation in the Amazon basin. With different circulation patterns, the future intensity and extent of water stress experienced by the Amazon forests may not be directly extrapolated from current seasonal and episodic droughts.

From the terrestrial point of view, despite the increasing water stress, an increasing trend of vegetation greenness, represented by increasing LAI, has been observed in many regions of the world since several decades (Zhu et al., 2016; Piao et al., 2020). The greening is largely due to higher atmospheric CO₂ concentration, which may increase the water use efficiency (the ratio of carbon uptake to water loss) and growth of plants. This may alleviate the negative effects from water stress, as suggested by experiments of artificial atmospheric CO₂ enrichment (Ainsworth and Long, 2004). However, the uncertainty due to greening is large. For example, in the high latitudes, current models do not agree on the magnitude of greening per CO₂ increase and the carbon uptake by plants (Winkler et al., 2019). The climate responses to greening has been shown to vary with regions, with warming in boreal region as the surface albedo is reduced, and cooling in arid regions as the evaporation is increased (Forzieri et al., 2017). Due to the contrasting mechanisms and the limited studies focusing on tropical forests, the biogeophysical effects of drought on the Amazon forests

and whether the Amazon remains as a carbon sink in the future are still unclear.

1.5 THESIS OVERVIEW

The overall aim of the thesis is to understand the impact of drought responses on the Amazon forests on land-atmosphere interactions under future climate. A modeling approach is adopted, and the key research tool is the land surface model JSBACH. The aim is addressed by answering the following research questions:

1.1 Is JSBACH able to capture the drought response in the Amazon?

1.2 If not, what are the missing processes in the model, and how to improve the model?

We answer the questions by assessing the capability of JSBACH to capture the drought response in the Amazon forests, which is characterized by the drought impacts on LAI and litter production. Model simulations are conducted and compared against the intensive observations from the rainfall reduction experiments in the Amazon forests (Nepstad et al., 2002; Fisher et al., 2007). Model modifications are implemented to improve the model. (Chapter 2)

2.1 What are the contributions of vegetation drought responses to the biogeochemical and biogeophysical drought effects under future climate?

2.2 How large is the uncertainty associated with the poor representation of vegetation response?

To answer the questions, we conduct land-atmosphere coupled experiments with Max Planck Institute Earth System Model (MPI-ESM) with JSBACH as the land component to simulate future climate under the RCP8.5 scenario. To disentangle the complex processes involved in the drought responses, we separate the climate responses to soil drying into (I) the effects of stomatal closure and reduced soil evaporation (the *direct effect*), and (II) the effects of enhanced leaf shedding due to soil drying (the *LAI effect*). To give an estimate on the uncertainty associated with different representations of leaf shedding and litter production, simulations of the standard and modified versions of JSBACH are conducted, and the partitioning of the direct and LAI effects are compared (Chapter 3).

3.1 Does an inclusion of drought mortality in JSBACH improve the model?

3.2 What are the impacts of drought-enhanced tree mortality on carbon budgets under future climate?

Currently, a drought-enhanced tree mortality does not exist in JSBACH. Therefore, we implement an empirical-based formulation based on available soil moisture of plants and evaluate the fidelity against the in-situ biomass measurement in the Amazon over the past decades. And then, we conduct experiments with the RCP8.5 scenario to investigate the effects of drought mortality on carbon budgets under future climate. (Chapter 4)

EVALUATING AND IMPROVING THE SIMULATED VEGETATION DROUGHT RESPONSES AT THE AMAZON FORESTS

2.1 INTRODUCTION

The responses of vegetation to drought can be characterized in several perspectives, including, but not limited to, the Leaf Area Index (LAI), the Gross Primary Production (GPP) or Net Primary Productinn (NPP) (e.g., Zhao and Running, 2010), and the vegetation indices of the Normalized Difference Vegetation Index (NDVI) or the Enhanced Vegetation Index (EVI) (e.g., Karnieli et al., 2010; Xu et al., 2011; Sruthi and Aslam, 2015; Lawal et al., 2019). However, NPP characterizes biogeochemical instead of biogeophysical effects, and large scale in-situ measurements of NPP are costly. And while the NDVI and EVI are able to provide information on the photosynthetic characteristics and leaf physiology, the relation to surface energy flux is only indirect. In addition, as the vegetation indices are remote-sensing based product and in-situ measurement is not operational, validation with site-level data is less feasible.

*Characterizing
vegetation drought
responses*

Therefore, in this chapter, we focus on the vegetation variable of LAI, with an eye on the relevance both biogeochemically and biogeophysically. A reduction in LAI will reduce transpiration, affecting albedo and roughness, which can in turn impact surface energy partition and wind speed. In fact, the control of LAI on global energy partition between the latent and sensible heat fluxes has been shown to increase with time (Forzieri et al., 2020). The LAI also affects how much carbon can be fixed in plants. It has been shown that LAI, along with leaf properties, drives the spatial and temporal variations of GPP across the Amazon forests (Flack-Prain et al., 2019). Additionally, we also characterize the drought response with the litter production, which is the amount of dead plant material falling to the ground, as the litter production is a good indicator of tropical forest function (Rowland et al., 2018). Part of the litter enters soil and other stays on the ground. The amount of litter entering soil will affect soil carbon and soil respiration, and the amount of litter staying on the ground will affect natural fire occurrence. In the both cases, litter production is able to influence carbon cycle.

*Importance of LAI
and litter production*

To evaluate the vegetation drought responses, observations on droughts are used. Several drought events have happened in the

*Limitations of
remote-sensing
products*

Amazon during the past decades. Observations on the Amazon forests during and after the drought has become possible due to the application of remote sensing in this region. However, remote sensing products still have some weaknesses in dense canopies such as in the tropical forests. For example, the measured LAI might be underestimated because of the saturation induced by the multi-story canopy structure (Turner et al., 1999; Tang et al., 2012). While remote sensing products of soil moisture is now also available, as data from passive microwaves represents only upper layer soil of top few centimeters, it is also less suitable for studying tropical forests, where the rooting depth of trees can be deep. An example of how difficult it is to study drought in the Amazon forests without enough in-situ data lies in the fact that contradictory conclusions have been shown for the impacts of the 2005 drought to the Amazon forests. While some studies have indicated a general greening because of less cloud cover and more solar radiation during the drought (e.g., Saleska et al., 2007), other studies have shown opposite results (e.g., Samanta et al., 2010, 2011). Furthermore, although the research focus of drought impacts on Amazon has been proposed to be the canopy physiological responses to drought and the changes in subcanopy fires during drought, the current remote sensing products nevertheless do not help much in resolving the issues (Asner and Alencar, 2010).

*Reasons to use data
from TFE
experiments*

For the purpose of evaluating and improving the model, intensive in-situ data from field campaign is therefore more desirable. Artificial rainfall reduction experiments have been conducted for different vegetations at different climate regimes (see e.g. Paschalis et al., 2020, for an overview). As for the rainfall reduction experiments done in forest biomes, it is usually the throughfall (rainfall penetrating the canopy) that is reduced, the experiments are also called Throughfall Exclusion (TFE) experiments in the literature. The TFE experiments in the Amazon forests are invaluable data to use as there are only very limited intensive observation on drought at the ecosystem level in tropical forests. Despite the fact that there are also other TFE experiments, they are either not conducted in tropical forests, or the spatial scales are too small. The results obtained from TFE experiments outside tropics may not be applicable to tropical forests, and the results obtained at smaller spatial scales might not represent the response at stand- and ecosystem-level. As JSBACH is usually run at global scale or coupled with atmospheric model, both at ecosystem scale, it is more relevant to capture the responses of forests at ecosystem level instead of at individual level.

Results from TAP

In one of the TFE experiment site at Tapajós National Forest (TAP), where the throughfall is excluded during the wet season, about 20% of LAI reduction was recorded (Nepstad et al., 2002). It was reported that after several years of experiment, the mortality increased the most among large trees, and the smallest stems were less responsive

(Nepstad et al., 2007). In a flux tower close to the TFE site, it was found that the carbon uptake by the canopy was largely controlled by phenology and light, with little influence from water limitation (Hutyra et al., 2007). The allocation of NPP was observed to change as well, with the aboveground NPP (wood and leaf production) shifted away from wood production (Brando et al., 2008). The allocation of carbon to foliage and roots were less affected (Davidson et al., 2008). One-dimensional soil water models have been used to simulate the soil water content (Belk et al., 2007; Markewitz et al., 2010). It is shown that large amount of hydraulic redistribution was not essential for accurately simulating the soil water content (Markewitz et al., 2010), although it has been shown to take place at this location (Rocha et al., 2004; Oliveira et al., 2005).

Another TFE experiment has been conducted at Caxiuanã National Forest (CAX), with the throughfall excluded not only for dry season, but for all year round (Fisher et al., 2007). While TAP did not have substantial drought stress in the first 2 years, the drought stress was larger in this site. The GPP declined by 13–14% and the transpiration declined for 30–40% (Fisher et al., 2007). It was found that the autotrophic respiration (R_a) from leaf and root was increased at the drought plot, with the source for consumption being the nonstructural carbohydrate (NSC). However, a clear response of NPP allocation was not found, indicating the possibility that the forest was adapting to drought in other ways (Metcalf et al., 2010). The results of tree mortality and aboveground biomass from the two TFE sites were consistent despite the fact that TAP and CAX are different in several aspects, suggesting that the vegetation drought responses in eastern Amazonian are similar (Costa et al., 2010). The photosynthetic capacity at the drought plot did not deviate much from the control plot, with the leaf dark respiration much increased (Rowland et al., 2015b). During the first 4 years of experiment, an initial shock response took place, where the reproductive litterfall (flowers and fruits) were largely declined and all litterfall were decoupled from the climate seasonality. After more than 10 years of drought, the litterfall is able to stabilize again, such that the reproductive litterfall was increased again and the relationships between litterfall and atmospheric variables were established (Rowland et al., 2018). The overall biomass loss due to increased mortality after year three is more than 40%. After more than 16 years of experiment, it is concluded that the long term response of drought cannot be extrapolated from short term response, as a long-term resilience with partial or full recovery of litterfall and allocation are shown (Meir et al., 2018).

In earlier development of land models such as the first-generation land surface schemes, the surface properties are fixed as parameters, including the LAI (Pitman, 2003). Recently, more and more models have started to simulate the LAI interactively. However, a mechanistic

Results from CAX

Previous effort to simulate leaf shedding

modeling of drought deciduousness has not been common. Theories have been proposed to explain the process of leaf shedding under plant water shortage. In the *hydraulic fuse* hypothesis, leaf shedding is proposed to slow water loss and protect the whole plant from losing too much hydraulic conductivity (Tyree et al., 1993). During droughts, the most peripheral plant organs (such as leaves) have the lowest water potential. If the vulnerability of leaves are not smaller than stems, then the leaves will cavitate before the stems, such that the water is kept in the stems and the stems can be protected from cavitation. It is predicted that the leaves will be shed or abscised. In this hypothesis, the leaves in effect function as a fuse to protect the whole plant from damage. The hydraulic fuse hypothesis has been applied to study the Seasonally Dry Tropical Forests (SDTF) in Panama. It was found that the leaf area was largely decreased when the critical level of transpiration rate above which the soil–plant conductance reaches zero was reduced below a threshold value. However, for some species, the leaf shedding does not stop water loss or loss in stem hydraulic conductivity, which is not in agreement with the hydraulic fuse hypothesis (Wolfe et al., 2016). On the other hand, using data from another SDTF in Costa Rica, the simulated LAI was shown to improve when a diversity of plant hydraulic traits was added to the model (Xu et al., 2016). Therefore, it is likely that the hydraulic fuse hypothesis is not able to explain the leaf shedding among different species and climates and it is also uncertain whether the results from SDTF is applicable to the less seasonal tropical forests in the Amazon.

*Importance to
evaluate and improve
JSBACH*

As the land component of MPI-ESM, the performance of JSBACH simulating important land properties is assessed in the International Land Model Benchmarking (ILAMB) project¹ (Collier et al., 2018). For the CMIP5 historical simulation, the MPI-ESM has a lower score of LAI in South America than over global land, indicating that the MPI-ESM is less capable of capturing leaf phenology in the Amazon compared with in rest of the world. The gap of the scores are not improved in the CMIP6 version of simulations, either. Meanwhile, many other models still have lower scores than the MPI-ESM, pointing to the fact that there is still room for improvement for current models simulating leaf phenology in the Amazon forests. As JSBACH contributes to several model comparison projects, including TRENDY (Sitch et al., 2015; Le Quéré et al., 2018) (as offline land model) and Coupled Model Intercomparison Projects (CMIPs) (as the land component of MPI-ESM), it is important to know the ability of JSBACH simulating drought responses in the Amazon forests. However, the ability of JSBACH simulating the vegetation drought responses of tropical rainforests has not been thoroughly investigated, and it was not included in the previous studies which evaluated the models against the TFE experiments (Powell et al., 2013; Joetzjer et al., 2014).

¹ Website: <https://www.ilamb.org>

To bridge the gap, in this chapter, we evaluate the LAI and litter production simulated by JSBACH against the observation from the TFE experiments in the Amazon. Based on the evaluation, we identify the weaknesses of the model and modify the model accordingly. The following sections present the evaluations and improvements.

2.2 METHODS

2.2.1 *The starting point: JSBACH v3.2 (FOM branch)*

The baseline model utilized in this thesis is the FOM² branch of the land surface model JSBACH v3.2 (hereafter *the standard JSBACH*). JSBACH is the land component of the MPI-ESM (Reick et al., 2013; Mauritsen et al., 2019). However, JSBACH can also be run alone in the offline mode with the meteorological data as forcing. Different vegetation land covers are represented in JSBACH as 11 Plant Functional Types (PFTs) (Table 2.1). Different PFTs have different parameters, and have different properties for including photosynthesis, phenology, and albedo. The plant photosynthesis is based on Farquhar model for C₃ plants and Collatz model for C₄ plants (Farquhar et al., 1980; Collatz et al., 1992). The carbon and nitrogen cycles of the terrestrial ecosystem can be simulated as interactive elements. The dynamical vegetation option can be switched on, such that the JSBACH functions as a Dynamic Global Vegetation Model (DGVM) to simulate the shift of land cover type (e.g. from forests to shrubs because of low water-availability). Disturbances to vegetation including wind-break and natural fire can also be switched on. There are different options of wood harvesting, in order to represent different practices of forests management. The soil physics consists of a five-layer scheme, with the deepest depth of about 10 m. Plants are able to take water from soil layers above the rooting depth. Although JSBACH does not explicitly include a groundwater component, the soil below the rooting depth can act as a reservoir to buffer the soil water.

*Description of
JSBACH*

In this study, the carbon cycle is interactive. The nitrogen cycle is switched off, in an effect that the plants are not limited by nutrients at all. For simplicity, we do not consider both types of disturbances. The dynamical vegetation is also switched off.

*Configuration used
in this study*

2.2.1.1 *Leaf dynamics*

The LAI is governed in JSBACH by the phenology module. The standard phenology module in JSBACH is LoGro-P, in which the leaf

² FOrrest Management

Table 2.1: Summary of the Plant Functional Types (PFTs) in JSBACH and the respective phenological categories.

PFT	phenological category
tropical evergreen	raingreen
tropical deciduous	raingreen
extra-tropical evergreen	evergreen
extra-tropical deciduous	summergreen
raingreen shrubs	raingreen
deciduous shrubs	summergreen
C ₃ grass	grass
C ₄ grass	grass
C ₃ pasture	grass
C ₄ pasture	grass
C ₃ /C ₄ crop	crop

dynamics is a combination of logistic growth and exponential decay³ and the growth of leaves is based on the following equation:

$$\frac{d\Lambda}{dt} = k\Lambda\left(1 - \frac{\Lambda}{\Lambda_{max}}\right) - p\Lambda \quad (2.1)$$

where Λ is LAI, Λ_{max} is the maximum LAI which can be supported by the plant, and k and p are the phenological parameters, representing the growth rate and shedding rate of leaves, respectively. In the FOM branch, instead of having fixed values for the maximum LAI (Λ_{max}), it is determined with the regrowth scheme, which considers the gradual growth of trees in the beginning of simulation or after wood harvesting (Naudts et al., manuscript in preparation, 2021). In the regrowth scheme, the maximum LAI is calculated by multiplying Specific Leaf Area (SLA) with leaf masses of individual trees, which is calculated by the allometric relationship with the biomass of individual trees. The biomass of individual trees are in turn calculated by dividing the total stand-level biomass with the number of trees in a stand, and the number of trees in a stand follows the self-thinning rule (Westoby, 1984).

The 11 PFTs are separated into five phenological categories (Table 2.1). According to the phenological categories, the conditions of how the phenological parameters k and p change are different. For example, for extra-tropical deciduous trees (*summergreen* phenology in JSBACH), the k and p values are switched to different sets during

³ Hence the name LoGro-P: Logistic Growth Phenology.

seasonal changes: When entering autumn, k is set to 0 and p is set to a large value, resulting in quick leaf shedding, and vice versa when entering spring. In the current study, we focus on the leaf phenology in the Amazon forests, which is predominately *raingreen* phenology in JSBACH.

The k and p for raingreen is determined as follows.

(I) When the relative soil moisture at root zone w is greater than the wilting point w_{wilt} and the Net Primary Production (NPP) is positive,

$$k = k_{growth}$$

$$p = p_{aging} + k_{growth} \begin{cases} 0, & \text{for } w_{crit} < w \\ \frac{w_{crit}-w}{w_{crit}-w_{wilt}} & \text{for } w_{wilt} < w < w_{crit}, \end{cases} \quad (2.2)$$

where the critical soil moisture w_{crit} is 0.65, w_{wilt} is 0.35, both in relative soil moisture, defined as soil moisture divided by field capacity. p_{aging} is 0.005 and k_{growth} is 0.08.

We note that because of the existence of the threshold w_{crit} , there is no difference in leaf growth whether the relative soil moisture is 0.65 or 1. Also the wilting point is universally set to 0.35, which does not consider local soil or vegetation properties.

(II) When w is less than w_{wilt} ,

$$k = 0$$

$$p = p_{dry}, \quad (2.3)$$

where $p_{dry} = 0.12$.

(III) When NPP is not positive, the LAI will not be updated.

2.2.1.2 Litter production

In JSBACH, the carbon stored in plants is divided into three pools: the green pool (C_G), the wood pool (C_W), and the reserve pool (C_R). The green pool is composed of leaves, as well as fine roots and vascular tissues; the wood pool contains woody material, and the reserve pool contains sugar and starches stored by the plants.

*Vegetation carbon
structure in
JSBACH*

Of the three vegetation carbon pools, the green pool is where the carbon of shed leaves is removed from. The size of the green pool is governed by the following equation:

$$\frac{dC_G}{dt} = NPP_{\triangleright G} - F_{litter} - F_{grazing}, \quad (2.4)$$

where C_G is green pool size, $NPP_{\triangleright G}$ is NPP allocating to green pool, F_{litter} is green litter (litter produced from leaves, fine roots and vascular tissues) and $F_{grazing}$ is carbon losses due to grazing. F_{litter} is given by the following equation:

$$F_{litter} = \frac{\gamma_G}{SLA} \max(r_{shed}\Lambda(t), -\frac{d\Lambda}{dt}), \quad (2.5)$$

where γ_G is the ratio of size of leaves to total green pool and assumed as a constant of 4; SLA is specific leaf area, and r_{shed} is the pre-defined inverse leaf longevity and is PFT-dependent.

We note that, in the standard JSBACH, litter is produced at the pre-defined aging rate multiplied by current LAI, unless the net LAI change is larger than the aging process. Therefore, in the standard JSBACH, leaf litter production is dependent only on current LAI or the net change of LAI, and is decoupled from the shedding rate used in phenology equation.

A summary of symbols used in the standard JSBACH is provided in Table 2.2.

Table 2.2: Summary of symbols used in the standard JSBACH. See text for details.

Symbol	Unit	Description
Λ	m^2/m^2	LAI
Λ_{max}	m^2/m^2	Maximum LAI which can be supported by the plant
k	1/day	LAI growth rate
p	1/day	LAI shedding rate
k_{growth}	1/day	Constant. LAI growth rate
p_{aging}	1/day	Constant. Component of LAI shedding rate due to aging
p_{dry}	1/day	Constant. LAI shedding rate when soil moisture is lower than wilting point
w	m^3/m^3	Soil moisture
w_{crit}	m^3/m^3	Critical soil moisture
w_{wilt}	m^3/m^3	Wilting point
C_G	$\text{mol(C)}/\text{m}^2$	Green pool size
$NPP_{\triangleright G}$	$\text{mol(C)}/\text{m}^2/\text{s}$	NPP allocated to green pool
F_{litter}	$\text{mol(C)}/\text{m}^2/\text{s}$	Green pool litter production rate
$F_{grazing}$	$\text{mol(C)}/\text{m}^2/\text{s}$	Green pool grazing rate
γ_G	—	Constant. Size ratio of total green pool to leaves
SLA	$\text{m}^2(\text{leaf})/\text{mol(C)}$	Specific leaf area
r_{shed}	1/day	Constant. A pre-defined inverse leaf longevity

2.2.2 Site description

To evaluate JSBACH, data from the two ecosystem-scale Throughfall Exclusion Experiments (TFEs) carried out in the eastern Amazon forests (Nepstad et al., 2002; Fisher et al., 2007) are used. The TFE experiments are composed of two 1-ha (100×100 m) plots: the controlled plot (CTR) and the experimental plot (EXP). At the EXP plot, the soil moisture is artificially reduced by deflecting away the throughfall (rainfall penetrating the canopy) with drainage structures installed 1–2 meters above the canopy floor. The two TFE sites are at TAP and CAX, both in Pará, Brazil (see Fig. 2.1 for their location in the Amazon). The design of the two TFE experiments are similar. The annual precipitation at both sites is 2000–2300 mm, with clear seasonality and wet season roughly between December and June. The soil at TAP is more clay-rich and deeper (60–80%; >100 m), and the soil at CAX is more sandier (70–83% sand) with a shallower water table at 15–20 m. At TAP, the experiment ran from 2000 to 2006, with the throughfall excluded only during the wet season. At CAX, the experiment started in 2001 and continued for at least 16 years, with the throughfall excluded all year round.

Comprehensive measurements were conducted at the sites at both CTR and EXP plots including LAI, soil moisture at different depth, diameter at breast height (which can be used to derive aboveground biomass (AGB)), and litter production from different parts of the trees.

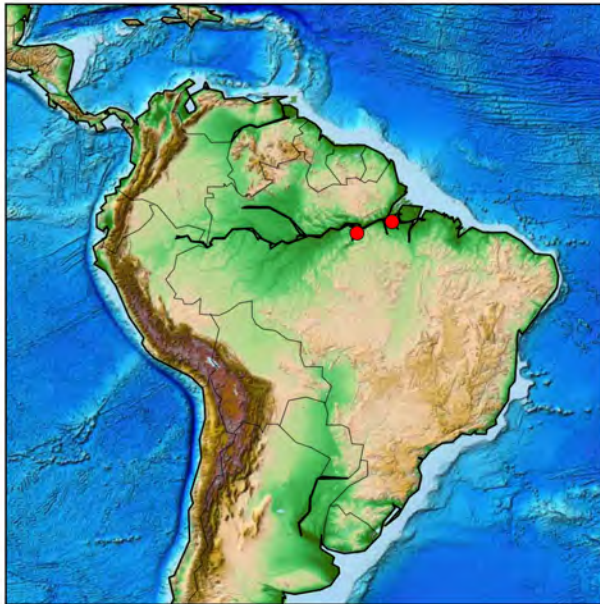


Figure 2.1: Location of the two throughfall exclusion experiments used in this study. Left: Tapajós National Forest (TAP); Right: Caxiuanã National Forest (CAX).

2.2.3 Model modifications and parameter tuning

As will be seen in Section 2.3, the standard JSBACH failed to reproduce the LAI and leaf litter production observed at the TFE experiment sites. To improve the model, several modifications are therefore implemented, which are mainly associated with the leaf dynamics and litter production (hereafter the *modified JSBACH*).

*Modification to leaf
phenology*

For the leaf dynamics, the three equations for different conditions are reduced to only one identical equation, which is also applied when w is less than w_{wilt} or NPP is not positive. The threshold for LAI to respond to water stress is removed through setting w_{crit} to 1. In the standard JSBACH, the wilting point w_{wilt} is assigned with a global invariant value. We replace it with a global map with spatial variation to incorporate soil and vegetation properties locally (Patterson, 1990). The growth rate k is now proportional to the NPP input to represent the carbon allocation to leaves. The shedding rate p is now decoupled from growth rate k and a new parameter p_{stress} is created to represent the component of shedding rate which is determined by water stress.

The following equations summarize the phenological parameters k and p in the new version:

$$\begin{aligned} k &= NPP \cdot k_{growth} \\ p &= p_{aging} + p_{stress} \begin{cases} \frac{w_{crit}-w}{w_{crit}-w_{wilt}}, & \text{for } w_{wilt} < w < w_{crit} = 1 \\ 1, & \text{for } w \leq w_{wilt} \end{cases} \end{aligned} \quad (2.6)$$

Plugging into the phenology formulation results in the following equation:

$$\frac{d\Lambda}{dt} = NPP \cdot k_{growth} \cdot \Lambda \left(1 - \frac{\Lambda}{\Lambda_{max}}\right) - \left[p_{aging} + p_{stress} \cdot \frac{1-w}{1-w_{wilt}}\right] \Lambda \quad (2.7)$$

All parameters in the modified model version are tuned against the observation at the TFE experiments to best reproduce the observed values. We choose the parameter set which gives the best results simulating LAI at EXP plot at TAP for the first two years of experiment.

The choice of TAP as the site for tuning is because concurrent comprehensive measurement of both soil moisture and LAI are only available at TAP (LAI was only measured every six months during the experiments at CAX). The usage of data only for the first two years (2000 and 2001) at EXP plot is because after two years, the effects of enhanced mortality have already manifested, which have affected the LAI and litter production (Brando et al., 2008). As a drought

dependent tree mortality has not been implemented in JSBACH, we do not tune the model against the data after two years⁴. There are three tunable parameters (k_{growth} , p_{aging} and p_{stress}), and we utilize the grid search method to optimize the parameters. In the grid search method, we exhaustively search through a reasonable range within the parameter space to find the best parameter. The parameters giving the smallest centered root-mean-square deviation (CRMSD) compared with observation is chosen, which is represented on the Taylor Diagram as having the least distance to the observation.

In the new formulation of phenology equation, there are three phenological parameters we need to decide: k_{growth} , p_{aging} , and p_{stress} . The searching range and step size of the grid search method is described below.

k_{growth} is $\{0.1, 0.3 \dots, 0.9\} \times 0.25$; p_{aging} and p_{stress} are both $\{1.0, 1.5, 2.0, 2.5 \dots, 4.5\} \times 10^{-3}$, meaning that a total of $5 \times 8 \times 8 = 320$ simulations are searched.

Fig. 2.2 is the Taylor Diagrams of observational and simulated LAI at EXP plot for the first two years. The parameters chosen accordingly is $k_{growth} = 0.125$, $p_{aging} = 1.0 \times 10^{-3}$, and $p_{stress} = 4.5 \times 10^{-3}$.

As for the production of leaf litter, since leaves are both growing and shedding simultaneously, the dependence of leaf litter production on net LAI change is replaced, and the litter production now accounts for directly the shed part of leaves. Besides, a new ratio of 2, representing the ratio of green litter to leaf litter, is updated (Girardin et al., 2016). The litter production now follows the equation:

$$F_{litter} = \frac{\gamma_G}{SLA} \cdot p\Lambda, \quad (2.8)$$

where γ_G is now 2, p is the shedding rate taken from the phenology model.

A summary of the modification to the model is provided in Table 2.3.

2.2.4 Simulation protocol

To compare JSBACH simulations with the observations made at the TFE sites, we conduct land-only simulations at site-level. Atmospheric forcing representing CTR and EXP plots are used to force the model.

At TAP, the 3-hourly meteorological data from the WATCH-WFDEI input data is used as forcing (Weedon et al., 2011; Weedon et al., 2014), with the precipitation, temperature, specific humidity, and wind

⁴ In this and the next chapter, the focus is on the effects of drought-induced leaf shedding. We will come back to the effects of enhanced tree mortality due to drought in Chapter 4.

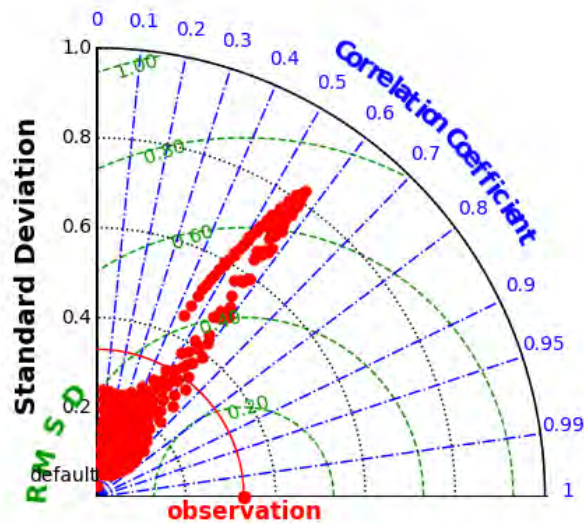


Figure 2.2: Taylor Diagrams of observational and simulated LAI at EXP plot for the first 2 years. The standard JSBACH is also shown on the diagram with the label "default".

speed replaced by the measurement from the nearby Km67 tower. The soil depth is set to 10 m, which is the deepest available in JSBACH, and the rooting depth is set to 3 m. Soil parameters are tuned to reproduce the observed soil moisture, which is as follows: The Clapp and Hornberger, 1978 exponent b is set to 1.15; the saturated hydraulic conductivity is 1.23×10^{-5} m/s; the saturated matrix potential is 0.533 m. The simulations cover from 2000 to 2006. One set of simulation is with the precipitation kept unchanged (CTR), and the other with the precipitation during wet season from January to June reduced to 50% of original value (EXP).

At CAX, all variables from the WATCH-WFDEI input data are used. The soil depth is also set to 10 m, while the rooting depth is set to 6 m. The soil physics parameters (Clapp and Hornberger, 1978 exponent b , saturated hydraulic conductivity, and saturated matrix potential) are the same as in TAP. The simulations period is from 2002 to 2007. As in the TFE experiment, the precipitation at EXP plot is reduced for all months.

2.3 RESULTS

The observed and simulated LAI and soil moisture at TAP are shown in Fig. 2.3. For the standard JSBACH, the simulated LAI shows several features which do not match the observations (Fig. 2.3, top). At the

Table 2.3: Summary of difference between standard and modified JSBACH. See text for details.

Symbol	Unit	Standard JSBACH	Modified JSBACH
w_{crit}	m^3/m^3	0.65	1
w_{wilt}	m^3/m^3	0.35	From a global map (Patterson, 1990)
k	1/day	Constant of 0.08	$NPP \times 0.125$
p_{aging}	1/day	Constant of 0.005	Constant of 0.001
p_{stress}	1/day	Constant. Coupled with k , which is 0.008	Decoupled from k . Constant of 0.0045
p_{dry}	1/day	Constant of 0.12	Not used.
F_{litter}	$\text{mol(C)}/m^2/s$	Proportional to current LAI or net change of LAI	Proportional to leaf shedding rate
γ_G	—	Constant of 4	Constant of 2
r_{shed}	1/day	Constant dependent on PFTs	Not used.

CTR plot, the simulated LAI remains at a constant value without any variability, except for the drastic decrease (about $3 \text{ m}^2/\text{m}^2$) during the end of 2002 and 2003, which both do not exist in observations. At the EXP plot, the simulated LAI is either at the same value as the CTR plot, or drops to a low value which is never observed during the experiment period (about $3 \text{ m}^2/\text{m}^2$; the lowest value at EXP plot in observation is about $4 \text{ m}^2/\text{m}^2$). At both CTR and EXP plots, a threshold behavior thus exists that the simulated LAI remains at the constant values until soil moisture is below a specific level (about $0.23 \text{ m}^3/\text{m}^3$). When below this level, LAI evolves with time, but the decrease and recovery are both much faster compared with the observations. The features are improved in the modified JSBACH (Fig. 2.3, bottom). The simulated LAI at both plots have now gentle variability. The response to drought at EXP plot is captured, with the correlation with the observation largely improved. The high biases at both plots are also reduced.

The improvement of the threshold behavior is clearly seen when we look at the relation between soil moisture and LAI. Fig. 2.4 shows the concurrent soil moisture and LAI at the EXP plot of the observation and simulation for the whole experimental period. In the observation, the soil moisture and LAI have a moderate linear correlation ($r = 0.519$). With a reduction of relative soil moisture from about 0.9 to 0.7, the LAI changes from about 5.5 to 4.5 (see figure caption for the calculation of relative soil moisture). In the standard JSBACH, the LAI does not change at all when relative soil moisture is above 0.65, and the slope of change when below 0.65 is also too high. The

Comparison of LAI

Relation between soil moisture and LAI

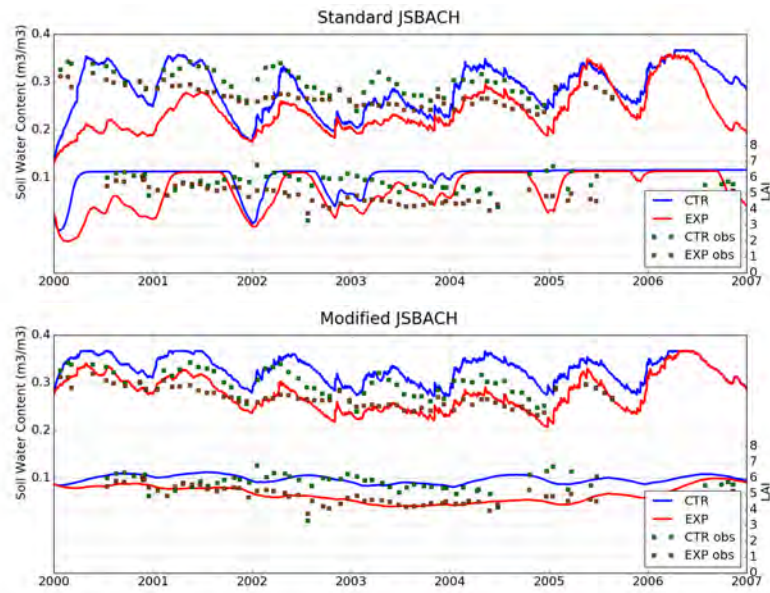


Figure 2.3: Time evolution of soil moisture (upper half) and LAI (lower half) of both observation and simulations at TAP. (Top) standard (Bot) modified JSBACH. Dots: observation; Lines: simulations.

linear correlation is also stronger than in the observation ($r = 0.831$), indicating a too-strong control of soil moisture on LAI. In the modified JSBACH, the threshold behavior is removed and the steep slope is improved. The linear correlation also reduces to a value closer to the observation ($r = 0.702$). While the linear correlation between observed soil moisture and LAI at EXP plot is moderate, the correlation of differences in LAI and soil moisture (ΔLAI and $\Delta(\text{soil moisture})$) between EXP and CTR plots is poor (not shown). This indicates that LAI is not a simple function of current soil moisture but also depends on other factors such as the NPP input. The inclusion of NPP input in determining LAI growth in the modified JSBACH thus helps explain the improvement.

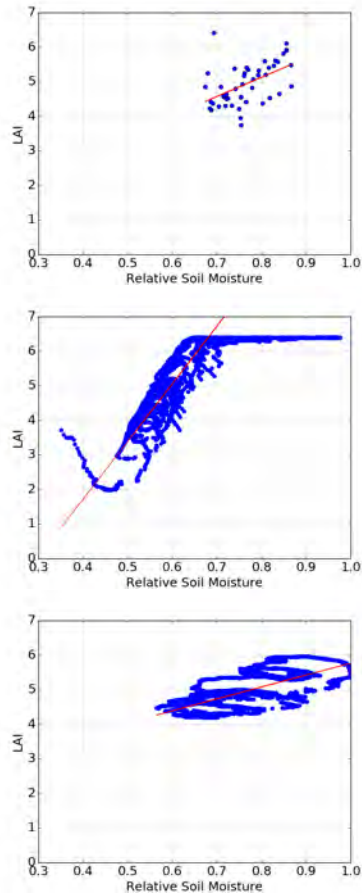


Figure 2.4: LAI versus relative soil moisture at the EXP plot at TAP. (Top) observation (slope = 5.53, $r = 0.519$) (Mid) standard JSBACH (slope = 16.7, $r = 0.831$) (Bot) modified JSBACH (slope = 3.45, $r = 0.702$). Relative soil moisture is calculated as volumetric soil moisture divided by field capacity. Red lines are regression lines. The regression line in the middle is calculated only when relative soil moisture < 0.65 .

The observed and simulated leaf litter production and soil moisture at TAP are shown in Fig. 2.5. As in the comparison of LAI, the standard JSBACH also simulates the leaf litter production with features not seen in the observation (Fig. 2.5, top). The production of leaf litter remains at low values close to zero for long stretches of time, with intermittent pulse-like jumps to high values. In comparison, the modified JSBACH simulates the leaf litter production with more appropriate magnitude and much less biases (Fig. 2.5, bottom). Although the magnitude and bias is much improved in the modified JSBACH, there is a time lag of about 90 days in leaf litter production.

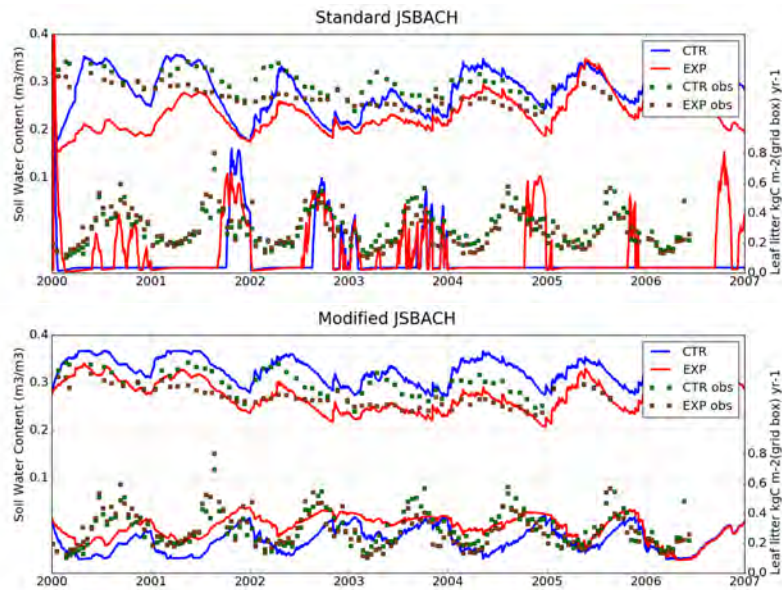


Figure 2.5: Time evolution of soil moisture (upper half) and leaf litter production (lower half) of both observation and simulations at TAP. (Top) standard (Bot) modified JSBACH. Dots: observation; Lines: simulations.

A comprehensive comparison of the ability of the standard and modified JSBACH to reproduce the observations at TAP is provided in Table 2.4 (note that the values at the EXP plot is only with data from the first 2 years to exclude the drought-enhanced mortality effects). For LAI, the improvement is apparent at the EXP plot, as the bias, variance and correlation are all much better for the modified JSBACH. Although the improvement is less prominent at the CTR plot (only the bias and CRMSD are better for the modified JSBACH), we note that it is more important to correctly simulate the drought response at the EXP plot than capturing the non-stressed LAI at the CTR plot within the context of understanding how the Amazon forests respond to future droughts. In addition, although our modification to JSBACH is without drought-enhanced tree mortality, the linear correlation between observation and simulation at EXP plot for all years is still high ($r = 0.720$), indicating that canopy-level leaf shedding is able to

explain about half of variance of the LAI reduction due to drought. For leaf litter production, the improvement is prominent at both CTR and EXP plots. With a lag of about 90 days, the modified JSBACH is able to reproduce the observation at both plots with high correlations, reduced biases and improved seasonal variability.

Table 2.4: Comparison between the standard and modified version of JSBACH at TAP, including simulated bias, differences of standard deviation (dSDev) between simulation and observation, centered root-mean-square deviation (CRMSD), and correlation coefficient with observation (CCoef). At the CTR plot, data from all years are used for calculation, while at the EXP plot, only data from the first 2 years are used. Values in bold indicates the respective model version performs better than its counterpart. Values in italic indicates the correlation is insignificant ($p > 0.1$).

Variable	Plot	Version	Bias	dSDev	CRMSD	CCoef
LAI	CTR	Standard	0.375	0.102	0.984	-0.273
		Modified	0.225	-0.299	0.628	<i>-0.015</i>
	EXP	Standard	-0.611	0.864	1.286	<i>-0.154</i>
		Modified	-0.070	-0.195	0.242	0.769
Leaf litter	CTR	Standard	-0.214	0.043	0.183	<i>0.124</i>
		Modified	-0.080^a	-0.031^a	0.087^a	0.655^a
	EXP	Standard	-0.181	0.063	0.230	<i>0.104</i>
		Modified	-0.035^a	-0.063^a	0.100^a	0.704^a

^acalculated with a lag of 90 days for the simulations

The phenology-related parameters in the modified JSBACH is tuned based on the observation at TAP. To test if the modified formulation and parameter are applicable to other sites in the Amazon forests, we carry out the same evaluation at CAX.

The observed and simulated LAI and soil moisture at CAX are shown in Fig. 2.6. Similar to TAP, the standard JSBACH simulates constant values of LAI at both CTR and EXP plots (Fig. 2.6, top; except for the ends of 2005 and 2006 at the EXP plot). Although measurements were carried out much less frequently at CAX than in TAP, the available observations are already enough to show that LAI is not constant during the experimental period. This is improved in the modified JSBACH (Fig. 2.6, bottom), which simulated gentle seasonal variability at both plots.

Shown in Fig. 2.7 is the observed and simulated leaf litter production and soil moisture at CAX. Also similar to TAP, the standard JSBACH simulates low leaf litter production most of the time at both CTR and EXP plots, with jumps to non-zero values only at the ends of dry seasons at the EXP plot (Fig. 2.7, top). In contrast, the modified JSBACH simulates the magnitudes and mean values correctly, despite

Comparison of LAI at CAX

Comparison of leaf litter production at CAX

also having a time lag of about 90 days to the observations (Fig. 2.7, bottom).

A comprehensive comparison of the ability of the standard and modified JSBACH to reproduce the observations at CAX is provided in Table 2.5. As in TAP, the modified JSBACH is able to reproduce the observed LAI and leaf litter production at both CTR and EXP plots. The evaluation at CAX shows that the improvement by the modified JSBACH at TAP applies also to the simulation at CAX.

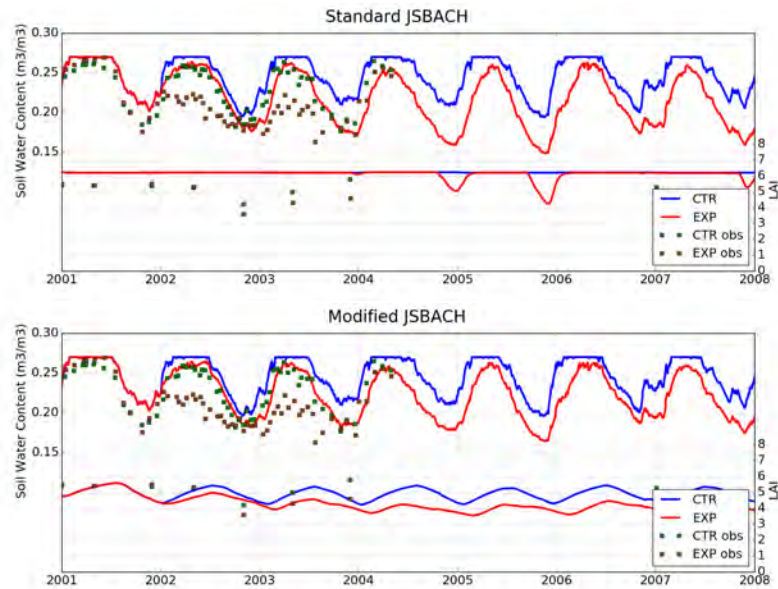


Figure 2.6: Time evolution of soil moisture (upper half) and LAI (lower half) of both observation and simulations at CAX. (Top) The standard and (Bot) modified JSBACH. Dots: observation; Lines: simulations.

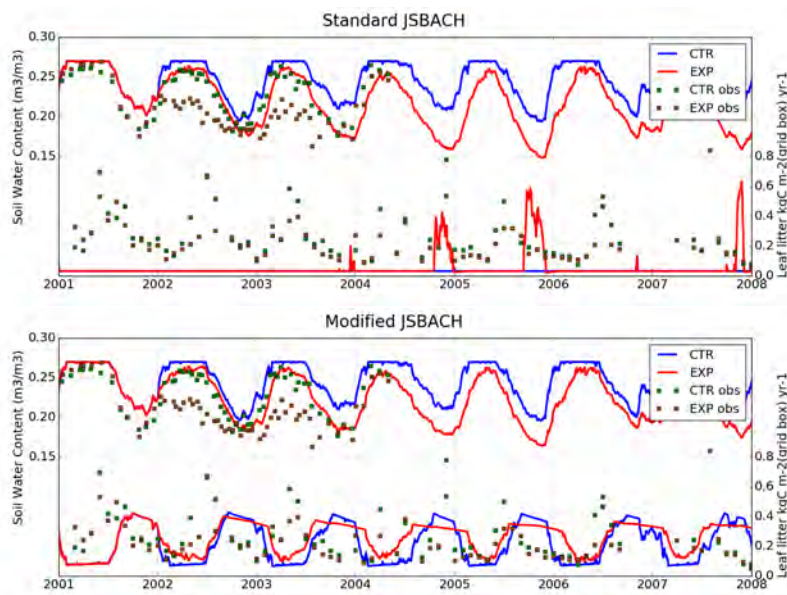


Figure 2.7: Time evolution of soil moisture (upper half) and leaf litter production (lower half) of both observation and simulations at CAX. (Top) The standard and (Bot) modified JSBACH. Dots: observation; Lines: simulations.

Table 2.5: Comparison between the standard and modified version of JSBACH at CAX, including simulated bias, differences of standard deviation between simulation and observation (dSDev), CRMSD, and correlation coefficient with observation (CCoef). At the CTR plot, data from all years are used for calculation, while at the EXP plot, only data from the first 2 years are used. Values in bold indicates the respective model version performs better than its counterpart. Values in italic indicates the correlation is insignificant ($p > 0.1$).

Variable	Plot	Version	Bias	dSDev	CRMSD	CCoef
LAI	CTR	Standard	0.987	-0.421	0.436	-0.177
		Modified	-0.404	-0.157	0.537	-0.098
	EXP	Standard	1.324	-0.668	0.681	0.088
		Modified	-0.269	-0.310	0.588	0.508
Leaf litter	CTR	Standard	-0.252	-0.323	0.328	-0.038
		Modified	-0.069^a	-0.195^a	0.322^a	0.243^a
	EXP	Standard	-0.287	-0.101	0.113	-0.005
		Modified	-0.087^a	-0.020^a	0.112^a	0.593^a

^acalculated with a lag of 90 days for the simulations

2.4 DISCUSSION

2.4.1 LAI

Previous studies have shown that current state-of-the-art models are unable to reproduce the response to drought in TFE experiments (Powell et al., 2013; Joetzjer et al., 2014). Our evaluation shows that the standard JSBACH is not an exception, as a threshold behavior exists in its simulation of LAI.

The threshold behavior simulated by the standard JSBACH consists of two parts: A constant LAI at the beginning, and a strong decline of LAI when the soil moisture is below a certain threshold. The constant LAI corresponds to the design in the standard JSBACH that, leaf growth is always the same when the relative soil moisture w is higher than 0.65, which is to simulate the low LAI seasonality of tropical evergreen trees compared to deciduous trees. However, from the observations at the CTR plot, it can be seen that there is still a slight seasonality (e.g., the annual range of CTR plot at TAP is larger than 2, which is more than 30% of the mean value; Fig. 2.3). Aside from rainfall seasonality, the reason of the LAI seasonality might include the seasonality in available solar radiation as well. Previous studies have also suggested leaf shedding as an acclimation strategy in response to

episodic drought. A constant LAI either throughout the year or under mild drought condition is therefore unrealistic.

On the other hand, a strong reduction in LAI following severe drought is also observed in the Amazon forests due to enhanced tree mortality. To maintain a stable LAI but still account for the drought stress, the standard JSBACH assumes a soil moisture threshold only below which LAI starts to reduce, and adds a strong dependence to soil water content. However, in the standard JSBACH, the LAI response to drought is too strong, and since the enhanced tree mortality is mechanistically different from the leaf shedding, the effects of the two should not be simulated at canopy-level with the same formulation.

Although the overall drought responses of forests may include enhanced tree mortality in severe conditions, by enabling JSBACH to simulate the mild LAI reduction within annual time scale and under mild drought, we can constraint the canopy-level responses of the Amazon forests to future droughts. The prediction of the overall responses to future droughts will also be facilitated when the enhanced tree mortality due to drought is included⁵. It is noteworthy that the linear correlation of simulated and observed LAI during the whole experimental period is not vastly lower than the first two years, indicating that the modified JSBACH is already able to reproduce large portion of the LAI variability despite lacking an implementation of enhanced mortality.

2.4.2 Leaf litter production

Similar to LAI, current vegetation models simulated litter flux with a large spread and are not able to reproduce the results at TFE sites well (Powell et al., 2013). The standard JSBACH simulates the litter flux at both TAP and CAX with negative biases. The annual-mean biases and variance are largely improved in the modified JSBACH although the parameter are not tuned against observations on litter flux, which indicates the fidelity of the modified formulation. However, the seasonality is still simulated with a 90-day lag. There are several candidates for the reason of the 90-day lag. While we assume the leaf shedding rate to depend solely on soil moisture, water stress is perceived by plants as insufficient soil water supply to the vapor pressure deficit, which represents atmospheric water demand and therefore involves both land and atmosphere conditions. Previous studies have also indicated that leaf demography (e.g., explicit representation of leaf ages, which is currently not represented in JSBACH) and the synchronization of leaf flushing and leaf litter production play important roles in simu-

⁵ See Chapter 4 for an estimate of the overall drought effects including drought mortality in the Amazon.

lating carbon flux seasonality in the Amazon forests (Wu et al., 2016; Manoli et al., 2018). However, as leaf demography has less impact on water and energy fluxes (Manoli et al., 2018), and we are currently more interested in the impacts of droughts on mean-state climate, we therefore leave the issue of leaf litter seasonality for future exploration.

2.4.3 *Implications for future model development*

The logistic equation in the formulation in the standard JSBACH aims to represent the common characteristics of plants that there is a physiological limit for number of leaves that a plant can grow. The limit might be rooted from the number of leaf buds grown in previous season, or the limited transport capacity of sapwoods. The logistic equation has been shown to be successful in simulating seasonal shift in temperate vegetation (see e.g., Dalmonech et al., 2015). Therefore, for the consistency of the modeled physiology, while we aim to modify the phenology for tropical forests, we opt to implement our modification within the current framework of the logistic equation.

A mechanistic formulation of leaf shedding requires detailed plant hydraulics. We note that JSBACH is an ecosystem-level vegetation model which is frequently used in a setup to represent the average condition of vegetation across a spatial scale of ~ 200 km. The large scale means that in tropical forests, the various species in the ecosystem is aggregated into just one PFT with one LAI value⁶. Therefore, plant hydraulics might also not be able to capture the hydraulic behavior of the tropical forest. Due to the insufficiency of soil and vegetation data at high resolution and the limitation of computational resources, coupled simulation of high-resolution at long-term time scale for future scenario is still not feasible. It is thus reasonable to utilize a data-driven method to tune the JSBACH with the intensive data from TFE experiment despite the lower complexity.

On the other hand, the LAI dynamics also depends on carbon allocation to leaves. For example, in energy limited region such as the tropical forests, the seasonality of LAI as well as productivity responds not only to water stress, but also to the input of photosynthetically active radiation. In this study, we account for the carbon allocation with the NPP input to leaf. However, we note that in JSBACH, the ratio of NPP allocation to different pools is fixed regardless of water stress. This might be a source of uncertainty as some studies have suggested that a shift in carbon allocation as a strategy against water stress⁷. However, as the behavior may not be universal, we leave the

⁶ While there are 11 PFTs in the JSBACH, there is only one representing tropical evergreen forest.

⁷ For example, more investment to roots and a reduction to leaves under water stress, in order to maximize water uptake and reduce transpiration.

issue for future exploration when more abundant in-situ measurement and understanding on related tree physiology is available.

2.5 CONCLUSIONS

In this chapter, we first present the evaluation on the ability of the land surface model JSBACH to capture the drought responses of LAI and leaf litter production at the two TFE (throughfall exclusion) experiments sites in the eastern Amazon forests. The evaluation shows that the drought responses of the standard JSBACH has a unrealistic threshold behavior. The threshold behavior consists of two part: A constant LAI with no response to reduction in soil moisture, and a too-sharp decrease in LAI when soil moisture is below a threshold. While under current climate, the biases caused by this threshold might be mild, due to the fact that the water stress will be larger under future climate, the threshold will be crossed more frequently and the LAI response to drought will likely to be overestimated.

To address the issue, several modifications are implemented to the model. A dependence on the NPP input to leaf is added to the leaf growth rate to account for the carbon allocated to leaves. The leaf shedding rate is separated into two components to represent the aging and water stress respectively. Litter production is now coupled with the shedding rate of the leaves. All phenological parameters are tuned against the LAI observations at the TFE experiments site at Tapajós National Forest (TAP).

The modified JSBACH improves the simulation of the LAI. Most notably, the LAI at EXP plot is simulated with much reduced bias, closer variability and better correlation ($r = 0.769$) to the observation. The litter production is also improved. At the EXP plot, the bias is reduced and the correlation is high ($r = 0.704$) when a lagged correlation of 30 days is applied. As studies have shown that the tree mortality has increased after two years of throughfall exclusion, we tune the model against only the LAI from the first two years. Nevertheless, the simulated LAI after two years does not deviate from the observation much. The linear correlation between observation and simulation at EXP plot for the whole experimental period is high, indicating that about half of the variance of the LAI reduction due to drought can be explained by the canopy-level leaf shedding.

Finally, the same analysis is conducted at another independent TFE experiment site at Caxiuanã National Forest (CAX). We show that the improvement applies not only to TAP, but also to CAX, which indicates the fidelity of the modified JSBACH.

SEPARATING THE DIRECT AND LAI EFFECTS OF DROUGHT UNDER FUTURE CLIMATE

3.1 INTRODUCTION

Soil moisture and climate have been known to couple together, with different coupling strength at different regions being identified in the Global Land-Atmosphere Coupling Experiment (GLACE) project (Koster et al., 2004). It was shown that, with better understanding of the soil moisture, the seasonal forecast of precipitation can be improved. Under the framework, the soil moisture should not be viewed as merely the boundary condition of the atmosphere, but as an interactive component of the climate system. Inspired by the GLACE project, the GLACE-CMIP5 provided a framework to quantify the impacts of soil moisture-climate coupling on future climate in CMIP5 simulations, with a focus on long-term (decadal) instead of seasonal or intraseasonal time scale. As for many regions of the world as well as the global mean, the soil is drier in the future, results from GLACE-CMIP5 can be used to investigate the drought effects under future climate.

In the GLACE-CMIP5 experiments, the effects of soil moisture on climate are given by comparing the reference simulation (with future climate forcing and interactive soil moisture) and simulation with future climate but prescribed historical soil moisture (1971–2000). It has been shown that drought has strong and consistent effects of increasing temperature (Seneviratne et al., 2013). Not only the mean temperature is linked to soil moisture, but also the temperature extremes increase due to projected soil moisture decrease (Lorenz et al., 2016). The experiments have also been used to study the effect of land-atmosphere interaction on aridity. In contrast to soil moisture, the aridity considers both the evaporative demand from the atmosphere and the water supply at the land surface, and is seen as more relevant for natural and societal systems. The aridity has been found to increase in a warming world. While previous studies have focused on the contribution from the oceanic warming and associated atmospheric processes, it was shown that the land also plays an important role as the land-atmosphere feedbacks can substantially amplify the global land aridity under global warming (Berg et al., 2016). A strong negative coupling between soil moisture and aridity was also found to occur

*BGP effects in
GLACE-CMIP5*

globally, in which the feedback of soil on the atmosphere is largely responsible (Zhou et al., 2019).

*BGC effects in
GLACE-CMIP5*

The biogeochemical effects of soil moisture deficit have also been studied with the GLACE-CMIP5 experiments. It has been shown that soil moisture contributes to reduction of the net biome productivity (NBP) under future climate¹. The reduction of NBP due to soil moisture is about the same magnitude as the land sink (NBP) itself. As both the annual mean and seasonal variability of soil moisture are different between the future and historical period (1971–2000), the contributions from the trend and seasonal variability were also assessed, with the both being of similar magnitudes. However, the importance of the soil moisture trend will become more important than the seasonal variability by the end of the 21st century (Green et al., 2019).

*Vegetation responses
are also important*

The climate impacts of droughts and heatwaves result not only from soil moisture deficit, but also from vegetation responses. Previous study on European spring and summer climate found that the effect of a drastic LAI change on mean temperature is about 25% the magnitude of the effect from soil moisture changes. In the heatwave of 2003 and 2007, a decrease in LAI can amplify the heatwave by 0.5K for daily maximum temperature, which is about half of the magnitude from soil moisture effect (Lorenz et al., 2013). Another study has been done on the extreme drought and heatwave of central and northern Europe in 2018. In this year, the spring was extremely warm and brightening but the precipitation deficit was only moderate. However, the summer drought was extreme. It was shown that the vegetation played an important role, as the spring condition stimulated the vegetation growth, which in turn contributed to soil water depletion and amplified the summer drought (Bastos et al., 2020). Therefore, considering its impacts on both biogeochemical and biogeophysical effects, the vegetation drought responses of the Amazon forests should be better quantified.

*Multiple scales of
vegetation drought
responses*

To quantify the vegetation drought responses of the Amazon forests, it is crucial to understand the effects of drought on forests. The drought effects on forests are multi scales, from stomatal closure at the leaf-level to leaf shedding at the canopy-level, and then to enhanced tree mortality at the stand-level. Previous studies including GLACE-CMIP5 have utilized models to study the drought effects of forest ecosystems. However, it has been pointed out that current models are not able to capture vegetation drought responses. Uncertainties therefore exist in the modeling results from previous studies, as their results mostly contain the combined drought effects at different scales. Sometimes, in a specific model, it is not clear at which levels are the drought effects included. For example, most models do not have a drought-

¹ Note that in contrast to the definition in the Global Carbon Budget, the NBP in this study includes the emission from land use and land cover change.

enhanced mortality, but the climate responses simulated by models are nevertheless indicated as drought effects. The insights from comparing results of different models are therefore diminished, as the model complexities are different.

To address this issue, in this chapter, we explicitly separate the drought effects at different scales, which has not been done before. Here, the *direct effect* of drought is defined as the effect induced by soil drying and stomatal closure. The *LAI effect* is defined as the effect induced by leaf shedding (LAI reduction). With the improved JSBACH, the direct and LAI effects are separated and their relative contributions to biogeochemical and biogeophysical effects under future climate are quantified. The uncertainty associated with LAI formulation and litter production is investigated by comparing the simulated future climate using MPI-ESM with the standard JSBACH and modified JSBACH as the land surface model. Furthermore, the uncertainty associated with the internal variability is given by a series of experiments consist of five ensemble members.

3.2 METHODS

3.2.1 Model configuration

To investigate the climatic effects of the Amazon forests to future drought, the atmospheric as well as terrestrial states should be considered together instead of only the land surface. Therefore, we conduct a series of land-atmosphere coupled simulations, where the JSBACH is coupled with the atmospheric general circulation model ECHAM (or equivalently, the MPI-ESM is run in an Atmospheric Model Inter-comparison Project (AMIP)-type configuration). The simulations is run globally and the spatial resolution is T63 (ca. 200 km).

In the AMIP-type configuration, the SST and sea ice concentration (SIC) are prescribed as the boundary condition. The SST and SIC are calculated by combining the trend during the 21st century under RCP8.5 scenario simulated by MPI-ESM (Mauritsen et al., 2019) and the spatial pattern from HadISST (Rayner et al., 2003). As we focus on the response of intact forests, anthropogenic land use and land cover change is not considered. The land use and land cover map is taken from 2010 of TRENDY simulation by JSBACH (Sitch et al., 2015; Le Quéré et al., 2018). The distributions of PFTs are shown in Fig. 3.1. As can be seen, most of the vegetation in the Amazon is tropical evergreen, with a small portion being raingreen shrubs (over eastern Brazil). Both of the PFTs belong to the raingreen phenology in JSBACH.

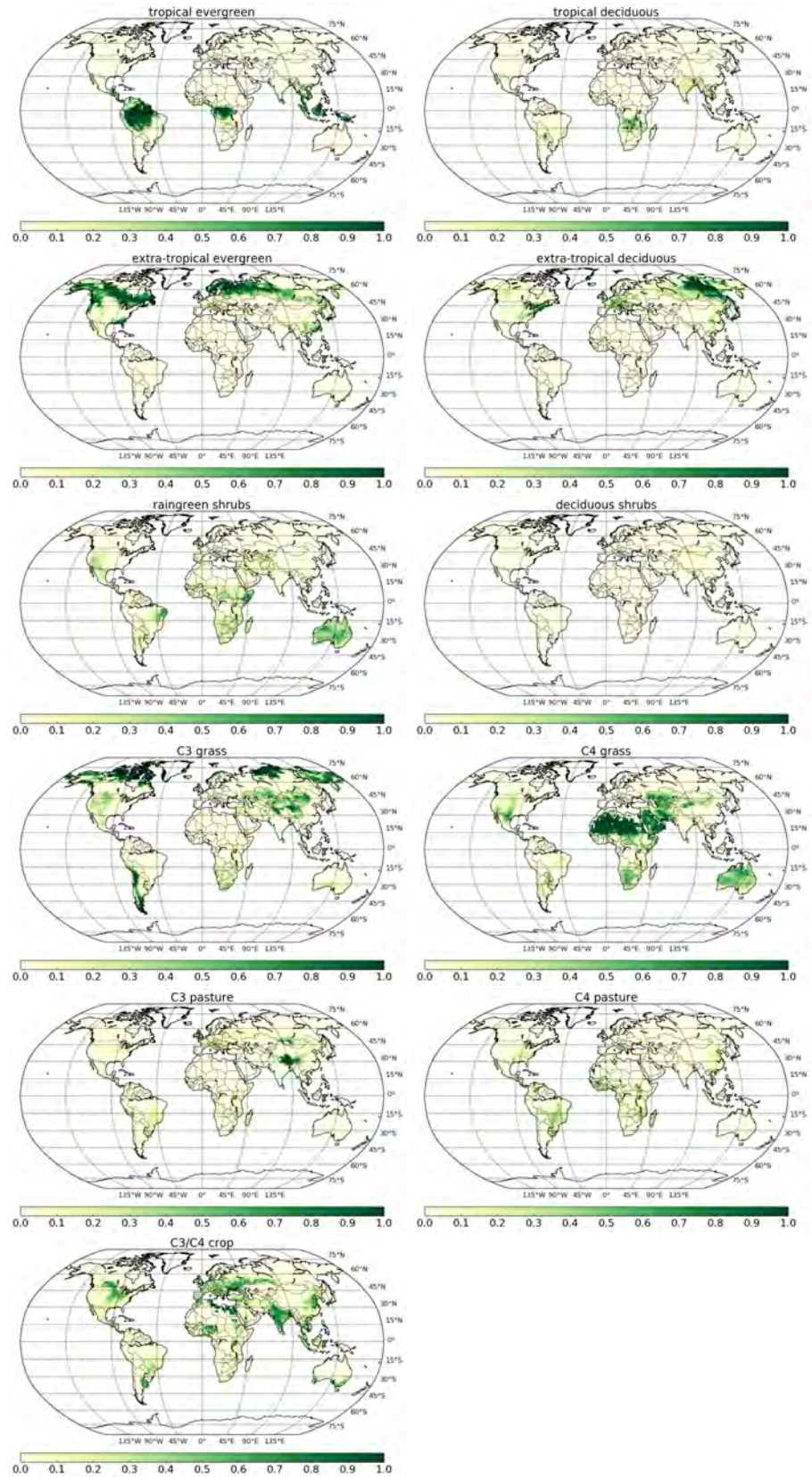


Figure 3.1: Cover fraction of the 11 Plant Functional Types in TRENDYv7.

3.2.2 Simulations

With the configuration and boundary conditions described above, the model is run with pre-industrial forcing for several hundred years, until the global soil carbon reaches equilibrium². After reaching equilibrium, the simulation is run with historical forcing from 1850 to 2014. And then, the reference simulation (21sm-21L; 21st-century-soil-moisture-21st-century-LAI) starts from 2015, with the business-as-usual RCP8.5 scenario as the greenhouse gas (GHG) forcing, and both soil moisture and LAI are interactive. Since the LAI is regulated both by soil moisture (which is expected to be lower in the future) and available carbon allocated to the leaves (which due to future higher CO₂ concentration, is higher in the future), the LAI in 21sm-21L includes the effects of both future GHG forcing and future water stress. In the first experimental simulation (20sm-20L; 20th-century-soil-moisture-20th-century-LAI), the soil moisture is prescribed according to the daily climatology from the historical simulation during 1971–2000, and the LAI is still interactive. The LAI in 20sm-20L therefore considers only future GHG forcing, but not the effects from future soil drying. Finally, in the second experimental simulation (21sm20L; 21st-century-soil-moisture-20th-century-LAI), the soil moisture is prescribed from 21sm-21L, and the LAI is prescribed from 20sm-20L. As the LAI in 21sm-20L is identical to 20sm-20L, the LAI considers only the effect of future GHG forcing but not future soil drying.

To separate the direct effect (soil drying and stomatal closure) and the LAI effect (LAI reduction), we compare the results between different simulations. The comparison between 21sm-20L and 20sm-20L gives the direct effect, as the only difference is the soil drying due to future GHG forcing. Similarly, the comparison between 21sm-21L and 21sm-20L gives the LAI effect, as the only difference is the LAI reduction due to future soil drying. Note that, as in all simulations the GHG forcing is identical (RCP8.5), taking differences between the simulations therefore cancel out the warming and other climatic effects from GHG forcing.

The simulations are conducted with the land surface model as both the standard and modified JSBACH. For both versions, simulations of five ensemble members are conducted. The different ensemble members are produced by starting the historical simulation from different days of the pre-industrial simulations.

A summary of the experiment design is provided in Table 3.1.

² In the absence of an interactive ocean, the humus in soil carbon is the component which needs the longest time to reach equilibrium.

Table 3.1: Design of the coupled experiments. 21sm-21L (sm: soil moisture; L: LAI) is the reference experiment where both the soil moisture and LAI are interactive. In 20sm-20L the soil moisture is prescribed with the 1971–2000 climatology and the LAI is interactive. In 21sm-20L the soil moisture is prescribed from 21sm-21L and the LAI is prescribed from 20sm-20L. The difference between 21sm-20L and 20sm-20L reveals the direct effect of drought from soil moisture and stomatal closure alone. The difference between 21sm-21L and 21sm-20L reveals the LAI effect of drought from the LAI reduction due to drier soil. The experiments are run with both the standard and modified JSBACH. For each experiment five ensemble members are conducted with different initial date.

Experiment name	GHG forcing	Soil moisture	LAI	LAI response to future GHG forcing	LAI response to future water stress
21sm-21L	RCP8.5	Interactive	Interactive	Yes	Yes
20sm-20L	RCP8.5	1971–2000 climatology	Interactive	Yes	
21sm-20L	RCP8.5	Prescribed from 21sm-21L	Prescribed from 20sm-20L	Yes	

3.3 RESULTS

By comparing the results from the different experiments as described in Section 3.2, the components of drought effects are isolated. In the following sections, the climatic effects caused solely by soil drying and stomatal responses of plants are referred to as the *direct effect*, whereas such caused by the reduction of LAI because of drier soil are termed the *LAI effect*. The *drought effects* then indicate the sum of the two effects.

3.3.1 Future decline of precipitation simulated by MPI-ESM

Before diving into the separated drought effects, we first look at how future climate is simulated by the MPI-ESM, with the focus on the precipitation changes.

The difference in precipitation between the end of the 21st century (2071–2085) and the 20th century (1971–2000) simulated by MPI-ESM is shown in Fig. 3.2. We note that the region with prominent reduction in precipitation is in central and southern North America, northeastern South America, South Africa, coastal West Africa and Europe. There is also an increase in precipitation in several regions, including central Africa, South Asia, Southeast Asia, and much of higher latitudes. The spatial patterns are generally in accordance with the CMIP6 multi-model mean (Cook et al., 2020, Fig. 9). When looking into South America (Fig. 3.2, lower panel), while the CMIP6 multi-model mean is a consistent reduction over the Amazon basin, MPI-ESM simulates a more prominent reduction over northeastern South America (Venezuela, the Guianas³, and northern Brazil; compare Fig. 3.2 lower left and right). In addition, a stripe pattern exists in parallel with the Andes, such that there are regions of precipitation increase in between the regions of decrease. The stripe pattern is likely due to the topography, as the Andes is in some regions higher than 4 km in elevation and affects the distribution of water vapor imported from the tropical Atlantic.

The spatial pattern and seasonality of the associated direct and LAI effects of drought during 2071–2084 are shown in Fig. 3.3. The spatial patterns of the direct and LAI effects are similar to the reduction in precipitation, with the strongest magnitude being over northeastern Amazon and a stripe pattern parallel to the Andes over the Southern Amazon (Fig. 3.3ab). The soil drying prevails all year round and is most severe during the dry season, in effect prolonging the dry season (Fig. 3.3c). When averaged annually, the magnitude of soil drying is 6% of the 1971–2000 value. The contrast between dry and wet season is

Spatial patterns of drought effects

³ Including French Guiana, Guyana, and Suriname

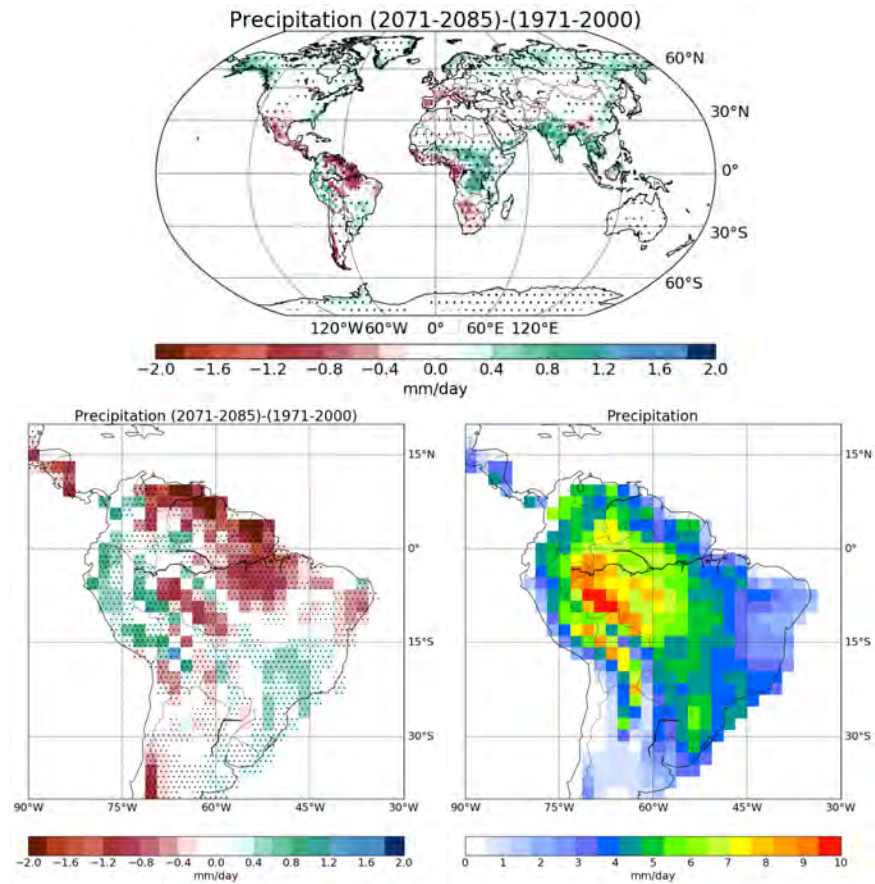


Figure 3.2: (Top and lower left) Precipitation between the end of the 21st century (2071–2085) and the 20th century (1971–2000). (Lower right) 1971–2000 averaged precipitation. Dots: All ensemble members agree on the sign of change.

also larger, with the annual range being 15% larger than in 1971–2000. The resultant annual mean LAI reduction is of similar magnitude (7%), and with a lag of a month after the soil drying (Fig. 3.3d). Therefore, under future climate, not only the mean state of soil is drier, but also the annual range is larger. The soil drying induces a LAI reduction of similar magnitude with a lag of approximately one month.

3.3.2 Biogeochemical effects: The carbon budgets

As a prominent reduction in precipitation as well as soil drying and LAI reduction are found in large parts of South America by the end of the 21st century, in this section we look at the how the carbon budgets at the Amazon forests evolve during the 21st century, and the contribution of the direct and LAI effects respectively.

Fig. 3.4 shows the 21st-century-evolution of carbon budgets of the Amazon forests as simulated in 21sm-21L (the reference simulation).

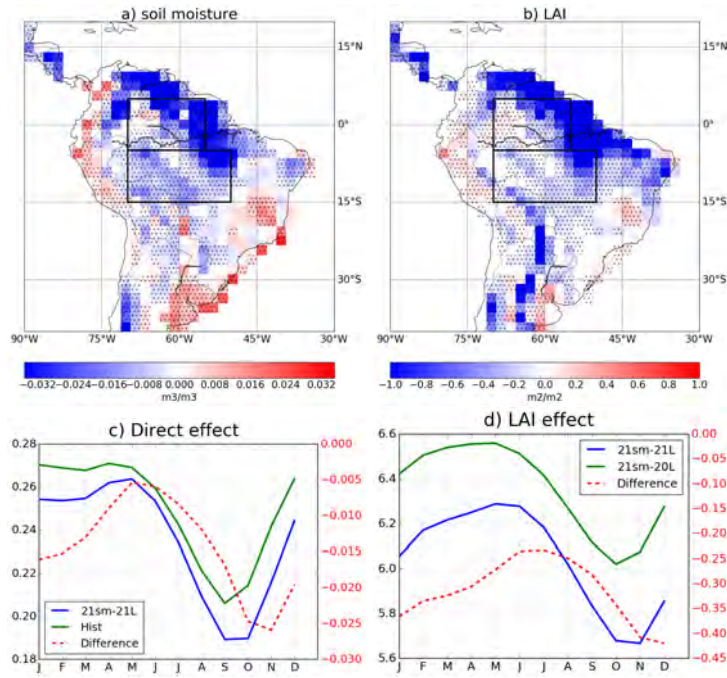


Figure 3.3: (a) Difference of soil moisture between 2071–2085 and 1971–2000 (m^3/m^3). (b) Difference of LAI because of difference in soil moisture in (a) during 2071–2085. (c) The seasonality of soil moisture of the historical and future (21sm-21L) experiments. The difference represents the direct effect. (d) The seasonality of LAI of 21sm-20L and 21sm-21L. The difference represents the LAI effect. Note the different scales of differences (the right y-axis) in (c) and (d). Dots: All ensemble members agree on the sign of change. The boxes in (a) and (b) indicate the Northern and Southern Amazon as defined in a study analyzing the precipitation of CMIP5 models over tropical South America (Yin et al., 2013).

Throughout the 21st century, the soil moisture has a significant negative trend, corresponding to 6.9% reduction of its 1971–2000 value per century. In contrast, the LAI in 21sm-21L has a significant positive trend (not shown), which is a manifestation of the CO_2 fertilization effect, as shown by e.g. Sitch et al., 2015. When considering only the soil drying, the LAI shows a negative trend of 7.9% lost per century (compared to the 1971–2000 mean LAI), which is slightly larger than the trend of soil moisture, and the interannual variability follows soil moisture closely ($r = 0.943$; Fig. 3.4a).

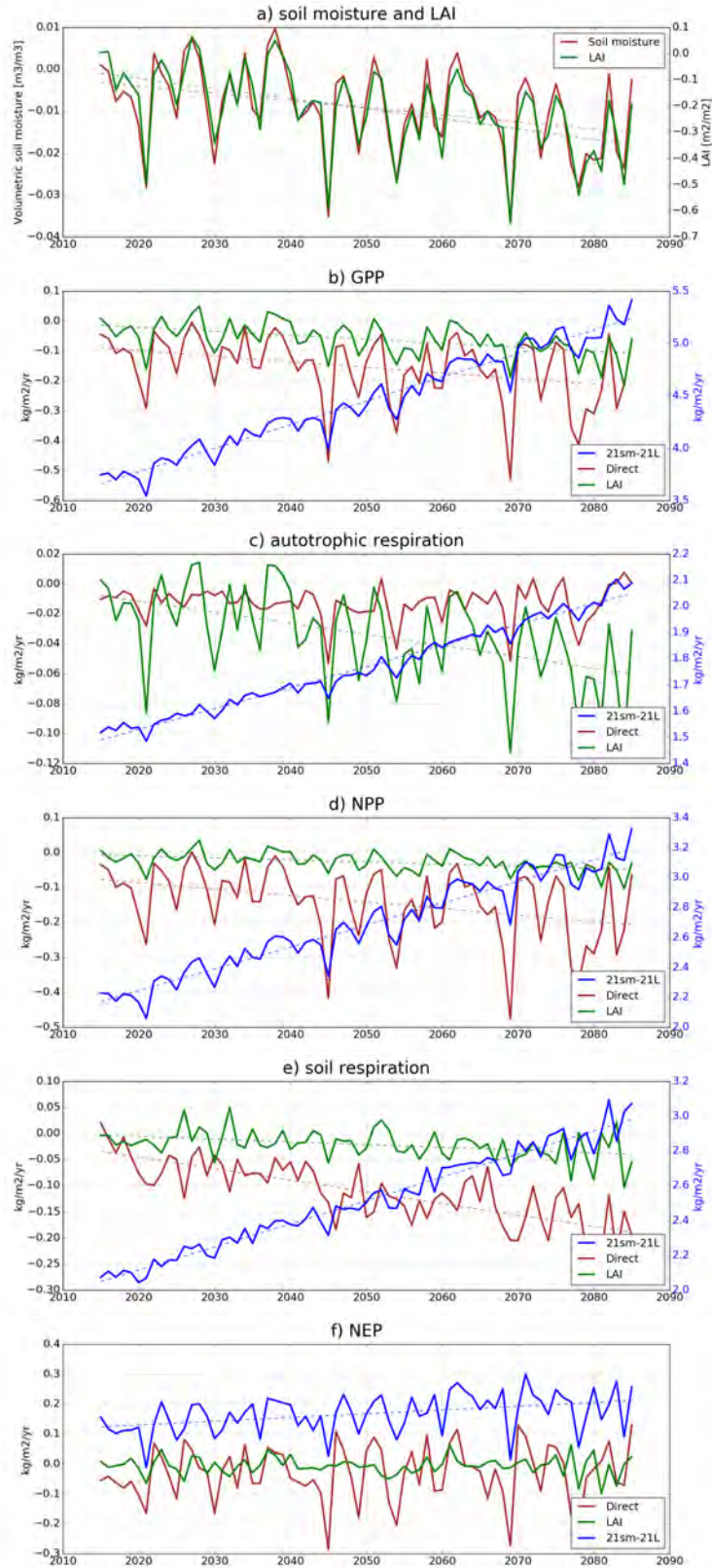


Figure 3.4: Evolution of (a) soil moisture and LAI (b) gross primary production (GPP) (c) autotrophic respiration (R_a) (d) NPP (e) soil respiration (R_a) (f) net ecosystem production (NEP) in the Amazon forests during the 21st century. Blue lines indicate 21sm-21L, which is the all-interactive simulation. Brown lines and green lines represent direct and LAI effects respectively. Dashed lines are linear regression lines and are shown only when $p < 0.05$. The region over which the area mean is taken is the boxes in Fig. 3.3.

Similar to the LAI, positive trends exist also for other carbon budget components in 21sm-21L, including gross primary production (GPP), autotrophic respiration (R_a), net primary production (NPP), soil respiration (R_s) and net ecosystem production (NEP; blue lines in Fig. 3.4b–f), indicating the strong controls of the rising CO_2 concentration on each carbon budget component. However, for most of the carbon budget components, the direct and LAI effects have negative trends, which cancels out part of the increasing trend. The direct and LAI effects on GPP are both negative and have negative trends with similar slopes, with the direct effect having larger magnitudes than the LAI effect (Fig. 3.4b). The direct effect on R_a is slightly negative without a significant trend, while the LAI effect is stronger and has a significant negative trend (Fig. 3.4c). The direct and LAI effects on NPP are both negative, with the former having more negative trend than the latter due to the contrasting features in GPP and R_a (Fig. 3.4d). The signs and trends of the R_s effects are similar to that of NPP, which are more negative and stronger from the direct effect than the LAI effect (Fig. 3.4e). The NEP, the sum of natural carbon sinks and sources of terrestrial ecosystem, is shown in Fig. 3.4f. A positive trend exists in 21sm-21L, indicating an increase in natural carbon uptake by the Amazon forests simulated in our model. In contrast, the direct and LAI effects on NEP are both negative and at the same order of magnitude as the NEP in 21sm-21L, indicating that the net carbon uptake by the Amazon forests is strongly reduced by future droughts.

Time series of biogeochemical effects

Fig. 3.5 shows the comparison of the direct and LAI effects on the carbon budget components over the Amazon forests during 2071–2085. The reduction of GPP due to the direct effect is double the magnitude of the LAI effect. Compared to the GPP reduction, the direct effect on R_a is weak. The LAI effect on R_a is stronger, compensating about half of reduction of LAI effect on GPP. Due to strong reduction in GPP and weak reduction in R_a , the direct effect on NPP reduction is strong. The magnitude is four times of the LAI effect. Conversely, the LAI effect on NPP reduction is weak, as the reduction in GPP is weak and the reduction in R_a is strong. For both the direct and LAI effects, the reduction in R_s is slightly less than the reduction in NPP. A large part of the NPP reduction is therefore cancelled out by the reduction in R_s . The net drought effects on NEP are negative. The magnitude of direct effect on NEP is about twice of the LAI effect. Compared with the NEP between 1971–2000, the NEP reduction due to direct and LAI effects correspond to reduction of 25.4% and 13.8% respectively, again indicating the strong impacts of future droughts on the natural carbon uptake of the Amazon forests.

Comparisons between the direct and LAI effects on carbon budgets

The direct and LAI effects on NPP, R_s , and NEP during the first (2015–2030) and the last (2070–2085) 15 years of the experiments are shown in Fig. 3.6. While for both the direct and LAI effects the NPP and R_s reduction become more prominent in the course of the 21st

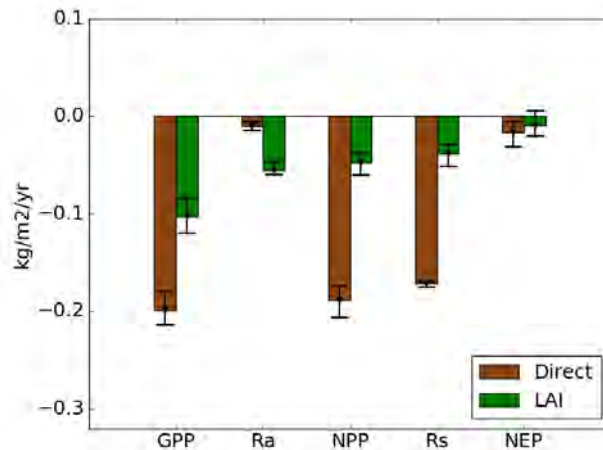


Figure 3.5: The direct and LAI effects on carbon budget components in the Amazon forests during 2071–2085. Bars represent ensemble means and whiskers represent range of ensemble members. Ra: Autotrophic respiration. Rs: Soil respiration.

century, the changes are different. The result is that the relative importance of the direct effects will change through time, and will be lower during 2070–2085 than 2015–2030. Although the LAI effect will be smaller than the direct effects for most of the 21st century, it will become more important by the end of this century.

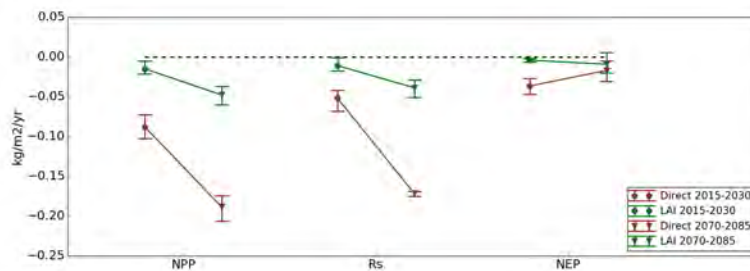


Figure 3.6: Comparison of NPP, soil respiration (Rs) and NEP due to the direct (brown) and LAI effects (green) during 2015–2030 and 2070–2085. Whiskers represent range of ensemble members.

*Large internal
variability for NEP
over large area*

In the responses of the carbon budget components, the ensemble members generally agree well with each other over the whole Amazon in the signs of change, including the weak response of R_a to direct effect (not shown). However, NEP is an exception. Despite the strong responses in NEP, the ensemble members agree with each other only in small regions (Fig. 3.7). The magnitudes of reduction in NPP and R_s are similar, such that in large parts of the Northern Amazon and almost the whole Southern Amazon the internal variability plays an important role in determining the sign of change. While the mean effects over the Amazon are prominent and often significant (Fig. 3.5),

for many of the grid points, whether the effect is positive or negative is subject to a large uncertainty.

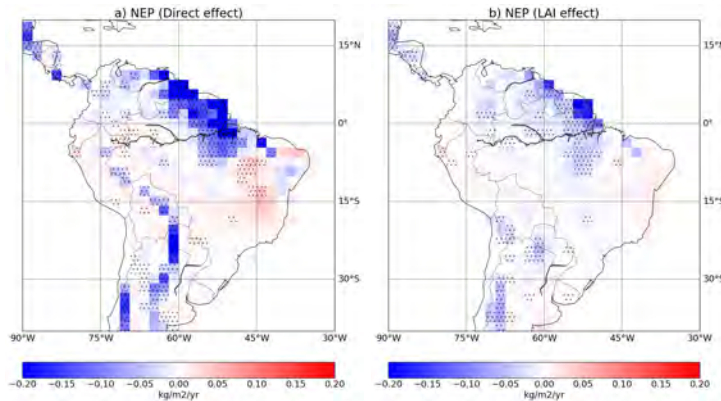


Figure 3.7: (a) The spatial pattern of the direct effect on NEP. (b) The spatial pattern of the LAI effect on NEP. Dots: All ensemble members agree on the sign of change.

3.3.3 Biogeophysical effects

Fig. 3.8 shows the 21st-century-evolution of selected variables related to biogeophysical effects in the Amazon forests. The soil evaporation in 21sm-21L (the reference simulation) has a positive trend, indicating that despite a decrease in precipitation under climate change, this region is still wet enough that the trend is driven by the increasing evaporative demand from the atmosphere. As the direct effect suppresses the moisture supply from the soil, a strong negative trend exists in the direct effect on soil evaporation (Fig. 3.8a). For transpiration, there is no significant trend in 21sm-21L. Despite the negative values of the direct effect on transpiration, no significant trend is simulated. Although the LAI effect on transpiration is weaker compared to the direct effect, it has a negative trend (Fig. 3.8b). For the total latent heat flux, the direct effect has a negative trend and the interannual variability correlates well with 21sm-21L throughout the 21st century (Fig. 3.8c). Due to the reduced water vapor released to the atmosphere from the direct effect, the low cloud cover is reduced and the net solar radiation at surface is increased. In 21sm-21L, a negative trend in low cloud cover and a positive trend in net surface solar radiation are simulated, both of which correlate well with the direct effect (Fig. 3.8de). Because of the feedback from the land-atmosphere interaction, both the direct and LAI effects cause an increase in surface temperature, with the direct effect having a significant positive trend (Fig. 3.8f).

*Time series of
biogeophysical effects*

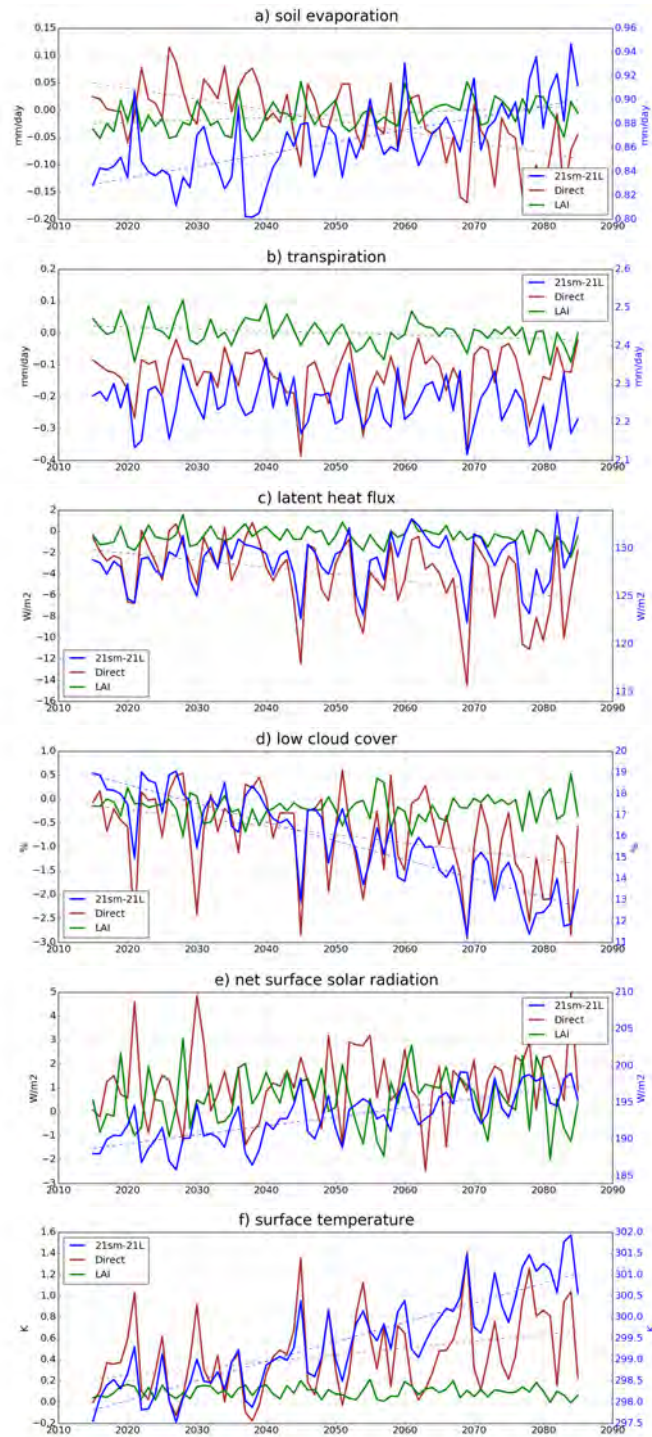


Figure 3.8: Evolution of (a) soil evaporation (b) transpiration (c) latent heat flux (d) low cloud cover (e) net surface solar radiation (f) surface temperature in the Amazon forests during the 21st century. Blue lines indicate 21sm-21L, which is the all-interactive reference simulation. Brown lines and green lines represent direct and LAI effects respectively. Dash lines are linear regression lines and are shown only when $p < 0.05$. The region over which the area mean is taken is the boxes in Fig. 3.3. Note the different scales of 21sm-21L (the right y-axis) and the drought effects (the left y-axis).

Fig. 3.9 summarizes the biogeophysical effects on surface energy budgets in the Amazon forests during 2071–2085. The direct effect is strong in reducing both soil evaporation and transpiration, with the latter being 30% higher, indicating that the contribution from stomatal response is larger than soil response. On the other hand, the LAI effect on soil evaporation is close to zero. As in the carbon budgets, in which the direct effect is stronger than the LAI effect, the latent heat flux reduction due to the direct effect is also stronger than the LAI effect. The direct effect also induces a reduction of more than 1% of low cloud cover. The reduction in low cloud cover corresponds to an enhancement of net surface solar radiation by more than 1.5 W/m^2 . Due to the change in surface energy budget partition, the surface temperature is higher for both the direct and LAI effects, with the former stronger than the latter by a factor of 7, and have a combined warming of 0.7K . While the drought effects of surface warming is consistent across the Amazon, the effects on precipitation have a dipole pattern. The reduction in soil moisture due to the direct effect results in an increase of precipitation over the Northern Amazon, and a decrease over the Southern Amazon. While the direct effect on precipitation change is prominent, the contribution from the LAI effect is small. The evaporative demand from the atmosphere, represented by the potential evapotranspiration (PET), is increased in both the Northern and Southern Amazon due to the direct effect. With the changes in precipitation and PET, we calculate the change in aridity, represented as the Aridity Index (AI, the ratio between precipitation and PET). Despite the consistent soil drying pattern across the Amazon (Fig. 3.3a), the signs of change of aridity are different in the Northern and Southern Amazon. The aridity is reduced in the Northern Amazon (an increase in AI), while in the Southern Amazon the aridity is increased (a decrease in AI). In both the Northern and Southern Amazon, the change in aridity is decided by the changes in precipitation, while the increased PET plays a smaller role.

The spatial pattern of the changes in precipitation during 2071–2085 due to the direct effect is shown in Fig. 3.10. The LAI effect is not shown as the magnitude is small in comparison. The pattern of an increase in the north and a decrease in the south is clear (Fig. 3.10a). The south-north cross section in Fig. 3.10b shows the distribution of wind and moisture in wet (21sm-20L) and dry minus wet (20sm-20L minus 21sm-20L) experiments. The drying over the Northern Amazon and the associated heating creates anomalous upward motion in locations where the original moisture is already abundant, favoring moist convection and hence enhance the precipitation there. On the other hand, reduced convection over the Southern Amazon leads to reduction in precipitation.

*Comparisons
between the direct
and LAI effects on
surface energy
budgets*

*Precipitation change
due to the direct
effects*

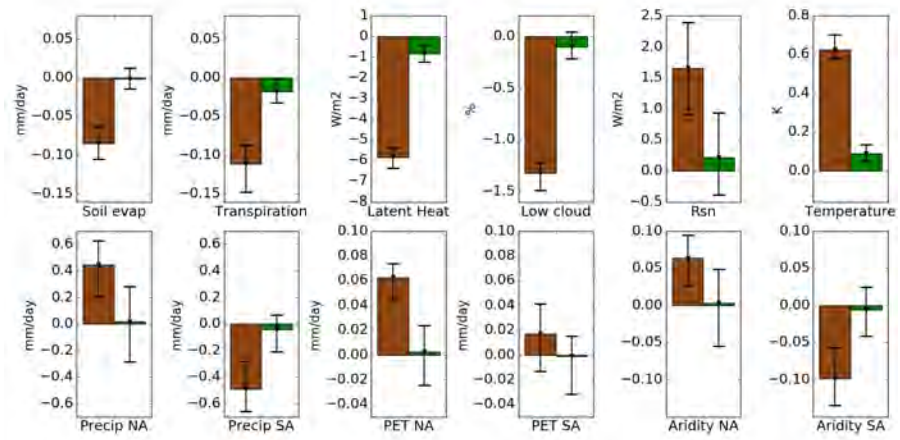


Figure 3.9: The direct and LAI effects on energy budget in the Amazon forests during 2071–2085. Bars represent ensemble means and whiskers are ensemble ranges. Soil evap: Soil evaporation. Rsn: Net surface shortwave radiation. Precip: Precipitation. PET: potential evapotranspiration. Aridity: Aridity Index, calculated as the ratio between precipitation and PET. NA: Northern Amazon. SA: Southern Amazon.

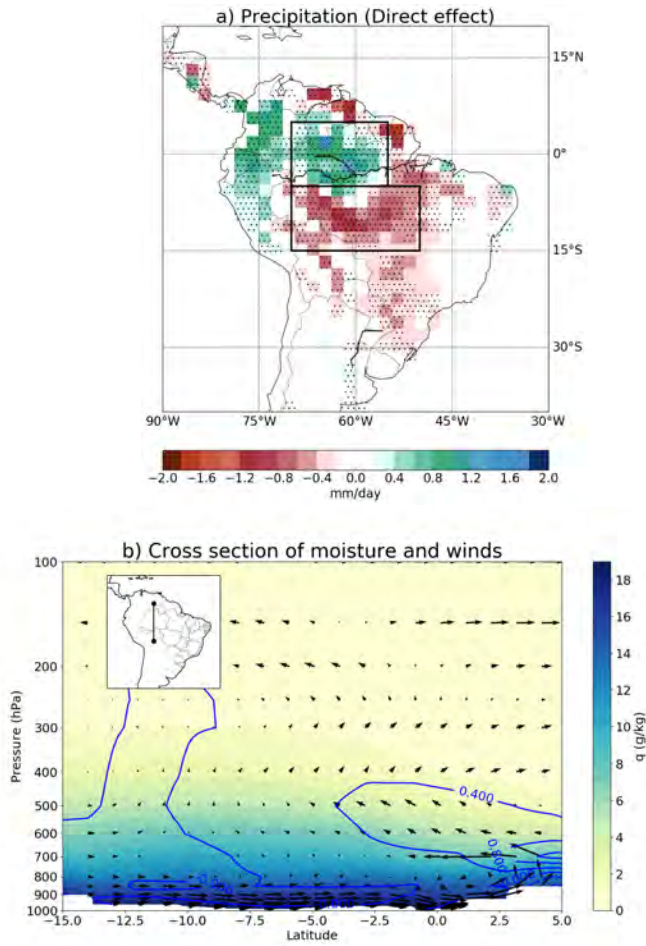


Figure 3.10: (a) Change in annual precipitation due to the direct effect during 2071–2085 (mm/day). (b) North-south cross section of wind and moisture field. Vector: (meridional wind, pressure velocity $(-10 \times \omega)$); contour: change in specific humidity; shading: specific humidity in the wet (21sm-20L) experiment.

3.3.4 Comparing the standard and modified JSBACH

To understand the influences of the model modification on the predicted drought effects, the same set of coupled experiments to separate the direct and LAI effects are conducted, with the land surface model being the standard version of JSBACH. Compared with the results using the modified JSBACH, the standard JSBACH simulates a similar magnitude of soil drying, but the magnitude of the LAI reduction is doubled (not shown).

Fig. 3.11 shows the comparison of the biogeochemical effects between the standard and modified JSBACH. As the standard JSBACH simulates a stronger responses of LAI to water stress, the LAI effect on GPP reduction is stronger than the direct effect. The reduction in R_a due to LAI effect is large and more than cancelling out the reduction in GPP, such that the LAI effect on NPP is an increase, which is opposite to the results of the modified JSBACH. Aside from the different sign of change of the LAI effect on NPP, the reduction in NPP from the direct effect is also weaker than in the modified JSBACH. Another major difference between the results of the standard and modified JSBACH is the sign of change of R_s from the LAI effect. The standard JSBACH simulates an increase in R_s from the LAI effect, while the modified JSBACH simulates a decrease. For the direct effect, the standard JSBACH simulates a decrease in R_s of magnitude slightly smaller than the decrease in NPP, which is similar to the results of the modified JSBACH. For both the direct and LAI effects, the net effects on NEP are decrease of magnitudes smaller than the results of the modified JSBACH. It is noteworthy that the uncertainty associated with the internal variability is large enough that the change in NEP from the direct effect might be positive.

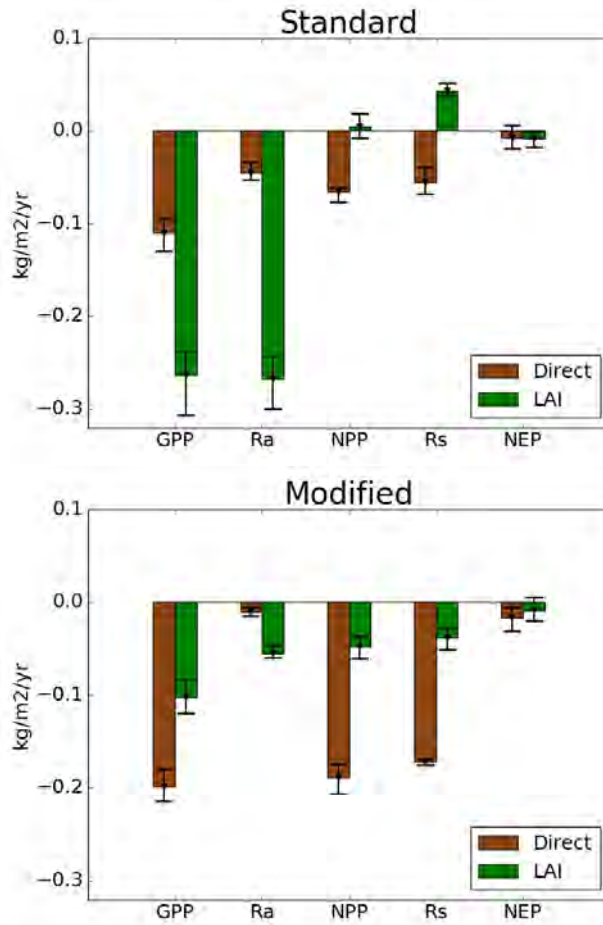


Figure 3.11: The comparison of the standard and modified JSBACH of the direct and LAI effects on carbon budget components in the Amazon forests during 2071–2085. Bars represent ensemble means and whiskers represent range of ensemble members. Ra: Autotrophic respiration. Rs: Soil respiration. The lower panel is the same as Fig. 3.5.

Fig. 3.12 shows the comparison of the biogeophysical effects between the standard and modified JSBACH. For the standard JSBACH, the LAI effect contributes to an increase in soil evaporation. The increase in soil evaporation is because more radiation is able to reach the surface to evaporate soil moisture, which can be seen from the more prominent reduction in LAI and transpiration than in the modified JSBACH. Although the LAI effect on reduction in latent heat flux is larger than in the modified JSBACH, the sum of the direct and LAI effects does not differ much from the modified JSBACH. The magnitudes of the increase in surface temperature are also similar to the results simulated by the modified JSBACH (0.8K vs. 0.7K). For the precipitation, PET and AI, the standard and modified JSBACH predict similar results at both the Northern and Southern Amazon.

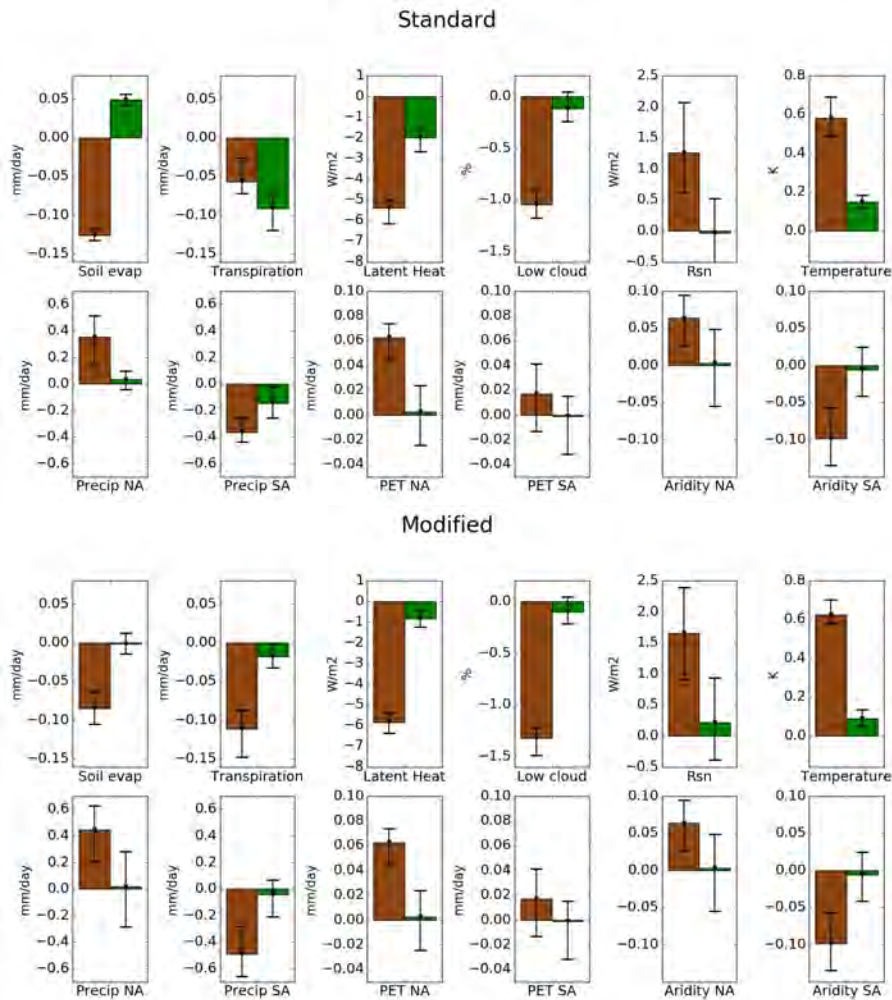


Figure 3.12: The comparison of the standard and modified JSBACH of the direct and LAI effects on energy budget in the Amazon forests during 2071–2085. Bars represent ensemble means and whiskers are ensemble ranges. Soil evap: Soil evaporation. Rsn: Net surface shortwave radiation. Precip: Precipitation. PET: potential evapotranspiration. Aridity: Aridity Index, calculated as the ratio between precipitation and PET. NA: Northern Amazon. SA: Southern Amazon. The lower panel is the same as Fig. 3.9.

3.4 DISCUSSION

3.4.1 *Improvement of JSBACH under coupled mode*

The improvement of model performance is also seen when coupled to the atmospheric model. For example, the standard JSBACH simulates an increase in soil evaporation due to the LAI effect. This is unlikely to happen in reality, because the canopy in the Amazon forests is dense and consist of multiple layers, and a mild reduction in LAI can barely impact the surface. In contrast, the modified JSBACH simulates nearly no change in soil evaporation from the LAI effect, which is more likely to be the reality.

In addition, the standard JSBACH simulates an increase in NPP from the LAI effect, which is due to the large reduction in R_a . In contrast, the modified JSBACH simulates only mild reduction in R_a from the LAI effect. Diverse responses of R_a to water stress have been suggested in previous studies. Increased leaf dark respiration as well as total ecosystem respiration was observed in the TFE experiments at CAX (Metcalf et al., 2010). On the contrary, studies based on natural drought events indicated reduced GPP and R_a of similar magnitude and therefore constant NPP (Doughty et al., 2015). A decline in leaf and wood respiration of $0.084 \text{ kg/m}^2/\text{yr}$ with a $0.5 \text{ m}^2/\text{m}^2/\text{yr}$ reduction in LAI was estimated in Meir et al., 2008. When compared with this estimate, the mild reduction in R_a simulated by the modified JSBACH is then closer than the large reduction simulated by the standard JSBACH, which indicates another improvement of JSBACH when coupled to the atmosphere.

3.4.2 *Biogeochemical and biogeophysical effects due to LAI*

In the studies making use of the GLACE-CMIP5 experiments to understand the impacts of drought on climate, the drought effects are often implicitly perceived as solely from the drier soil (e.g., Seneviratne et al., 2013; Berg et al., 2016; Green et al., 2019) and even as the response from vegetation is included, it is not quantified. In this study, we separate the direct and LAI effects and quantify the contribution from the LAI effect. For the carbon budgets, the contribution of LAI effect on NEP reduction during 2071–2085 is 35% of the combined drought effects. As the combined drought effects induce 40% of NEP reduction compared with the 1971–2000 value, the LAI effect alone is able to reduce about 14% of the natural carbon uptake. Across the composition of NEP (GPP, R_a , NPP, and R_s), the ratios of the magnitude of the direct to LAI effects are different, ranging from 0.2 for R_a , to 4.4 for R_s . Therefore, studies on the mechanisms of all the

*LAI effect is
important for both
BGC and BGP*

underlying variables are necessary for further process understanding. For the biogeophysical effects, the contribution of the LAI effect on increasing surface temperature is 12%. Although the contribution of the LAI effect is smaller in biogeophysical effects, we note that the magnitude of surface warming due to drought effects ($\sim 0.7\text{K}$) is close to the magnitude of the warming induced in a total-deforestation scenario of the Amazon forests (Lejeune et al., 2015), which is not trivial. Therefore, for both the biogeochemical and biogeophysical effects, the contribution of the LAI effect is important and should be carefully considered in the models.

The experimental setup in this study enables quantification of both model uncertainty and the uncertainty arising from the internal variability. Comparison of the results between the standard and modified JSBACH gives the model uncertainty, which is associated with different ways of simulating a physical process (in this study the formulation of LAI and leaf litter production), and the internal variability is given by the spread of results among the five ensemble members. For the process uncertainty, as the carbon budgets are simulated quite differently in the standard and modified JSBACH (Fig. 3.11), for biogeochemical effects the model uncertainty due to the formulation of LAI and leaf litter production is large. The sign of change in NPP and R_s from the LAI effect are different between the standard and modified JSBACH, which is caused solely by modifying the LAI and leaf litter formulation, indicating that having a better LAI response to water stress can be equally important as having better formulations of the respiration fluxes themselves. For the biogeophysical effects, the differences between the standard and modified JSBACH are smaller (Fig. 3.12), indicating that the process uncertainty is smaller. For the internal variability, except for the NEP, the carbon budgets generally have smaller uncertainties. As the biogeophysical effects are more subject to climate variability, some of the biogeophysical variables have large uncertainties, such as the surface net solar radiation, precipitation, and PET. To sum up, for the biogeochemical effects, the model uncertainty is larger than internal variability, while for the biogeophysical effects the model uncertainty and internal variability is often of the similar magnitude.

Another difference between the biogeochemical and biogeophysical effects is that while the spatial patterns of biogeochemical effects are more homogeneous, a pattern of north-south dipole exists in some biogeophysical variables such as precipitation and aridity. Some studies have argued consistent drying over the Amazon forests as the precipitation consists of high amount of recycled moisture (e.g., Zemp et al., 2017). However, a whole-basin reduction in precipitation due to soil drying is not supported by the results in this study. Instead, a meridional dipole of increase in the north and decrease in the south is simulated, which indicates a redistribution of precipitation and is

*Comparison between
model uncertainty
and internal
variability*

*BGP effects can be
non-local*

dominated by dynamical feedback. A redistribution in precipitation is also found in several model simulations conducted on deforestation scenarios (Lejeune et al., 2015). Reduced precipitation over wetter soil in the Amazon forests has also been simulated by previous studies with different models (Harper et al., 2014; Lin et al., 2015), indicating that ET is not the sole factor determining precipitation in this region and that dynamical mechanisms are important in determining precipitation response.

*Aridity reduced in
the north and
increased in the
south*

A globally enhanced aridity due to soil drying has been predicted by previous studies (e.g., Berg et al., 2016). In our results a consistent enhanced aridity due to drought is not found over the whole Amazon forests. Instead, the aridity change due to drought follows the pattern of precipitation change. The aridity is reduced in the Northern Amazon and an enhancement is only found in the Southern Amazon. Since the Southern Amazon may be subject to a tipping point of drastic vegetation shift (e.g., Nobre et al., 2016; Fearnside, 2018), a rainfall reduction and aridity enhancement over the Southern Amazon may further endanger the vegetation there in the future.

3.5 CONCLUSIONS

In this chapter, a series of coupled land-atmosphere simulations are conducted, in order to separate the direct and LAI drought effects under future RCP8.5 climate. The *direct effect* of drought refers to the climatic effect caused solely by soil drying and stomatal responses of plants, while the *LAI effect* of drought is the effect caused by the reduction of LAI because of drier soil.

With the configuration of this study, which does not include nutrient limitation, disturbances (wind-break and fires), vegetation cover change (both natural and anthropogenic), the natural carbon sink of the Amazon forests (net ecosystem productivity; NEP) will still be growing throughout the 21st century. Although without significant trends, the direct and LAI drought effects are at the same order of magnitude as the carbon sink, indicating that the drought effects are able to cancel out an important portion of the carbon sink. For all other carbon budget components, the greenhouse gas (GHG) forcing is causing positive trends, while the drought effects always have different signs as the GHG forcing and have trends of getting stronger, which acts to cancel out the effect of GHG forcing.

The results of separating the direct and LAI effects shows that the LAI effect is nonnegligible for both the biogeochemical and biogeophysical effects. Generally, the LAI effect plays larger roles in biogeochemical effects than in biogeophysical effects. By the end of the 21st century (2071–2085), the contribution of the LAI effect relative

to the combined direct and LAI drought effects in reducing natural carbon uptake is 35%. For increasing the surface temperature, the contribution is 12%.

The same set of experiments are conducted with both the standard and modified JSBACH. Comparing the simulations between the two versions shows that for the biogeochemical effects, the model uncertainty associated with the formulation of LAI and leaf litter production is large. The direct and LAI drought effects on carbon budget components can be very different between the two versions. For the biogeophysical effects, the standard and modified JSBACH are more consistent. Therefore studies with the GLACE-CMIP5 experiments on biogeophysical effects are subject to less uncertainties from the poor representation of vegetation drought responses, while large uncertainties and biases exist in the predictions of future carbon budgets by current vegetation models (e.g. in Green et al., 2019). To address the question, better strategy in modeling leaf phenology including more mechanically-based or data-driven approach as implemented in this study should be adopted.

MODELING DROUGHT-INDUCED TREE MORTALITY AND ITS IMPACTS UNDER FUTURE CLIMATE

4.1 INTRODUCTION

Following the past few decades of climate change, it has been found that at least some of largest forests in the world have already experienced the drought and heat stress and have been responding with enhanced tree mortality. The pattern is across different climate regimes globally, even includes places which are usually not considered water-limited (Allen et al., 2010). Records from multiple long-term monitoring plots across the Amazonia were used to assess forest response to the 2005 drought. It was found that the long-term carbon sink before 2005 was reversed. The total impact from the drought was 1.2 to 1.6 Pg¹ (Phillips et al., 2009). Using data from more than 100 monitoring plots in both Amazonia and Borneo, it is shown that larger trees are more at risk of drought. In Amazonia, trees with low wood density are also more at risk of drought-enhanced mortality, independent of the sizes. Evidences also exist that the impacts from drought might be lagged for several years (Phillips et al., 2010). Drought-enhanced mortality has also been observed in the TFE experiments, where tree mortality increased after two years of experiment, and the mortality enhancement was more prominent for larger trees, which store more carbon (Nepstad et al., 2007). Therefore, it is important to understand the mechanism under the enhancement of tree mortality.

Evidences of increasing drought mortality

There are several drivers for the increasing tree mortality at the moist tropical forests, include rising temperature and vapor pressure deficit (VPD), liana abundance, wind events and fire. The CO₂ fertilization is also likely to drive the increasing mortality via stand thinning or acceleration of tree growth to reach the larger but more vulnerable heights (Mcdowell et al., 2018). Among these drivers, the rising temperature and VPD as well as fire are related to droughts. Drought-enhanced tree mortality is not caused by a single process. At the individual tree level, the most important mechanisms for drought mortality include hydraulic failure and carbon starvation (Choat et al., 2018).

Drivers of tree mortality

Hydraulic failure indicates that, as soil moisture is too low or the atmospheric evaporative demand is too large, the tension in the xylem becomes higher. The high xylem tension creates air bubbles in the

Hydraulic failure

¹ petagrams; 1 Pg = 10¹⁵ g.

xylem (a phenomenon called *embolism* or *cavitation*), which block the water transport from roots to leaves. The hydraulic failure hypothesis states that the cavitation is responsible for tree death due to drought.

Carbon starvation

On the other hand, the carbon starvation hypothesis states that during extreme drought, as the stomata are closed and photosynthesis is lowered, carbon supply is reduced and plants will start to consume the stored carbohydrate. When both the supply and storage is not able to meet the demand of maintenance, tree death is also likely to happen.

Biotic attacks and fires

Both of hydraulic failure and carbon starvation have been shown able to predict drought mortality, and an interdependence between the two is likely to exist. In addition, the biotic attacks are also responsible for tree mortality. However, it should not be separated from other factors. It should be viewed that under drought conditions, the resistance of trees to biotic attacks is lowered through the aforementioned mechanisms, such that the biotic attacks are easier to cause tree deaths (Mcdowell et al., 2013). Under drought conditions, more litterfall is produced by the trees, which is the fuel for fire. Meanwhile, as the atmosphere is drier, the fire occurrence is also increased, which cause tree deaths as well.

Methods to predict mortality

In order to predict drought with models, several metrics have been proposed. For example, the Climatic Water Deficit (CWD) has been applied in temperate trees and shown to have good predictability. CWD is defined as the difference between water demand and supply of plants. As the plant water demand is determined by the atmospheric water demand, it can be represented by Potential Evapotranspiration (PET). The plant water supply is determined by available water in soil and plant physiology, which can be represented by evapotranspiration (ET). In previous studies (e.g., Anderegg et al., 2015), the CWD was applied to *Populus tremuloides*² to assess whether the mortality is increased when CWD is large. When applied to the measurement in southwestern United States, a threshold of CWD above which an apparent increase in tree mortality is found. Another proposed candidate to simulate drought is the growth efficiency, defined as the stemwood growth per individual leaf area (Mcdowell et al., 2018). Some metrics have also been proposed for the purpose of detection and early-warning of tree mortality. For example, an equation based on the non-photosynthetically active vegetation (NPV), which can be broadly defined as senescent leaves, bark, snags, and coarse woody debris, was constructed with mortality after the drought in 2002 in southwestern United States and then applied to predict the mortality after the drought in 2012. When examined on the drought in the

² Commonly known as quaking aspen or American aspen, a native deciduous tree widely distributed in North America.

Amazon, the results were also promising (Huang and Anderegg, 2012; Anderegg et al., 2019).

As few models have incorporated a drought mortality, the mortality under future climate has not been well-studied. In this chapter, we implement the drought-enhanced mortality to JSBACH, with an empirical formulation based on the plant available soil water. We force JSBACH with the climate under RCP8.5 scenario and investigate the impacts of drought mortality on the carbon budgets in the Amazon.

4.2 METHODS

4.2.1 Implementation of drought mortality

An empirical equation based on the TFE experiments at both TAP and CAX is proposed in Meir et al., 2015, which is based on the availability of soil moisture for the plants.

The availability of soil moisture is expressed via relative extractable water (REW), which is the fraction of the maximum plant available water (PAW_{\max}), and PAW_{\max} is the available soil moisture between field capacity (θ_{fc} , typically -33 kPa) and wilting point (θ_{wp} , typically -1500 kPa). However, the determination of exact θ_{fc} and θ_{wp} is difficult. It is therefore common to set θ_{fc} as the maximum of observed volumetric soil water content, and θ_{wp} as the minimum of observed volumetric soil water. In this way, the REW can be estimated via:

$$REW = \frac{\theta - \theta_{\min}}{\theta_{\max} - \theta_{\min}} \quad (4.1)$$

where θ is the volumetric soil water content; θ_{\min} is the minimum volumetric soil water content; θ_{\max} is the maximum volumetric soil water content.

In Meir et al., 2015, a piece-wise linear regression is carried out to the observed REW and mortality at the TFE experiments at TAP and CAX, and it is shown that when REW is lower than 0.51, the tree mortality starts to increase significantly.

In JSBACH, vegetation carbon is separated into green pool, wood pool and reserve pool. Woody parts of plants compose the wood pool. Carbon is removed from the wood pool according to a turnover time, in order to represent the background mortality. The dynamics of the wood pool is as follows:

$$\frac{dC_W}{dt} = NPP_{>W} - \frac{C_W}{\tau_W}, \quad (4.2)$$

where C_W is wood pool size, $NPP_{>W}$ is NPP allocated to wood pool, and τ_W is the wood turnover time.

In the standard JSBACH, τ_W is fixed to be 30 years. Therefore, woody part of trees are removed from the wood pool at a constant rate and independent of water stress.

To implement a drought-enhanced mortality, we modify the turnover time of wood pool in response to REW. The turnover time is kept unchanged when REW is larger than 0.51, and is reduced (corresponding to more removal of carbon from the wood pool) when the REW is lower than 0.51. The advantage of modifying the turnover time of wood pool to remove carbon from vegetation is that, in the regrowth scheme, when the total biomass is reduced, the maximum LAI and thereby the LAI are reduced.

4.2.2 Evaluation at TFE site at TAP

To evaluate the influences of the implemented drought mortality on LAI and litter production, we conduct the site-level experiment at TAP as in Chapter 2. A detailed comparison of the results between the leaf shedding version (called *the modified JSBACH* and used in Chapter 2 and 3) and the drought mortality version of JSBACH is provided in Table 4.1. Note that to account for the effects of drought mortality in the observation, now at the EXP plot data from all years are used for comparison, instead of only the first two years as done in Chapter 2. The LAI at CTR plot is not significantly improved: The bias and CRMSD is reduced and dSDev is increased, but the correlation is still insignificant. However, at the EXP plot the CRMSD and correlation are both improved. Although the bias and dSDev are slightly larger, we note that the leaf shedding version has performed nearly perfect for the two terms (bias = 0.001 and dSDev = 0.000 respectively). Although the litter production is not improved, it is also not significantly worse than the leaf shedding version. We therefore conclude that the comparisons against the TFE experiments at TAP lend us additional support to the applicability of the implemented empirical formulation of drought mortality.

4.2.3 Simulation protocol

In this chapter, offline (land-only) simulations are conducted. With the atmosphere only as forcing but not interactive, the land and the atmosphere are decoupled. However, as the focus is on the effect of drought mortality on carbon budgets, the influence from land-atmosphere interaction is for now ignored.

The spatial resolution is T63 (ca. 200 km). The simulated region is limited to the Amazon region. The atmospheric variables output by ECHAM from the experiments in Chapter 3 are used to force the

Table 4.1: Comparison between LFSD (leaf shedding version) and MORT (both leaf shedding and mortality) of JSBACH at TAP, including simulated bias, differences of standard deviation (dSDev) between simulation and observation, centered root-mean-square deviation (CRMSD), and correlation coefficient with observation (CCoef). At both CTR and EXP plot, data from all years are used for calculation. Values in bold indicates the respective model version performs better than its counterpart. Values in italic indicates the correlation is insignificant ($p > 0.1$).

Variable	Plot	Version	Bias	dSDev	CRMSD	CCoef
LAI	CTR	LFSD	0.225	-0.299	0.628	<i>-0.015</i>
		MORT	0.187	-0.305	0.621	<i>0.003</i>
	EXP	LFSD	0.001	0.000	0.399	0.720
		MORT	-0.194	-0.004	0.357	0.774
Leaf litter	CTR	LFSD	<i>-0.080^a</i>	<i>-0.031^a</i>	0.087^a	0.655 ^a
		MORT	0.135 ^a	0.053 ^a	0.127 ^a	0.655^a
	EXP	LFSD	0.019^a	<i>-0.037^a</i>	0.110	0.485^a
		MORT	0.292 ^a	0.052 ^a	0.157 ^a	0.484 ^a

LFSD: Leaf shedding

MORT: Leaf shedding + Mortality

^acalculated with a lag of 90 days for the simulations

JSBACH. The pre-industrial forcing is used to drive JSBACH until the humus in the soil reaches equilibrium. Then, the model is run with historical forcing from 1852 to 2014. From 2015 on, the model is forced with the climate under RCP8.5 scenario.

The experiments are carried out with different versions of JSBACH. The first experiment is conducted with the standard JSBACH, which is without the improved leaf shedding and litter production (hereafter *STND*); the second is conducted with the modified JSBACH, which is with the improved leaf shedding and litter production, as described in Chapter 2 (hereafter *LFSD*); the final experiment is conducted with the version in which both the drought mortality, the improved leaf shedding and litter production are implemented (hereafter *MORT*).

4.3 RESULTS

The precipitation over the Amazon region of both the historical period (1852–2014) and future scenario is shown in Fig. 4.1. During the historical period, a positive trend of precipitation exists in spite of the large interannual variability. On the contrary, there is no significant trend under future climate. The mean state is lower and the interannual variability is higher under RCP8.5 compared with the historical period,

Precipitation of historical and future (RCP8.5) periods

in agreement with results from previous studies that precipitation in the Amazon will be reduced and become more extreme in the future.

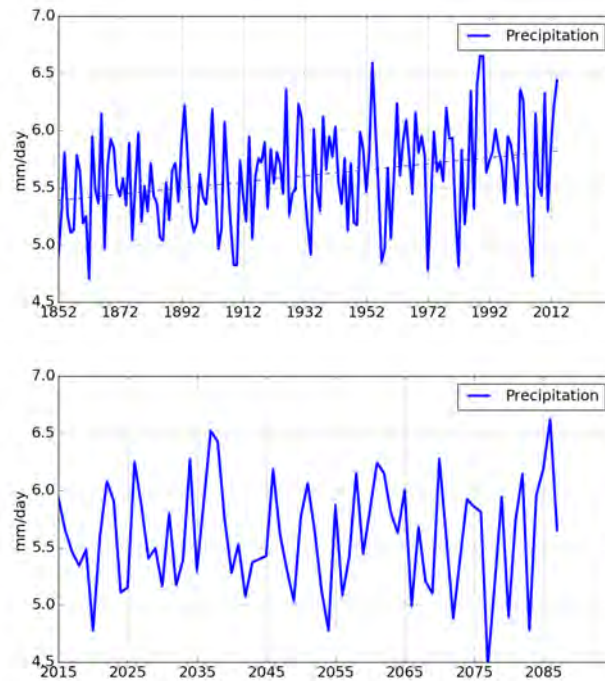


Figure 4.1: Precipitation over the Amazon from 1852 to 2014 (top) and from 2015 to 2085 under RCP8.5 (bottom). Note that a positive trend exists for the historical period (1852–2014), but not for the future scenario.

*Vegetation carbon in
spin-up and
historical periods*

The vegetation carbon simulated in the pre-industrial spin-up is shown in Fig. 4.2 (Top). The equilibrium states are different for the three model versions, with STND slightly higher than LFSD and MORT being especially lower than the others. The vegetation carbon simulated during the historical period is shown in Fig. 4.2 (Mid). Interestingly, the vegetation carbon simulated by LFSD surpasses STND in 1960s, while MORT remains low compared with the others. The LAI of LFSD also surpasses STND (Fig. 4.2, Bot), but only during a few decades later than 1960s, indicating that LAI is not the primary reason of why LFSD has higher vegetation carbon than STND. Both LAI and litter production (representing growth and carbon removal from plants respectively) play roles in determining the time when LFSD has more vegetation carbon than STND.

*Comparisons of
productivity and
mortality to the
observation*

To understand whether JSBACH captures the trend of biomass growth during the historical period, we compare the simulations with the large set of biomass measurement data in the Amazon forests (Brienen et al., 2015). Fig. 4.3 shows the comparison of productivity, biomass mortality and annual biomass change, respectively. An increasing trend in productivity is found in the observation, and

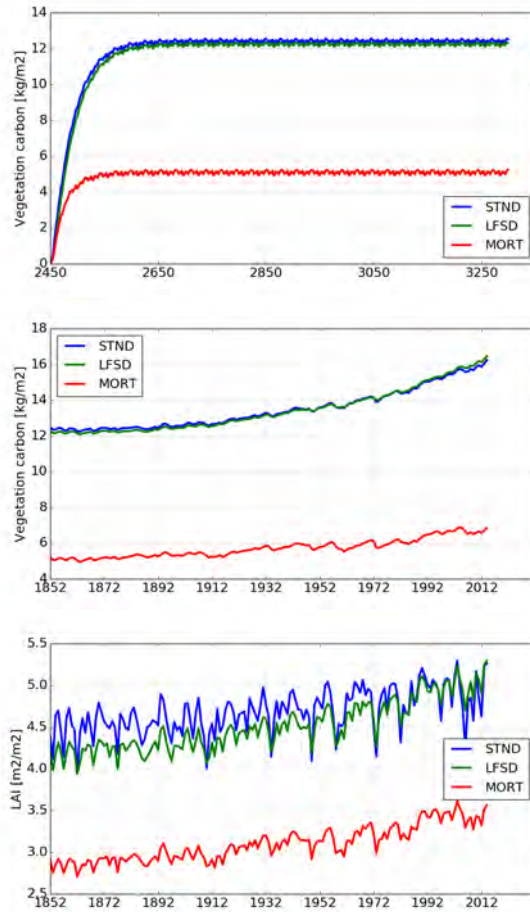


Figure 4.2: Comparisons of total vegetation carbon between the simulations of the (Top) spin-up and (Mid) historical period; (Bot) Comparisons of LAI between the simulations of the historical period.

the trend is captured in all model versions. All model versions have medium to high correlation with the observation, with MORT having the highest correlation ($r = 0.786$). For the biomass mortality, the observation has a significant increasing trend, which is also captured by all model versions with MORT having the closest slope to the observation. However, the correlation between model simulation and observation is only significant for STND and LFSD ($r = 0.427$ and $r = 0.520$ respectively). The annual change of vegetation carbon, calculated as the difference between productivity and biomass mortality, shows a decreasing trend, indicating a saturation of biomass growth. However, none of the model versions capture the trend, and none of the model versions correlate with observation significantly.

Additionally, to understand the ability of JSBACH simulating the spatial pattern of biomass distribution in the Amazon forests, the simulations are compared with a gridded data of the aboveground biomass in the Amazon (Saatchi et al., 2007). Fig. 4.4 shows the spatial

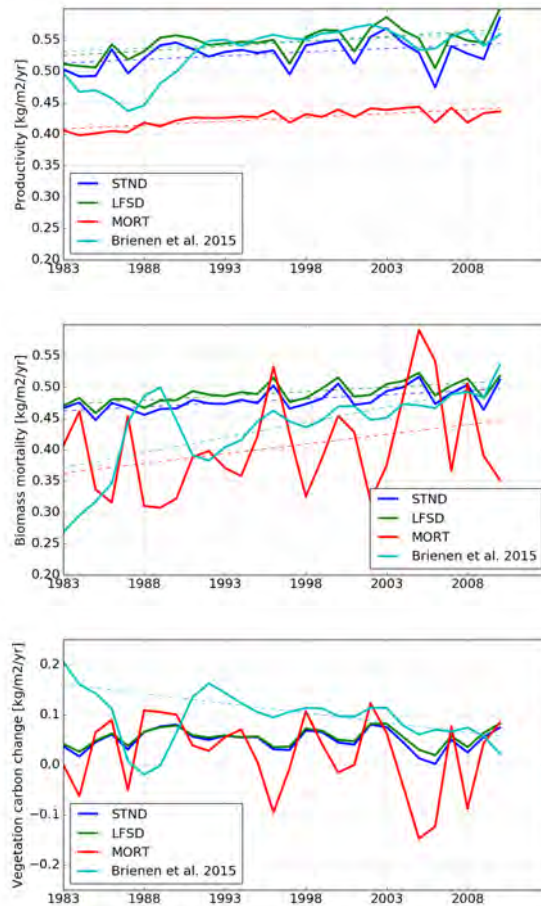


Figure 4.3: Comparisons between observation from Brienen et al., 2015 and the simulations.

patterns of the observation-based estimate and the simulations of the biomass in the Amazon. The AGB is simulated with low biases in all model versions. We note that only MORT captures better the contrast between the Northern and Southern Amazon (the black boxes in Fig. 4.4), while both STND and LFSD simulate the biomass homogeneously with less spatial variability compared to the observation.

*Comparisons under
future climate*

The comparison of the model results under future climate is shown in Fig. 4.5. To eliminate the influence of the different mean states at the beginning of RCP8.5 runs, the y-axes of MORT on the figures are shifted. Both STND and LFSD has exponential growth throughout the 21st century. However, for MORT, a linear growth exists only until the 2050s. After the 2050s, the vegetation carbon stays at the same level without a clear trend. Due to the hiatus, the vegetation carbon growth throughout the simulation period of MORT is only about 36% of LFSD. The reduced vegetation carbon of 3.75 kg/m² corresponds to a basin reduction of 26.9 Pg, which is roughly 20 times of the impact from

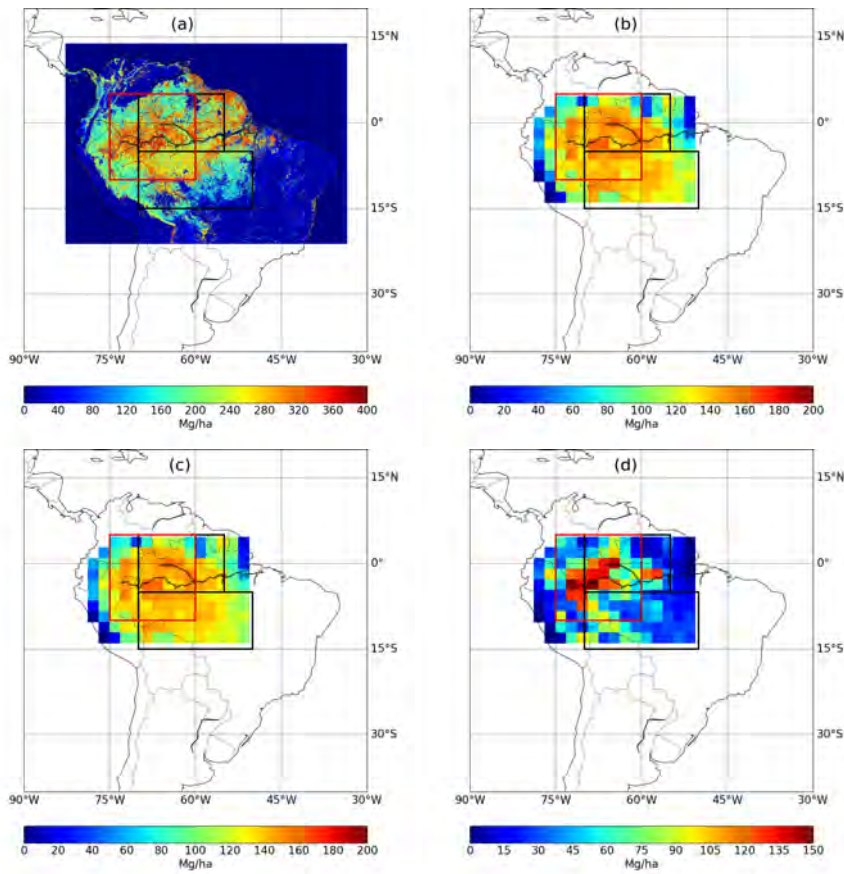


Figure 4.4: Comparisons of biomass map pattern from (a) observation (Saatchi et al., 2007), (b) STND, (c) LFSO, and (d) MORT. Note that the colorbars are different among figures. The black boxes indicate the Northern and Southern Amazon, and the red box is northwestern Amazon, as defined in Yin et al., 2013.

the drought in 2005³. To understand the cause of the difference in vegetation after the 2050s, we look into the time evolution of NPP (Fig. 4.5, Bot). For all model versions, positive trends exist throughout the simulation period. For MORT, although the slope of trend is smaller compared with STND and LFSO, a similar hiatus as in vegetation carbon does not exist. Therefore, the difference in vegetation carbon growth between MORT and the others is caused not by their difference in NPP, but from the difference in mortality, which removes carbon from the plants and is higher for MORT than the others.

Fig. 4.6 shows the difference of vegetation carbon between 2015 and 2085 in the three simulations. The patterns of STND and LFSO are similar, with a homogeneous increase over both the Northern and Southern Amazon. In contrast, the pattern of MORT shows large

³ The drought impact on biomass was estimated to be 1.2 to 1.6 Pg in Phillips et al., 2009.

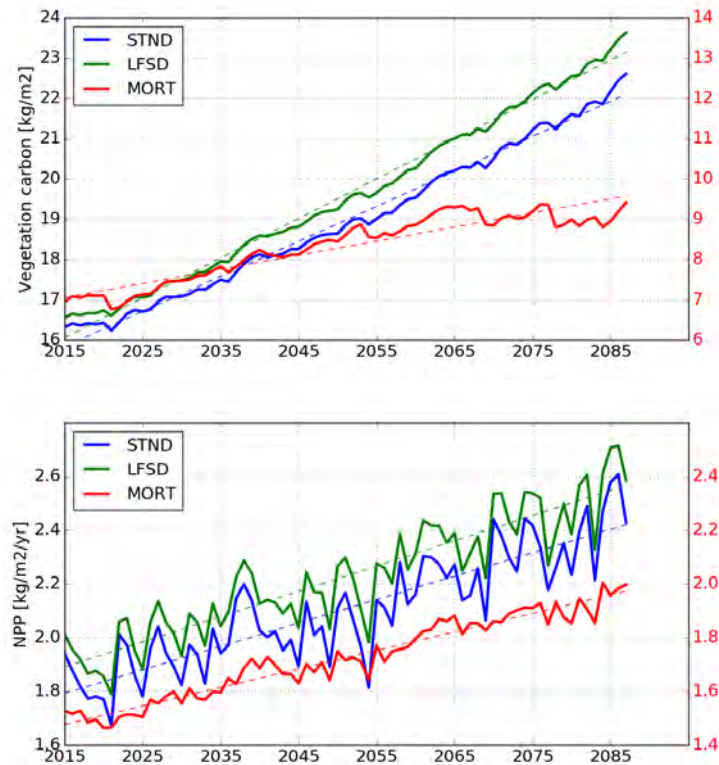


Figure 4.5: Comparisons between models of (Upper) vegetation carbon and (Lower) net primary production (NPP). Note that MORT has a shifted y-axis as shown at the right hand side (red).

heterogeneity, with the largest increase over the northwestern Amazon and only zero to slightly increase over the Southern Amazon.

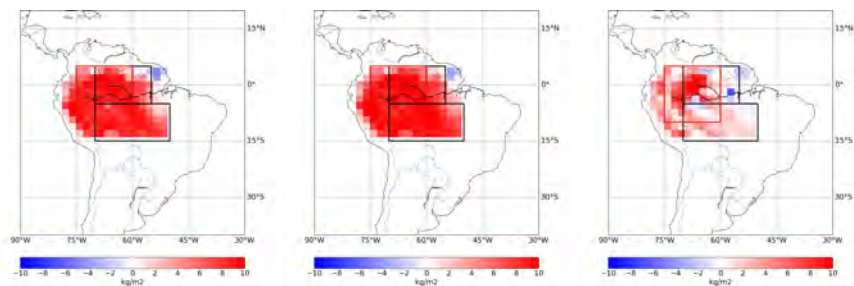


Figure 4.6: Comparison of the difference in vegetation carbon between 2015 and 2085. (Left) STND (Mid) LFSD (Right) MORT.

4.4 DISCUSSIONS AND CONCLUSIONS

In this chapter, we implemented a drought-enhanced tree mortality to JSBACH based on an empirical formulation proposed in Meir et al., 2015. The formulation is derived from the results at the two

TFE experiment sites in the Amazon, and is based on the relative extractable water (REW) of soil, which aims to represent the portion of soil water which is accessible for plants.

First, we conducted site-level simulation at the TFE experiment at TAP and compared the results from the model version with leaf shedding (LFSD) and with both leaf shedding and mortality (MORT). The results showed that MORT is able to simulate the LAI at EXP plot slightly better than LFSD, providing support for the applicability of the implemented drought mortality to JSBACH.

To estimate the impacts of drought mortality under future climate, we conducted land-only experiments under the business-as-usual RCP8.5 scenario with three model versions: STND (the standard version), LFSD (leaf shedding), and MORT (both leaf shedding and mortality). The simulated mean state of LAI and vegetation carbon of MORT in present day is significantly lower than STND and LFSD, and all of the three versions simulate low biases in aboveground biomass (AGB) compared with the observation. The vegetation carbon simulated by LFSD has been lower than STND for the whole spin-up and historical period until the 1960s, and surpasses STND after then, which is in agreement with our conclusion in Chapter 2 that the standard JSBACH might overestimate drought responses when the mean state is drier.

Despite the large biases in AGB, when comparing the simulated annual productivity and biomass mortality (as the carbon sink and source respectively) with the observation, the magnitudes of the simulations are close to the observation. Among the model versions, LFSD and MORT are better than STND to reproduce the trend and variability of both productivity and mortality during the late 20th century, although the net change of biomass is less certain. When compared with the biomass intensity map in the Amazon, MORT is the only model version able to simulate the pattern of more abundant biomass in the Northern Amazon, while STND and LFSD both simulate a homogeneous pattern across the Amazon, which is not seen in the observation.

Finally, the results under future climate showed that for MORT, the vegetation carbon is saturated and remain in hiatus after the 2050s. The vegetation carbon growth throughout the 21st century is largely reduced compared with other version, which is only 36% of LFSD. The impact on stored carbon is roughly 20 times of the impacts from the drought in 2005. The saturation is more prominent over Southern and northeastern Amazon and it is not induced by reduction in productivity, which has significant trends for all three model versions, but rather by the biomass removal due to drought mortality.

CONCLUSIONS AND OUTLOOKS

5.1 CONCLUSIONS

In this thesis, we study the impact of forest drought response on land-atmosphere interactions, with a focus on the Amazon rainforests.

The Amazon forests are the largest rainforests and carbon reservoirs of the world. The Amazon forests also play important roles in regional climate as a lot of evapotranspiration is generated at the Amazon forests and then recycled as precipitation. The Amazon region is however predicted to experience more meteorological drought in the future, with a decreased mean state of precipitation and increased seasonal variability.

Previous studies have shown that current vegetation models are poor in capturing vegetation drought responses in the Amazon forests. As the land surface model JSBACH is an important member contributing to various model intercomparison projects both in land-only and coupled configuration, an evaluation on and improvement to JSBACH in simulating vegetation drought responses in the Amazon forests can not only help bridge the gaps between models and observations, but also provide insights for the modeling community. Specifically, we have answered the following questions, which have been raised in Chapter 1.

1.1 Is JSBACH able to capture the drought response in the Amazon? (Chapter 2)

- No. JSBACH can not reproduce either the LAI or litter production as observed in the field campaign of artificial drought experiment conducted in the Amazon forest.
- For the LAI, JSBACH has a threshold behavior, which consists of two stages of responses. At first, the LAI is kept at a constant value when the soil moisture is above a threshold. When the soil moisture drops below the threshold, the LAI declines too fast with a unrealistically steep slope. When the soil moisture recovers above the threshold again, the regrowth of LAI is also too fast.
- For the litter production, the simulations of JSBACH have systematic low biases. The litter production is at a rate close to zero

for most time of the year, and has intermittent pulse-like jumps to extreme values.

1.2 If not, what are the missing processes in the model, and how to improve the model?

- In the standard JSBACH, in order to have a low seasonal variability, a threshold value of soil moisture is assumed. Meanwhile, to account for LAI reduction when soil moisture falls to extreme low value, a steep slope is assigned to the LAI-soil moisture relationship. However, this disagrees with the LAI observation, which has a mild seasonality and mild response to drought before mortality is increased.
- As can be seen from the seasonality of LAI and carbon fluxes of the Amazon forests, the canopy growth is not only limited by available water, but also controlled by the carbon allocation to leaves, which is in turn determined by allocation strategy of the plants and available radiation input for photosynthesis. It is through the canopy that the water, energy and carbon budgets are coupled together and affects the land-atmosphere interaction. However, the interaction is now partially missing in JSBACH.
- To improve the model, a dependence of leaf growth rate on NPP allocation to leaves is implemented, and the leaf shedding rate is separated into two components representing leaf aging and leaf shedding due to water stress respectively. The intensive data from artificial drought experiments are used to tune the model.
- The implications for future model development include:
 - The canopy growth (LAI growth) should be coupled with the plant production or carbon allocation to the canopy, in order to simulate the seasonality of LAI and correctly incorporate the interaction between climate and vegetation growth.
 - Drought responses of different scales should be modeled at the respective scale. A reduction of canopy cover due to enhanced tree mortality should not be compensated with an overestimated leaf shedding rate as in the standard JSBACH.
 - The results reached by tuning against the intensive data from field campaign is promising. Therefore, when more mechanistically-based method is not available, a data-driven method as done in this study should be adopted.

2.1 What are the contributions of vegetation drought responses to the biogeochemical and biogeophysical drought effects under future climate? (Chapter 3)

- In terms of the biogeochemical effects, the LAI effect contributes to reductions in all carbon budget components, including GPP, R_a , NPP, R_s and NEP. The relative importances compared with the direct effect are different. The LAI effect is smaller than the direct effect, except for R_a , where the contribution from LAI effect is much stronger than from direct effect. For the reduction in natural carbon uptake (NEP), the magnitude of the LAI effect is 35% compared to the total drought effects.
- In terms of the biogeophysical effects, the contributions from the LAI effect is proportionally smaller than the direct effect, except for the bare soil evaporation, where the contribution from the LAI effect is negligible. The land-atmosphere interaction acts to amplify the warming through a reduction in low cloud cover and an increase in net surface solar radiation. The surface temperature is increased by the drought effects. The magnitude of warming induced by the LAI effect is 12% compared to the total drought effects.

2.2 How large is the uncertainty associated with the poor representation of vegetation response?

- For the carbon budgets, the model uncertainty associated the formulation of LAI and litter production is large, and much larger than the uncertainty related to internal variability. The poor representation of vegetation drought response therefore produces large uncertainties in the estimates of drought on carbon budgets such as (Green et al., 2019).
- For the biogeophysical effects, the model uncertainty is comparable to the uncertainty related to internal variability. However, in contrast to previous studies, the aridity in the Amazon forests is found to be determined by the pattern of change in precipitation, which corresponds to an increase in the Northern Amazon and a decrease in the Southern Amazon.

3.1 Does an inclusion of drought mortality in JSBACH improve the model? (Chapter 4)

- Yes. Compared to the standard JSBACH (*STND*), the versions with modified leaf shedding and litter production (*LFSD*, as used in Chapter 3) and drought mortality (*MORT*) are better in capturing the trend of biomass productivity and biomass mortality during the 1983 to 2010.
- The spatial pattern of aboveground biomass (AGB) in the Amazon basin, which is the highest in central Amazonia and roughly half over the southern part of basin, is captured only in *MORT*, in which the drought mortality is implemented.

3.2 What are the impacts of drought-enhanced tree mortality on carbon budgets under future climate?

- With the drought mortality, the vegetation carbon growth from during the 21st century is only 36%. The impact of drought mortality on biomass is 20 times of the impact on biomass of the drought in 2005.
- The fact that the vegetation carbon simulated by the model version with improved leaf shedding surpass the standard JSBACH is in agreement to our assumption in Chapter 2, which states that the standard JSBACH is likely to overestimate the drought responses.

5.2 OUTLOOKS

While in this study, we have answered the research questions concerning the vegetation drought responses in the Amazon forest, some related questions remain to be addressed. In the following, some further questions and recommendations for future studies are discussed.

Tropical forests outside of Amazon rainforests

Aside from the Amazon rainforests, large areas of rainforests are also located in Congo Basin and Southeast Asia. Although an increasing trend of drought will not necessarily happen in these forests, the deforestation is a common threat. For example, deforestation has also been increasing quickly in Borneo and Sumatra. While the biogeochemical functions of the forests in terms of carbon storage are similar, their roles in the regional climate might be different. For example, the responses of rainforests in Congo Basin and Southeast Asia to drought and deforestation might be different from the Amazon. It has been shown that the resilience to drought in Borneo has also been shown to be lower from in the Amazon (Phillips et al., 2010). The results obtained in this study therefore are not applicable to the rest of tropical rainforests. More ground-based observations on the effects of drought and deforestation as well as modeling studies are needed to help enhance our understanding at the regions.

Improving seasonality of LAI and carbon fluxes

While we have largely improved the biases and correlation of LAI at the drought plot in the TFE experiment, we note that the litter production is simulated still with a lag of phase of about 90 days. The

correlation at the control plot is also not as good as at the drought plot. Although in this study, the seasonal variability was not discussed in detail as we focused on the long term effect, better simulations of seasonality might be important for short-term and regional scale study. Previous studies have proposed some methods to improve the issue. For example, distinguishing new leaves and old leaves might be helpful, as the photosynthetic capacities of the two are different. A change of allocation strategy between root and canopy due to seasonal drought or episodic drought is also likely to affect the canopy seasonality. More model-data comparisons should be conducted in order to address this issue.

Inclusion of a mechanistically-based mortality

The results in Chapter 4 indicated a large reduction of natural carbon sink due to drought mortality. However, several uncertainties exist in our simulations. We note that as the mortality formulation implemented is empirical and based on the results from the TFE experiments under current climate and without full mechanical basis, the threshold is likely only with limited representativeness. Under drought condition in the future, the temperature above the canopy will become higher, resulting in higher VPD, which is not created in the TFE experiments. Uncertainties therefore exist in the results from the REW-based drought mortality. In addition, the strength of the land-atmosphere interaction was fixed as the simulation is offline without an interactive atmosphere. The fact that vegetation carbon is underestimated in MORT also indicates that the drought mortality is too strong in the formulation, and the response of natural carbon sink to future drought in reality therefore should lie somewhere between LFSD and MORT. Several models have implemented plant hydraulic, and promising results have been obtained (Kennedy et al., 2019; De Kauwe et al., 2020). Therefore, enhancement of representation in both hydrology and plant hydraulics should be considered in future model development of JSBACH.

A.1 THE DROUGHT EFFECTS OUTSIDE THE AMAZON

When we take the difference between the output of 21sm-20L and 20sm-20L, as the prescription of LAI and soil moisture is for every grid point, for each grid point on the map, the effect comes from the sum of local effect and the nonlocal effect of the rest of the world.

We have conducted another simulation, where only the LAI and soil moisture over the South America are prescribed. In this set of simulations, for the grid points in South America, there are only effects locally from South America; for grid points outside South America, the effects are from South America.

Taking the differences between the two set of experiments therefore can give us an estimate on the magnitudes of nonlocal effects. For example, looking at South America gives us the remote effects of drying elsewhere on South America. An example of comparison of the two experiment sets is shown in Fig. A.1. As the patterns and magnitudes over the South America at the upper and lower panels are similar, we conclude that the remote effects from outside of South America is small.

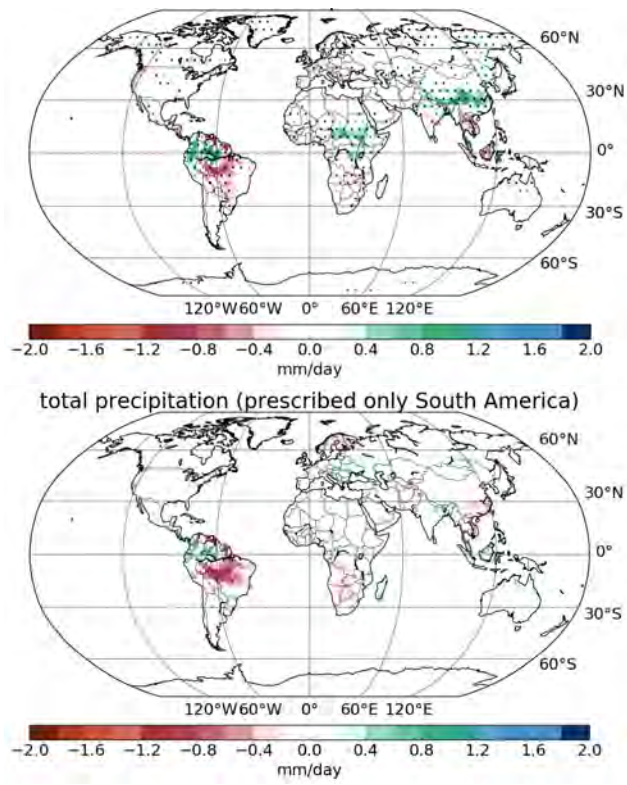


Figure A.1: Precipitation from the direct effect in (Upper) globally prescribed and (Lower) only South America prescribed experiments.

APPENDIX TO CHAPTER 4

B.1 ALTERNATIVES FOR IMPLEMENTING DROUGHT MORTALITY

In this section, we test several metrics, which do not utilize an explicit plant hydraulics, to find out the suitable candidates to implement to the JSBACH in order to estimate the future impacts of drought-enhanced mortality in the Amazon forests.

Climatic water deficit

CWD is the cumulative difference between PET and actual ET. We test if a threshold of CWD for tree mortality also applies to the tropical forests in the Amazon. To calculate the CWD in the Amazon, both the PET and ET are required. The PET and ET data is from Moderate Resolution Imaging Spectroradiometer (MODIS) (MOD16A2) data. The resolution is 0.05 degree. The mortality data is from the measurement on biomass from 321 plots over three decades in the Amazon forests (Brienen et al., 2015). The relations between CWD and mortality at various plots in the Amazon are shown in Fig. B.1. In contrast to the results from the previous study, there is no clear threshold in CWD for mortality. Moreover, the mortality does not increase with increasing CWD either. In Fig. B.1, the period for CWD accumulation is 12 months. However, the results do not change when the CWD is accumulated for 24 or 36 months (not shown). We therefore conclude that the CWD threshold does not apply at the tropical forests.

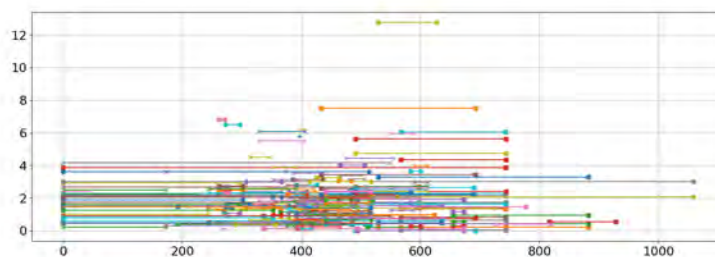


Figure B.1: Climatic water deficit (CWD) accumulated with 12 months. The mortality data is from Brienen et al., 2015. X-axis: CWD; Y-axis: biomass mortality.

Growth efficiency

Growth efficiency, defined as the stemwood growth per individual leaf area, is a common current method for mortality (Mcdowell et al., 2018). The growth efficiency simulated by JSBACH is shown in Fig. B.2. As can be seen, the JSBACH simulates an increase in growth efficiency instead of a decrease. The growth efficiency is therefore not suitable for predicting mortality in JSBACH.

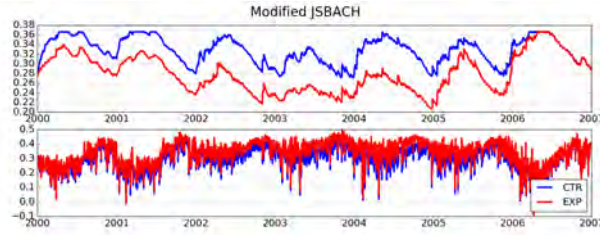


Figure B.2: (Upper) Soil moisture and (Lower) growth efficiency at both control (CTR) and drought (EXP) plots as simulated by the modified JSBACH.

B.2 METHODS*Comparison to Brien et al., 2015 data*

The wood productivity in models is calculated by multiplying total NPP with 0.3.

The biomass mortality is calculated as the difference between the annual wood productivity and the biomass in the woody part of plants.

The change of biomass is calculated by directly taking differences of the biomass of woody part between years.

Comparison to Saatchi et al., 2007 data

The biomass data from Saatchi et al., 2007 classifies the biomass into 11 categories. We convert the categories to the mean value of the respective bins. For the bins of larger than 400 Mg/ha, we take 450 Mg/ha.

The AGB is calculated in models by multiplying the total vegetation carbon with 0.7.



FORMAL REMARK ABOUT THE USE OF "WE" IN THIS THESIS

The research has been conducted under the supervision of Prof. Dr. Julia Pongratz and Dr. Kim Naudts, as well as input from other colleagues. The first person plural is therefore chosen to present the work.

Nevertheless, this thesis can mainly be viewed as a solitary work, as substantial parts of the research ideas are developed by the author. In addition, model development, data analysis and manuscript writing are conducted by the author.

BIBLIOGRAPHY

- Ainsworth, Elizabeth A. and Stephen P. Long (2004). "What have we learned from 15 years of free-air CO₂ enrichment (FACE)? A meta-analytic review of the responses of photosynthesis, canopy properties and plant production to rising CO₂." In: *New Phytologist* 165.2, pp. 351–372. DOI: [10.1111/j.1469-8137.2004.01224.x](https://doi.org/10.1111/j.1469-8137.2004.01224.x) (cit. on p. 4).
- Allen, Craig D. et al. (2010). "A global overview of drought and heat-induced tree mortality reveals emerging climate change risks for forests." In: *Forest Ecology and Management* 259.4, pp. 660–684. DOI: [10.1016/j.foreco.2009.09.001](https://doi.org/10.1016/j.foreco.2009.09.001) (cit. on p. 57).
- Anderegg, William R L, Alan Flint, Cho-Ying Huang, Lorraine Flint, Joseph a Berry, Frank W. Davis, John S Sperry, and Christopher B Field (2015). "Tree mortality predicted from drought-induced vascular damage." In: *Nature Geoscience* 8.5, pp. 367–371. DOI: [10.1038/ngeo2400](https://doi.org/10.1038/ngeo2400) (cit. on p. 58).
- Anderegg, William R. L., Leander D. L. Anderegg, and Cho-ying Huang (2019). "Testing early warning metrics for drought-induced tree physiological stress and mortality." In: *Global Change Biology* 25.7, gcb.14655. DOI: [10.1111/gcb.14655](https://doi.org/10.1111/gcb.14655) (cit. on p. 59).
- Asner, Gregory P. and Ane Alencar (2010). "Drought impacts on the Amazon forest: The remote sensing perspective." In: *New Phytologist* 187.3, pp. 569–578. DOI: [10.1111/j.1469-8137.2010.03310.x](https://doi.org/10.1111/j.1469-8137.2010.03310.x) (cit. on p. 8).
- Barichivich, Jonathan, Emanuel Gloor, Philippe Peylin, Roel J. W. Brienen, Jochen Schöngart, Jhan Carlo Espinoza, and Kanhu C. Pattnayak (2018). "Recent intensification of Amazon flooding extremes driven by strengthened Walker circulation." In: *Science Advances* 4.9, eaat8785. DOI: [10.1126/sciadv.aat8785](https://doi.org/10.1126/sciadv.aat8785) (cit. on p. 4).
- Bastos, A. et al. (2020). "Direct and seasonal legacy effects of the 2018 heat wave and drought on European ecosystem productivity." In: *Science Advances* 6.24, pp. 1–14. DOI: [10.1126/sciadv.aba2724](https://doi.org/10.1126/sciadv.aba2724) (cit. on p. 32).
- Belk, Elizabeth L., Daniel Markewitz, Todd C. Rasmussen, Eduardo J Maklouf Carvalho, Daniel C. Nepstad, and Eric A. Davidson (2007). "Modeling the effects of throughfall reduction on soil water content in a Brazilian Oxisol under a moist tropical forest." In: *Water Resources Research* 43.8, pp. 1–14. DOI: [10.1029/2006WR005493](https://doi.org/10.1029/2006WR005493) (cit. on p. 9).
- Berg, Alexis et al. (2016). "Land-atmosphere feedbacks amplify aridity increase over land under global warming." In: *Nature Climate Change* 6, 869 EP – (cit. on pp. 4, 31, 52, 54).

- Brando, Paulo M, Daniel C Nepstad, Eric A Davidson, Susan E Trumbore, David Ray, and Plínio Camargo (2008). "Drought effects on litterfall, wood production and belowground carbon cycling in an Amazon forest: results of a throughfall reduction experiment." In: *Philosophical transactions of the Royal Society of London. Series B, Biological sciences* 363.1498, pp. 1839–48. DOI: [10.1098/rstb.2007.0031](https://doi.org/10.1098/rstb.2007.0031) (cit. on pp. 9, 16).
- Brienen, R. J.W. et al. (2015). "Long-term decline of the Amazon carbon sink." In: *Nature* 519.7543, pp. 344–348. DOI: [10.1038/nature14283](https://doi.org/10.1038/nature14283) (cit. on pp. 62, 64, 77, 78).
- Busch, Jonah, Jens Engelmann, Susan C. Cook-Patton, Bronson W. Griscom, Timm Kroeger, Hugh Possingham, and Priya Shyamsundar (2019). "Potential for low-cost carbon dioxide removal through tropical reforestation." In: *Nature Climate Change* 9.6, pp. 463–466. DOI: [10.1038/s41558-019-0485-x](https://doi.org/10.1038/s41558-019-0485-x) (cit. on p. 1).
- Cardoso, Domingos et al. (2017). "Amazon plant diversity revealed by a taxonomically verified species list." In: *Proceedings of the National Academy of Sciences* 114.40, pp. 10695–10700. DOI: [10.1073/pnas.1706756114](https://doi.org/10.1073/pnas.1706756114) (cit. on p. 1).
- Chadwick, Robin, Peter Good, Gill Martin, and David P. Rowell (2015). "Large rainfall changes consistently projected over substantial areas of tropical land." In: *Nature Climate Change* 6, 177 EP – (cit. on p. 1).
- Choat, Brendan, Timothy J. Brodribb, Craig R. Brodersen, Remko A. Duursma, Rosana López, and Belinda E. Medlyn (2018). "Triggers of tree mortality under drought." In: *Nature* 558.7711, pp. 531–539. DOI: [10.1038/s41586-018-0240-x](https://doi.org/10.1038/s41586-018-0240-x) (cit. on p. 57).
- Christenhusz, Maarten J.M. and James W. Byng (2016). "The number of known plants species in the world and its annual increase." In: *Phytotaxa* 261.3, p. 201. DOI: [10.11646/phytotaxa.261.3.1](https://doi.org/10.11646/phytotaxa.261.3.1) (cit. on p. 1).
- Clapp, Roger B. and George M. Hornberger (1978). "Empirical equations for some soil hydraulic properties." In: *Water Resources Research* 14.4, pp. 601–604. DOI: [10.1029/WR014i004p00601](https://doi.org/10.1029/WR014i004p00601) (cit. on p. 18).
- Collatz, GJ, M Ribas-Carbo, and JA Berry (1992). "Coupled Photosynthesis-Stomatal Conductance Model for Leaves of C₄ Plants." In: *Functional Plant Biology* 19.5, p. 519. DOI: [10.1071/PP9920519](https://doi.org/10.1071/PP9920519) (cit. on p. 11).
- Collier, Nathan, Forrest M. Hoffman, David M. Lawrence, Gretchen Keppel-Aleks, Charles D. Koven, William J. Riley, Mingquan Mu, and James T. Randerson (2018). "The International Land Model Benchmarking (ILAMB) System: Design, Theory, and Implementation." In: *Journal of Advances in Modeling Earth Systems* 10.11, pp. 2731–2754. DOI: [10.1029/2018MS001354](https://doi.org/10.1029/2018MS001354) (cit. on p. 10).
- Cook, B. I., J. S. Mankin, K. Marvel, A. P. Williams, J. E. Smerdon, and K. J. Anchukaitis (2020). "Twenty-First Century Drought Projections in the CMIP6 Forcing Scenarios." In: *Earth's Future* 8.6. DOI: [10.1029/2019EF001461](https://doi.org/10.1029/2019EF001461) (cit. on pp. 1, 37).

- Costa, Carlos Lola da et al. (2010). "Effect of seven years of experimental drought on the aboveground biomass storage of an eastern Amazonian rainforest." In: *New Phytologist* 187, pp. 579–591. DOI: [10.1111/j.1469-8137.2010.03309.x](https://doi.org/10.1111/j.1469-8137.2010.03309.x) (cit. on p. 9).
- Dalmonech, Daniela, Sönke Zaehle, Gregor J. Schürmann, Victor Brovkin, Christian Reick, and Reiner Schnur (2015). "Separation of the Effects of Land and Climate Model Errors on Simulated Contemporary Land Carbon Cycle Trends in the MPI Earth System Model version 1*." In: *Journal of Climate* 28.1, pp. 272–291. DOI: [10.1175/JCLI-D-13-00593.1](https://doi.org/10.1175/JCLI-D-13-00593.1) (cit. on p. 28).
- Davidson, Eric A., Daniel C. Nepstad, Françoise Yoko Ishida, and Paulo M. Brando (2008). "Effects of an experimental drought and recovery on soil emissions of carbon dioxide, methane, nitrous oxide, and nitric oxide in a moist tropical forest." In: *Global Change Biology* 14.11, pp. 2582–2590. DOI: [10.1111/j.1365-2486.2008.01694.x](https://doi.org/10.1111/j.1365-2486.2008.01694.x) (cit. on p. 9).
- De Kauwe, Martin G. et al. (2020). "Identifying areas at risk of drought-induced tree mortality across South-Eastern Australia." In: *Global Change Biology* 26.10, pp. 5716–5733. DOI: [10.1111/gcb.15215](https://doi.org/10.1111/gcb.15215) (cit. on p. 73).
- Doughty, Christopher E. et al. (2015). "Drought impact on forest carbon dynamics and fluxes in Amazonia." In: *Nature* 519.7541, pp. 78–82. DOI: [10.1038/nature14213](https://doi.org/10.1038/nature14213) (cit. on p. 52).
- Duffy, Philip B., Paulo Brando, Gregory P. Asner, and Christopher B. Field (2015). "Projections of future meteorological drought and wet periods in the Amazon." In: *Proceedings of the National Academy of Sciences* 112.43, pp. 13172–13177. DOI: [10.1073/pnas.1421010112](https://doi.org/10.1073/pnas.1421010112) (cit. on p. 1).
- Farquhar, G. D., S. von Caemmerer, and J. A. Berry (1980). "A biochemical model of photosynthetic CO₂ assimilation in leaves of C₃ species." In: *Planta* 149.1, pp. 78–90. DOI: [10.1007/BF00386231](https://doi.org/10.1007/BF00386231) (cit. on p. 11).
- Fearnside, Philip M. (2018). "Brazil's Amazonian forest carbon: the key to Southern Amazonia's significance for global climate." In: *Regional Environmental Change* 18.1, pp. 47–61. DOI: [10.1007/s10113-016-1007-2](https://doi.org/10.1007/s10113-016-1007-2) (cit. on p. 54).
- Feldpausch, T R et al. (2016). "Amazon forest response to repeated droughts." In: *Global Biogeochemical Cycles* 30.7, pp. 964–982. DOI: [10.1002/2015GB005133](https://doi.org/10.1002/2015GB005133) (cit. on p. 3).
- Fisher, Rosie A., M. Williams, A. Lola da Costa, Y. Malhi, R. F. da Costa, S. Almeida, and P. Meir (2007). "The response of an Eastern Amazonian rain forest to drought stress: Results and modelling analyses from a throughfall exclusion experiment." In: *Global Change Biology* 13.11, pp. 2361–2378. DOI: [10.1111/j.1365-2486.2007.01417.x](https://doi.org/10.1111/j.1365-2486.2007.01417.x) (cit. on pp. 3, 5, 9, 15).

- Flack-Prain, Sophie, Patrick Meir, Yadvinder Malhi, Thomas Luke Smallman, and Mathew Williams (2019). "The importance of physiological, structural and trait responses to drought stress in driving spatial and temporal variation in GPP across Amazon forests." In: *Biogeosciences* 16.22, pp. 4463–4484. DOI: [10.5194/bg-16-4463-2019](https://doi.org/10.5194/bg-16-4463-2019) (cit. on p. 7).
- Forzieri, Giovanni, Ramdane Alkama, Diego G. Miralles, and Alessandro Cescatti (2017). "Satellites reveal contrasting responses of regional climate to the widespread greening of Earth." In: *Science* 356.6343, pp. 1180–1184. DOI: [10.1126/science.aal1727](https://doi.org/10.1126/science.aal1727) (cit. on p. 4).
- Forzieri, Giovanni et al. (2020). "Increased control of vegetation on global terrestrial energy fluxes." In: *Nature Climate Change* 10.4, pp. 356–362. DOI: [10.1038/s41558-020-0717-0](https://doi.org/10.1038/s41558-020-0717-0) (cit. on p. 7).
- Friedlingstein, Pierre et al. (2019). "Global Carbon Budget 2019." In: *Earth System Science Data* 11.4, pp. 1783–1838. DOI: [10.5194/essd-11-1783-2019](https://doi.org/10.5194/essd-11-1783-2019) (cit. on p. 1).
- Gatti, L. V. et al. (2014). "Drought sensitivity of Amazonian carbon balance revealed by atmospheric measurements." In: *Nature* 506.7486, pp. 76–80. DOI: [10.1038/nature12957](https://doi.org/10.1038/nature12957) (cit. on p. 3).
- Girardin, Cécile A J et al. (2016). "Seasonal trends of Amazonian rainforest phenology, net primary productivity, and carbon allocation." In: *Global Biogeochemical Cycles* 30.5, pp. 700–715. DOI: [10.1002/2015GB005270](https://doi.org/10.1002/2015GB005270) (cit. on p. 17).
- Green, Julia K., Sonia I. Seneviratne, Alexis M. Berg, Kirsten L. Findell, Stefan Hagemann, David M. Lawrence, and Pierre Gentine (2019). "Large influence of soil moisture on long-term terrestrial carbon uptake." In: *Nature* 565.7740, pp. 476–479. DOI: [10.1038/s41586-018-0848-x](https://doi.org/10.1038/s41586-018-0848-x) (cit. on pp. 4, 32, 52, 55, 71).
- Harper, Anna, Ian T. Baker, A. Scott Denning, David A. Randall, Donald Dazlich, and Mark Branson (2014). "Impact of evapotranspiration on dry season climate in the Amazon forest." In: *Journal of Climate* 27.2, pp. 574–591. DOI: [10.1175/JCLI-D-13-00074.1](https://doi.org/10.1175/JCLI-D-13-00074.1) (cit. on p. 54).
- Huang, Cho-Ying and William R. L. Anderegg (2012). "Large drought-induced aboveground live biomass losses in southern Rocky Mountain aspen forests." In: *Global Change Biology* 18.3, pp. 1016–1027. DOI: [10.1111/j.1365-2486.2011.02592.x](https://doi.org/10.1111/j.1365-2486.2011.02592.x) (cit. on p. 59).
- Huang, Yuanyuan, Stefan Gerber, Tongyi Huang, and Jeremy W. Lichstein (2016). "Evaluating the drought response of CMIP5 models using global gross primary productivity, leaf area, precipitation, and soil moisture data." In: *Global Biogeochemical Cycles* 30.12, pp. 1827–1846. DOI: [10.1002/2016GB005480](https://doi.org/10.1002/2016GB005480) (cit. on p. 3).
- Hubbell, S. P., F. He, R. Condit, L. Borda-de Agua, J. Kellner, and H. ter Steege (2008). "How many tree species are there in the Amazon and how many of them will go extinct?" In: *Proceedings of the National*

- Academy of Sciences* 105.Supplement 1, pp. 11498–11504. DOI: [10.1073/pnas.0801915105](https://doi.org/10.1073/pnas.0801915105) (cit. on p. 1).
- Hutyra, Lucy R., J. William Munger, Scott R. Saleska, Elaine Gottlieb, Bruce C. Daube, Allison L. Dunn, Daniel F. Amaral, Plinio B. de Camargo, and Steven C. Wofsy (2007). “Seasonal controls on the exchange of carbon and water in an Amazonian rain forest.” In: *Journal of Geophysical Research: Biogeosciences* 112.3, pp. 1–16. DOI: [10.1029/2006JG000365](https://doi.org/10.1029/2006JG000365) (cit. on p. 9).
- Joetzjer, E., H. Douville, C. Delire, and P. Ciais (2013). “Present-day and future Amazonian precipitation in global climate models: CMIP5 versus CMIP3.” In: *Climate Dynamics* 41.11-12, pp. 2921–2936. DOI: [10.1007/s00382-012-1644-1](https://doi.org/10.1007/s00382-012-1644-1) (cit. on p. 1).
- Joetzjer, E. et al. (2014). “Predicting the response of the Amazon rainforest to persistent drought conditions under current and future climates: A major challenge for global land surface models.” In: *Geoscientific Model Development* 7.6, pp. 2933–2950. DOI: [10.5194/gmd-7-2933-2014](https://doi.org/10.5194/gmd-7-2933-2014) (cit. on p. 3, 10, 26).
- Karnieli, Arnon, Nurit Agam, Rachel T. Pinker, Martha Anderson, Marc L. Imhoff, Garik G. Gutman, Natalya Panov, and Alexander Goldberg (2010). “Use of NDVI and Land Surface Temperature for Drought Assessment: Merits and Limitations.” In: *Journal of Climate* 23.3, pp. 618–633. DOI: [10.1175/2009JCLI2900.1](https://doi.org/10.1175/2009JCLI2900.1) (cit. on p. 7).
- Kennedy, Daniel, Sean Swenson, Keith W. Oleson, David M. Lawrence, Rosie Fisher, Antonio Carlos Lola da Costa, and Pierre Gentine (2019). “Implementing Plant Hydraulics in the Community Land Model, Version 5.” In: *Journal of Advances in Modeling Earth Systems* 11.2, pp. 485–513. DOI: [10.1029/2018MS001500](https://doi.org/10.1029/2018MS001500) (cit. on p. 73).
- Klein, Tamir (2014). “The variability of stomatal sensitivity to leaf water potential across tree species indicates a continuum between isohydric and anisohydric behaviours.” In: *Functional Ecology* 28.6. Ed. by Shuli Niu, pp. 1313–1320. DOI: [10.1111/1365-2435.12289](https://doi.org/10.1111/1365-2435.12289) (cit. on p. 2).
- Koster, Randal D. et al. (2004). “Regions of strong coupling between soil moisture and precipitation.” In: *Science* 305.5687, pp. 1138–1140. DOI: [10.1126/science.1100217](https://doi.org/10.1126/science.1100217) (cit. on p. 31).
- L’Heureux, Michelle L., Sukyoung Lee, and Bradfield Lyon (2013). “Recent multidecadal strengthening of the Walker circulation across the tropical Pacific.” In: *Nature Climate Change* 3.6, pp. 571–576. DOI: [10.1038/nclimate1840](https://doi.org/10.1038/nclimate1840) (cit. on p. 4).
- Laan-Luijkx, I. T. van der et al. (2015). “Response of the Amazon carbon balance to the 2010 drought derived with CarbonTracker South America.” In: *Global Biogeochemical Cycles* 29.7, pp. 1092–1108. DOI: [10.1002/2014GB005082](https://doi.org/10.1002/2014GB005082) (cit. on p. 3).
- Lawal, Shakirudeen, Christopher Lennard, Christopher Jack, Piotr Wolski, Bruce Hewitson, and Babatunde Abiodun (2019). “The observed and model-simulated response of southern African vegetation to

- drought." In: *Agricultural and Forest Meteorology* 279, p. 107698. DOI: [10.1016/j.agrformet.2019.107698](https://doi.org/10.1016/j.agrformet.2019.107698) (cit. on p. 7).
- Le Quéré, Corinne et al. (2018). "Global Carbon Budget 2018." In: *Earth System Science Data* 10.4, pp. 2141–2194. DOI: [10.5194/essd-10-2141-2018](https://doi.org/10.5194/essd-10-2141-2018) (cit. on pp. 10, 33).
- Lejeune, Quentin, Edouard L. Davin, Benoit P. Guillod, and Sonia I. Seneviratne (2015). "Influence of Amazonian deforestation on the future evolution of regional surface fluxes, circulation, surface temperature and precipitation." In: *Climate Dynamics* 44.9-10, pp. 2769–2786. DOI: [10.1007/s00382-014-2203-8](https://doi.org/10.1007/s00382-014-2203-8) (cit. on pp. 53, 54).
- Lewis, Simon L., Paulo M. Brando, Oliver L. Phillips, Geertje M.F. Van Der Heijden, and Daniel Nepstad (2011). "The 2010 Amazon drought." In: *Science* 331.6017, p. 554. DOI: [10.1126/science.1200807](https://doi.org/10.1126/science.1200807) (cit. on p. 2).
- Lin, Yen-Heng, Min-Hui Lo, and Chia Chou (2015). "Potential negative effects of groundwater dynamics on dry season convection in the Amazon River basin." In: *Climate Dynamics*. DOI: [10.1007/s00382-015-2628-8](https://doi.org/10.1007/s00382-015-2628-8) (cit. on p. 54).
- Lorenz, Ruth, Edouard L. Davin, David M. Lawrence, Reto Stöckli, and Sonia I. Seneviratne (2013). "How important is vegetation phenology for European climate and heat waves?" In: *Journal of Climate* 26.24, pp. 10077–10100. DOI: [10.1175/JCLI-D-13-00040.1](https://doi.org/10.1175/JCLI-D-13-00040.1) (cit. on p. 32).
- Lorenz, Ruth et al. (2016). "Influence of land-atmosphere feedbacks on temperature and precipitation extremes in the GLACE-CMIP5 ensemble." In: *Journal of Geophysical Research: Atmospheres* 121.2, pp. 607–623. DOI: [10.1002/2015JD024053](https://doi.org/10.1002/2015JD024053) (cit. on pp. 4, 31).
- Malhi, Yadvinder, J. Timmons Roberts, Richard A. Betts, Timothy J. Killeen, Wenhong Li, and Carlos A. Nobre (2008). "Climate Change, Deforestation, and the Fate of the Amazon." In: *Science* January, pp. 169–172. DOI: [10.1126/science.1146961](https://doi.org/10.1126/science.1146961) (cit. on p. 1).
- Manoli, Gabriele, Valeriy Y. Ivanov, and Simone Fatichi (2018). "Dry-Season Greening and Water Stress in Amazonia: The Role of Modeling Leaf Phenology." In: *Journal of Geophysical Research: Biogeosciences* 123.6, pp. 1909–1926. DOI: [10.1029/2017JG004282](https://doi.org/10.1029/2017JG004282) (cit. on p. 28).
- Marengo, José A., Carlos A. Nobre, Javier Tomasella, Marcos D. Oyama, Gilvan Sampaio de Oliveira, Rafael de Oliveira, Helio Camargo, Lincoln M. Alves, and I. Foster Brown (2008). "The drought of Amazonia in 2005." In: *Journal of Climate* 21.3, pp. 495–516. DOI: [10.1175/2007JCLI1600.1](https://doi.org/10.1175/2007JCLI1600.1) (cit. on p. 2).
- Markewitz, Daniel, Scott Devine, Eric A. Davidson, Paulo Brando, and Daniel C. Nepstad (2010). "Soil moisture depletion under simulated drought in the Amazon: Impacts on deep root uptake." In: *New Phytologist* 187.3, pp. 592–607. DOI: [10.1111/j.1469-8137.2010.03391.x](https://doi.org/10.1111/j.1469-8137.2010.03391.x) (cit. on p. 9).

- Mauritsen, Thorsten et al. (2019). "Developments in the MPI-M Earth System Model version 1.2 (MPI-ESM1.2) and Its Response to Increasing CO₂." In: *Journal of Advances in Modeling Earth Systems* 11.4, pp. 998–1038. DOI: [10.1029/2018MS001400](https://doi.org/10.1029/2018MS001400) (cit. on pp. 11, 33).
- May, Wilhelm, Markku Rummukainen, Frederique Chéruey, Stefan Hagemann, and Arndt Meier (2017). "Contributions of soil moisture interactions to future precipitation changes in the GLACE-CMIP5 experiment." In: *Climate Dynamics* 49.5-6, pp. 1681–1704. DOI: [10.1007/s00382-016-3408-9](https://doi.org/10.1007/s00382-016-3408-9) (cit. on p. 4).
- McGregor, Shayne, Axel Timmermann, Malte F. Stuecker, Matthew H. England, Mark Merrifield, Fei-Fei Jin, and Yoshimitsu Chikamoto (2014). "Recent Walker circulation strengthening and Pacific cooling amplified by Atlantic warming." In: *Nature Climate Change* 4.10, pp. 888–892. DOI: [10.1038/nclimate2330](https://doi.org/10.1038/nclimate2330) (cit. on p. 4).
- Mcdowell, Nate G. et al. (2013). "Evaluating theories of drought-induced vegetation mortality using a multimodel-experiment framework." In: *New Phytologist* 200.2, pp. 304–321. DOI: [10.1111/nph.12465](https://doi.org/10.1111/nph.12465) (cit. on p. 58).
- Mcdowell, Nate et al. (2018). "Drivers and mechanisms of tree mortality in moist tropical forests." In: *New Phytologist*. DOI: [10.1111/nph.15027](https://doi.org/10.1111/nph.15027) (cit. on pp. 57, 58, 78).
- Meir, P., D. B. Metcalfe, A. C.L. Costa, and R. A. Fisher (2008). "The fate of assimilated carbon during drought: Impacts on respiration in Amazon rainforests." In: *Philosophical Transactions of the Royal Society B: Biological Sciences* 363.1498, pp. 1849–1855. DOI: [10.1098/rstb.2007.0021](https://doi.org/10.1098/rstb.2007.0021) (cit. on p. 52).
- Meir, Patrick, Tana E. Wood, David R. Galbraith, Paulo M. Brando, Antonio C L Da Costa, Lucy Rowland, and Leandro V. Ferreira (2015). "Threshold Responses to Soil Moisture Deficit by Trees and Soil in Tropical Rain Forests: Insights from Field Experiments." In: *BioScience* 65.9, pp. 882–892. DOI: [10.1093/biosci/biv107](https://doi.org/10.1093/biosci/biv107) (cit. on pp. 59, 66).
- Meir, Patrick, Maurizio Mencuccini, Oliver Binks, Antonio Lola Da Costa, Leandro Ferreira, and Lucy Rowland (2018). "Short-term effects of drought on tropical forest do not fully predict impacts of repeated or long-term drought: Gas exchange versus growth." In: *Philosophical Transactions of the Royal Society B: Biological Sciences* 373.1760. DOI: [10.1098/rstb.2017.0311](https://doi.org/10.1098/rstb.2017.0311) (cit. on p. 9).
- Metcalfe, D. B. et al. (2010). "Shifts in plant respiration and carbon use efficiency at a large-scale drought experiment in the eastern Amazon." In: *New Phytologist* 187.3, pp. 608–621. DOI: [10.1111/j.1469-8137.2010.03319.x](https://doi.org/10.1111/j.1469-8137.2010.03319.x) (cit. on pp. 9, 52).
- Nepstad, D C et al. (2002). "The effects of partial throughfall exclusion on canopy processes, aboveground production, and biogeochemistry of an Amazon forest." In: *Journal of Geophysical Research: Atmospheres*

- 107.D20, LBA 53-1-LBA 53-18. DOI: [10.1029/2001JD000360](https://doi.org/10.1029/2001JD000360) (cit. on pp. [3](#), [5](#), [8](#), [15](#)).
- Nepstad, Daniel C., Ingrid Marisa Tohver, Ray David, Paulo Moutinho, and Georgina Cardinot (2007). "Mortality of large trees and lianas following experimental drought in an amazon forest." In: *Ecology* 88.9, pp. 2259–2269. DOI: [10.1890/06-1046.1](https://doi.org/10.1890/06-1046.1) (cit. on pp. [9](#), [57](#)).
- Nobre, Carlos A., Gilvan Sampaio, Laura S. Borma, Juan Carlos Castilla-Rubio, José S. Silva, and Manoel Cardoso (2016). "Land-use and climate change risks in the amazon and the need of a novel sustainable development paradigm." In: *Proceedings of the National Academy of Sciences of the United States of America* 113.39, pp. 10759–10768. DOI: [10.1073/pnas.1605516113](https://doi.org/10.1073/pnas.1605516113) (cit. on p. [54](#)).
- Oliveira, Rafael S., Todd E. Dawson, Stephen S. O. Burgess, and Daniel C. Nepstad (2005). "Hydraulic redistribution in three Amazonian trees." In: *Oecologia* 145.3, pp. 354–363. DOI: [10.1007/s00442-005-0108-2](https://doi.org/10.1007/s00442-005-0108-2) (cit. on p. [9](#)).
- Pan, Yude et al. (2011). "A Large and Persistent Carbon Sink in the World's Forests." In: *Science* 333.6045, pp. 988–993. DOI: [10.1126/science.1201609](https://doi.org/10.1126/science.1201609) (cit. on p. [1](#)).
- Paschalis, Athanasios et al. (2020). "Rainfall manipulation experiments as simulated by terrestrial biosphere models: Where do we stand?" In: *Global Change Biology* January, pp. 1–20. DOI: [10.1111/gcb.15024](https://doi.org/10.1111/gcb.15024) (cit. on p. [8](#)).
- Patterson, K. A. (1990). "Global distribution of total and total-available soil water-holding capacities." In: *Msc. Thesis* 119 (cit. on pp. [16](#), [19](#)).
- Phillips, Oliver L et al. (2009). "Drought Sensitivity of the Amazon Rainforest." In: *Science* 323.5919, pp. 1344–1347. DOI: [10.1126/science.1164033](https://doi.org/10.1126/science.1164033) (cit. on pp. [57](#), [65](#)).
- Phillips, Oliver L et al. (2010). "Drought-mortality relationships for tropical forests." In: *New Phytologist* 187.3, pp. 631–646. DOI: [10.1111/j.1469-8137.2010.03359.x](https://doi.org/10.1111/j.1469-8137.2010.03359.x) (cit. on pp. [57](#), [72](#)).
- Phillips, Oliver L. et al. (2017). "Carbon uptake by mature Amazon forests has mitigated Amazon nations' carbon emissions." In: *Carbon Balance and Management* 12.1, pp. 1–9. DOI: [10.1186/s13021-016-0069-2](https://doi.org/10.1186/s13021-016-0069-2) (cit. on p. [1](#)).
- Piao, Shilong et al. (2020). "Characteristics, drivers and feedbacks of global greening." In: *Nature Reviews Earth & Environment* 1.1, pp. 14–27. DOI: [10.1038/s43017-019-0001-x](https://doi.org/10.1038/s43017-019-0001-x) (cit. on p. [4](#)).
- Pitman, A. J. (2003). "The evolution of, and revolution in, land surface schemes designed for climate models." In: *International Journal of Climatology* 23.5, pp. 479–510. DOI: [10.1002/joc.893](https://doi.org/10.1002/joc.893) (cit. on p. [9](#)).
- Powell, Thomas L. et al. (2013). "Confronting model predictions of carbon fluxes with measurements of Amazon forests subjected to experimental drought." In: *New Phytologist* 200.2, pp. 350–365. DOI: [10.1111/nph.12390](https://doi.org/10.1111/nph.12390) (cit. on pp. [3](#), [10](#), [26](#), [27](#)).

- Rayner, N. A., D. E. Parker, E. B. Horton, C. K. Folland, L. V. Alexander, D. P. Rowell, E. C. Kent, and A. Kaplan (2003). "Global analyses of sea surface temperature, sea ice, and night marine air temperature since the late nineteenth century." In: *Journal of Geophysical Research D: Atmospheres* 108.14. DOI: [10.1029/2002jd002670](https://doi.org/10.1029/2002jd002670) (cit. on p. 33).
- Reick, C. H., T. Raddatz, V. Brovkin, and V. Gayler (2013). "Representation of natural and anthropogenic land cover change in MPI-ESM." In: *Journal of Advances in Modeling Earth Systems* 5.3, pp. 459–482. DOI: [10.1002/jame.20022](https://doi.org/10.1002/jame.20022) (cit. on p. 11).
- Rocha, Humberto R. da, Michael L. Goulden, Scott D. Miller, Mary C. Menton, Leandro D. V. O. Pinto, Helber C. de Freitas, and Adelaine M. e Silva Figueira (2004). "SEASONALITY OF WATER AND HEAT FLUXES OVER A TROPICAL FOREST IN EASTERN AMAZONIA." In: *Ecological Applications* 14.sp4, pp. 22–32. DOI: [10.1890/02-6001](https://doi.org/10.1890/02-6001) (cit. on p. 9).
- Rowland, L. et al. (2015a). "Modelling climate change responses in tropical forests: Similar productivity estimates across five models, but different mechanisms and responses." In: *Geoscientific Model Development* 8.4, pp. 1097–1110. DOI: [10.5194/gmd-8-1097-2015](https://doi.org/10.5194/gmd-8-1097-2015) (cit. on p. 3).
- Rowland, Lucy et al. (2015b). "After more than a decade of soil moisture deficit, tropical rainforest trees maintain photosynthetic capacity, despite increased leaf respiration." In: *Global Change Biology* 21.12, pp. 4662–4672. DOI: [10.1111/gcb.13035](https://doi.org/10.1111/gcb.13035) (cit. on p. 9).
- Rowland, Lucy, Antonio C.L. da Costa, Alex A.R. Oliveira, Samuel S. Almeida, Leandro V. Ferreira, Yadvinder Malhi, Dan B. Metcalfe, Maurizio Mencuccini, John Grace, and Patrick Meir (2018). "Shock and stabilisation following long-term drought in tropical forest from 15 years of litterfall dynamics." In: *Journal of Ecology* 106.4, pp. 1673–1682. DOI: [10.1111/1365-2745.12931](https://doi.org/10.1111/1365-2745.12931) (cit. on pp. 7, 9).
- Ruiz-Vásquez, Melissa, Paola A. Arias, J. Alejandro Martínez, and Jhan Carlo Espinoza (2020). "Effects of Amazon basin deforestation on regional atmospheric circulation and water vapor transport towards tropical South America." In: *Climate Dynamics* 54.9-10, pp. 4169–4189. DOI: [10.1007/s00382-020-05223-4](https://doi.org/10.1007/s00382-020-05223-4) (cit. on p. 1).
- Saatchi, S. S., R. A. Houghton, R. C. Dos Santos Alvalá, J. V. Soares, and Y. Yu (2007). "Distribution of aboveground live biomass in the Amazon basin." In: *Global Change Biology* 13.4, pp. 816–837. DOI: [10.1111/j.1365-2486.2007.01323.x](https://doi.org/10.1111/j.1365-2486.2007.01323.x) (cit. on pp. 63, 65, 78).
- Saatchi, S., S. Asefi-Najafabady, Y. Malhi, L. E. O. C. Aragao, L. O. Anderson, R. B. Myneni, and R. Nemani (2013). "Persistent effects of a severe drought on Amazonian forest canopy." In: *Proceedings of the National Academy of Sciences* 110.2, pp. 565–570. DOI: [10.1073/pnas.1204651110](https://doi.org/10.1073/pnas.1204651110) (cit. on p. 2).

- Saleska, S R, K Didan, A R Huete, and H R da Rocha (2007). "Amazon Forests Green-Up During 2005 Drought." In: *Science* 318.5850, pp. 612–612. DOI: [10.1126/science.1146663](https://doi.org/10.1126/science.1146663) (cit. on p. 8).
- Samanta, Arindam, Sangram Ganguly, Hirofumi Hashimoto, Sadashiva Devadiga, Eric Vermote, Yuri Knyazikhin, Ramakrishna R. Nemani, and Ranga B. Myneni (2010). "Amazon forests did not green-up during the 2005 drought." In: *Geophysical Research Letters* 37.5, pp. 1–5. DOI: [10.1029/2009GL042154](https://doi.org/10.1029/2009GL042154) (cit. on p. 8).
- Samanta, Arindam, Sangram Ganguly, and Ranga B. Myneni (2011). "MODIS Enhanced Vegetation Index data do not show greening of Amazon forests during the 2005 drought." In: *New Phytologist* 189.1, pp. 11–15. DOI: [10.1111/j.1469-8137.2010.03516.x](https://doi.org/10.1111/j.1469-8137.2010.03516.x) (cit. on p. 8).
- Seneviratne, Sonia I. et al. (2013). "Impact of soil moisture-climate feedbacks on CMIP5 projections: First results from the GLACE-CMIP5 experiment." In: *Geophysical Research Letters* 40.19, pp. 5212–5217. DOI: [10.1002/grl.50956](https://doi.org/10.1002/grl.50956) (cit. on pp. 31, 52).
- Sitch, S. et al. (2015). "Recent trends and drivers of regional sources and sinks of carbon dioxide." In: *Biogeosciences* 12.3, pp. 653–679. DOI: [10.5194/bg-12-653-2015](https://doi.org/10.5194/bg-12-653-2015) (cit. on pp. 10, 33, 39).
- Sruthi, S. and M.A. Mohammed Aslam (2015). "Agricultural Drought Analysis Using the NDVI and Land Surface Temperature Data; a Case Study of Raichur District." In: *Aquatic Procedia* 4, pp. 1258–1264. DOI: [10.1016/j.aqpro.2015.02.164](https://doi.org/10.1016/j.aqpro.2015.02.164) (cit. on p. 7).
- Tang, Hao, Ralph Dubayah, Anu Swatantran, Michelle Hofton, Sage Sheldon, David B. Clark, and Bryan Blair (2012). "Retrieval of vertical LAI profiles over tropical rain forests using waveform lidar at La Selva, Costa Rica." In: *Remote Sensing of Environment* 124, pp. 242–250. DOI: [10.1016/j.rse.2012.05.005](https://doi.org/10.1016/j.rse.2012.05.005) (cit. on p. 8).
- Trugman, A. T., D. Medvigy, J. S. Mankin, and W. R. L. Anderegg (2018). "Soil Moisture Stress as a Major Driver of Carbon Cycle Uncertainty." In: *Geophysical Research Letters*, pp. 1–9. DOI: [10.1029/2018GL078131](https://doi.org/10.1029/2018GL078131) (cit. on p. 3).
- Turner, David P., Warren B. Cohen, Robert E. Kennedy, Karin S. Fassnacht, and John M. Briggs (1999). "Relationships between Leaf Area Index and Landsat TM Spectral Vegetation Indices across Three Temperate Zone Sites." In: *Remote Sensing of Environment* 70.1, pp. 52–68. DOI: [10.1016/S0034-4257\(99\)00057-7](https://doi.org/10.1016/S0034-4257(99)00057-7) (cit. on p. 8).
- Tyree, M. T., H. Cochard, P. Cruiziat, B. Sinclair, and T. Ameglio (1993). "Drought-induced leaf shedding in walnut: evidence for vulnerability segmentation." In: *Plant, Cell and Environment* 16.7, pp. 879–882. DOI: [10.1111/j.1365-3040.1993.tb00511.x](https://doi.org/10.1111/j.1365-3040.1993.tb00511.x) (cit. on p. 10).
- Weedon, G. P., S. Gomes, P. Viterbo, W. J. Shuttleworth, E. Blyth, H. Österle, J. C. Adam, N. Bellouin, O. Boucher, and M. Best (2011). "Creation of the WATCH forcing data and its use to assess global and regional reference crop evaporation over land during the twentieth

- century." In: *Journal of Hydrometeorology* 12.5, pp. 823–848. DOI: [10.1175/2011JHM1369.1](https://doi.org/10.1175/2011JHM1369.1) (cit. on p. 17).
- Weedon, Graham P., Gianpaolo Balsamo, Nicolas Bellouin, Sandra Gomes, Martin J. Best, and Pedro Viterbo (2014). "The WFDEI meteorological forcing data set: WATCH Forcing Data methodology applied to ERA-Interim reanalysis data." In: *Water Resources Research* 50.9, pp. 7505–7514. DOI: <https://doi.org/10.1002/2014WR015638> (cit. on p. 17).
- Westoby, Mark (1984). "The Self-Thinning Rule." In: pp. 167–225. DOI: [10.1016/S0065-2504\(08\)60171-3](https://doi.org/10.1016/S0065-2504(08)60171-3) (cit. on p. 12).
- Winkler, Alexander J., Ranga B. Myneni, Georgii A. Alexandrov, and Victor Brovkin (2019). "Earth system models underestimate carbon fixation by plants in the high latitudes." In: *Nature Communications* 10.1. DOI: [10.1038/s41467-019-08633-z](https://doi.org/10.1038/s41467-019-08633-z) (cit. on p. 4).
- Wolfe, Brett T., John S. Sperry, and Thomas A. Kursar (2016). "Does leaf shedding protect stems from cavitation during seasonal droughts? A test of the hydraulic fuse hypothesis." In: *New Phytologist* 212.4, pp. 1007–1018. DOI: [10.1111/nph.14087](https://doi.org/10.1111/nph.14087) (cit. on p. 10).
- Wu, Jin et al. (2016). "Leaf development and demography explain photosynthetic seasonality in Amazon evergreen forests." In: *Science* 351.6276, pp. 972–976. DOI: [10.1126/science.aad5068](https://doi.org/10.1126/science.aad5068) (cit. on p. 28).
- Xu, Liang, Arindam Samanta, Marcos H. Costa, Sangram Ganguly, Ramakrishna R. Nemani, and Ranga B. Myneni (2011). "Widespread decline in greenness of Amazonian vegetation due to the 2010 drought." In: *Geophysical Research Letters* 38.7, pp. 2–5. DOI: [10.1029/2011GL046824](https://doi.org/10.1029/2011GL046824) (cit. on p. 7).
- Xu, Xiangtao, David Medvigy, Jennifer S. Powers, Justin M. Becknell, and Kaiyu Guan (2016). "Diversity in plant hydraulic traits explains seasonal and inter-annual variations of vegetation dynamics in seasonally dry tropical forests." In: *New Phytologist* 212.1, pp. 80–95. DOI: [10.1111/nph.14009](https://doi.org/10.1111/nph.14009) (cit. on p. 10).
- Yang, Yan, Sassan S. Saatchi, Liang Xu, Yifan Yu, Sungho Choi, Nathan Phillips, Robert Kennedy, Michael Keller, Yuri Knyazikhin, and Ranga B. Myneni (2018). "Post-drought decline of the Amazon carbon sink." In: *Nature Communications* 9.1, p. 3172. DOI: [10.1038/s41467-018-05668-6](https://doi.org/10.1038/s41467-018-05668-6) (cit. on p. 3).
- Yin, Lei, Rong Fu, Elena Shevliakova, and Robert E. Dickinson (2013). "How well can CMIP5 simulate precipitation and its controlling processes over tropical South America?" In: *Climate Dynamics* 41.11–12, pp. 3127–3143. DOI: [10.1007/s00382-012-1582-y](https://doi.org/10.1007/s00382-012-1582-y) (cit. on pp. 39, 65).
- Zemp, Delphine Clara, Carl Friedrich Schleussner, Henrique M.J. Barbosa, Marina Hirota, Vincent Montade, Gilvan Sampaio, Arie Staal, Lan Wang-Erlandsson, and Anja Rammig (2017). "Self-amplified Amazon forest loss due to vegetation-atmosphere feedbacks." In:

- Nature Communications* 8, pp. 1–10. DOI: [10.1038/ncomms14681](https://doi.org/10.1038/ncomms14681) (cit. on p. 53).
- Zeng, Ning, Jin Ho Yoon, Jose A. Marengo, Ajit Subramaniam, Carlos A. Nobre, Annarita Mariotti, and J. David Neelin (2008). “Causes and impacts of the 2005 Amazon drought.” In: *Environmental Research Letters* 3.1. DOI: [10.1088/1748-9326/3/1/014002](https://doi.org/10.1088/1748-9326/3/1/014002) (cit. on p. 2).
- Zhao, M. and S. W. Running (2010). “Drought-Induced Reduction in Global Terrestrial Net Primary Production from 2000 Through 2009.” In: *Science* 329.5994, pp. 940–943. DOI: [10.1126/science.1192666](https://doi.org/10.1126/science.1192666) (cit. on p. 7).
- Zhou, Sha, A. Park Williams, Alexis M. Berg, Benjamin I. Cook, Yao Zhang, Stefan Hagemann, Ruth Lorenz, Sonia I. Seneviratne, and Pierre Gentine (2019). “Land–atmosphere feedbacks exacerbate concurrent soil drought and atmospheric aridity.” In: *Proceedings of the National Academy of Sciences of the United States of America* 116.38, pp. 18848–18853. DOI: [10.1073/pnas.1904955116](https://doi.org/10.1073/pnas.1904955116) (cit. on pp. 4, 32).
- Zhu, Zaichun et al. (2016). “Greening of the Earth and its drivers.” In: *Nature Climate Change* 6.August, early online. DOI: [10.1038/NCLIMATE3004](https://doi.org/10.1038/NCLIMATE3004) (cit. on p. 4).

This thesis was typeset using the `classicthesis` template developed by André Miede and Ivo Pletikosić (available at: <https://bitbucket.org/amiede/classicthesis/>).

VERSICHERUNG AN EIDES STATT

Hiermit versichere ich an Eides statt, dass ich die vorliegende Dissertation mit dem Titel: „Impact of Forest Drought Response on Land-Atmosphere Interactions“ selbstständig verfasst und keine anderen als die angegebenen Hilfsmittel – insbesondere keine im Quellenverzeichnis nicht benannten Internet-Quellen – benutzt habe. Alle Stellen, die wörtlich oder sinngemäß aus Veröffentlichungen entnommen wurden, sind als solche kenntlich gemacht. Ich versichere weiterhin, dass ich die Dissertation oder Teile davon vorher weder im In- noch im Ausland in einem anderen Prüfungsverfahren eingereicht habe und die eingereichte schriftliche Fassung der auf dem elektronischen Speichermedium entspricht.

Hamburg, 8. December 2020

Hao-wei Wey

Hinweis / Reference

Die gesamten Veröffentlichungen in der Publikationsreihe des MPI-M
„Berichte zur Erdsystemforschung / Reports on Earth System Science“,
ISSN 1614-1199

sind über die Internetseiten des Max-Planck-Instituts für Meteorologie erhältlich:
<http://www.mpimet.mpg.de/wissenschaft/publikationen.html>

*All the publications in the series of the MPI -M
„Berichte zur Erdsystemforschung / Reports on Earth System Science“,
ISSN 1614-1199*

*are available on the website of the Max Planck Institute for Meteorology:
<http://www.mpimet.mpg.de/wissenschaft/publikationen.html>*

